

AD-A085 740

MECHANICAL TECHNOLOGY INC LATHAM N Y

F/G 13/9

THE DEVELOPMENT OF AN AUTOMATED ROLLER INSPECTION SYSTEM USING --ETC(U)

NOV 79 M # EUSEPI

F33615-77-C-3142

UNCLASSIFIED

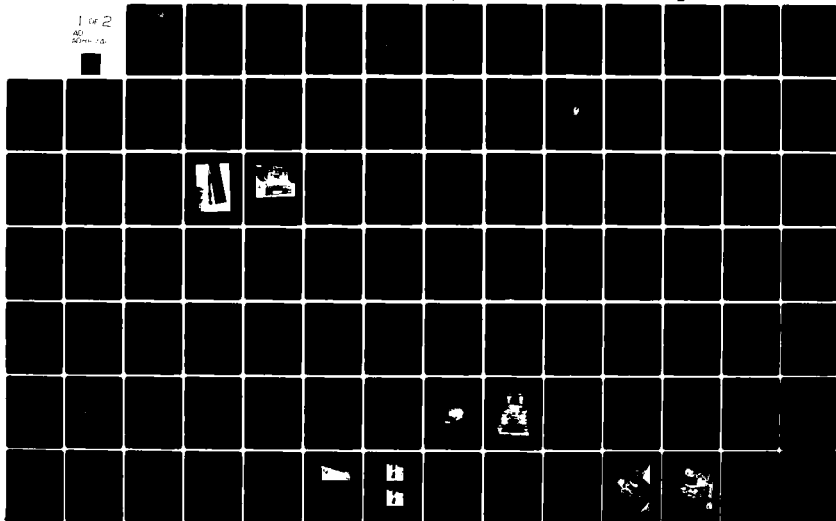
MTI-79TR60

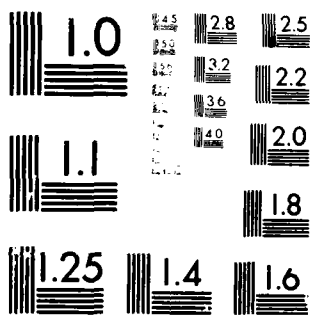
AFAL-TR-79-2076

NL

1 of 2

AD
A085 740





MICROCOPY RESOLUTION TEST CHART
NATIONAL BUREAU OF STANDARDS-1963-A

AFAPL-TR-79-2076

LEVEL

2

ADA 085740

**THE DEVELOPMENT OF AN
AUTOMATED ROLLER INSPECTION SYSTEM
USING NONCONTACTING SENSORS**

MARTIN W. EUSEPI
MECHANICAL TECHNOLOGY INCORPORATED
968 ALBANY-SHAKER ROAD
LATHAM, NEW YORK 12110

DTIC
ECTE
JUN 16 1980
D

November 1979

TECHNICAL REPORT AFAPL-TR-79-2076
Final Report for Period November 1977 to February 1979

Approved for public release; distribution unlimited

AIR FORCE AERO-PROPULSION LABORATORY
AIR FORCE WRIGHT AERONAUTICAL LABORATORIES
AIR FORCE SYSTEMS COMMAND
WRIGHT-PATTERSON AIR FORCE BASE, OHIO 45433

DDC FILE COPY


80 6 12 093

NOTICE

When Government drawings, specifications, or other data are used for any purpose other than in connection with a definitely related Government procurement operation, the United States Government thereby incurs no responsibility nor any obligation whatsoever; and the fact that the government may have formulated, furnished, or in any way supplied the said drawings, specifications, or other data, is not to be regarded by implication or otherwise as in any manner licensing the holder or any other person or corporation, or conveying any rights or permission to manufacture, use, or sell any patented invention that may in any way be related thereto.

This report has been reviewed by the Information Office, (ASD/OIP) and is releasable to the National Technical Information Service (NTIS). At NTIS, it will be available to the general public, including foreign nations.

This technical report has been reviewed and is approved for publication.

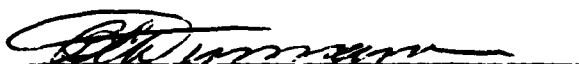


DR. JIM F. DILL
Project Engineer



HOWARD F. JONES
Chief, Lubrication Branch

FOR THE COMMANDER



BLACKWELL C. DUNNAM
Chief, Fuels and Lubrication Division

If your address has changed, if you wish to be removed from our mailing list, or if the addressee is no longer employed by your organization please notify AFAPL/SFL, WPAFB, OH 45433 to help us maintain a current mailing list.

Copies of this report should not be returned unless return is required by security considerations, contractual obligations, or notice on a specific document.

SECURITY CLASSIFICATION OF THIS PAGE (When Data Entered)

19 REPORT DOCUMENTATION PAGE		READ INSTRUCTIONS BEFORE COMPLETING FORM
1. REPORT NUMBER AFAPL TR-79-2876	2. GOVT ACCESSION NO. AD A085 740	3. RECIPIENT'S CATALOG NUMBER
4. TITLE (and Subtitle) THE DEVELOPMENT OF AN AUTOMATED ROLLER INSPECTION SYSTEM USING NONCONTACTING SENSORS.		5. TYPE OF REPORT & PERIOD COVERED Final Report - 11/77-2/79
7. AUTHOR(s) Martin W. Eusepi		6. PERFORMING ORG. REPORT NUMBER IMTI-79TR611
9. PERFORMING ORGANIZATION NAME AND ADDRESS Mechanical Technology Incorporated 968 Albany-Shaker Road Latham, New York 12110		8. CONTRACT OR GRANT NUMBER(s) F33615-77-C-3142
11. CONTROLLING OFFICE NAME AND ADDRESS Air Force Aero-Propulsion Laboratory Air Force Wright Aeronautical Laboratories Air Force Systems Command Wright-Patterson Air Force Base, Ohio 45433		10. PROGRAM ELEMENT, PROJECT, TASK AREA & WORK UNIT NUMBERS 12 189
14. MONITORING AGENCY NAME & ADDRESS (if different from Controlling Office) Final Rept. Nov 77 - Feb 79		12. REPORT DATE Nov 79
		13. NUMBER OF PAGES
		15. SECURITY CLASS. (of this report) Unclassified
		15a. DECLASSIFICATION/DOWNGRADING SCHEDULE
16. DISTRIBUTION STATEMENT (of this Report) Approved for Public Release; Distribution Unlimited		
17. DISTRIBUTION STATEMENT (of the abstract entered in Block 20, if different from Report)		
18. SUPPLEMENTARY NOTES		
19. KEY WORDS (Continue on reverse side if necessary and identify by block number) roller-bearings noncontacting measurements automated inspection high DN bearing rollers		
20. ABSTRACT (Continue on reverse side if necessary and identify by block number) An automated computer oriented inspection system for measuring the dimensional characteristics of high DN bearing rollers has been designed. The system is based on the use of non-contacting miniature capacitance probes having a sensitivity of 1000 volts/in. and a line scan camera employing photo diodes combined with an enlarging lens system to provide a 40×10^{-6} in./count sensitivity. The automated inspection system design is based on the results of a laboratory investigation of gaging techniques and the performance evaluation of non automated breadboard versions of the system.		

DD FORM 1 JAN 73 1473 EDITION OF 1 NOV 68 IS OBSOLETE

224550
SECURITY CLASSIFICATION OF THIS PAGE (When Data Entered)

TABLE OF CONTENTS

<u>Section</u>	<u>Page</u>
LIST OF ILLUSTRATIONS	vi
LIST OF TABLES	viii
I INTRODUCTION	1
II SUMMARY.	3
1. Laboratory Evaluation	3
2. Breadboard Gage Design	4
3. Breadboard Evaluation	4
4. Prototype Automatic Gage Design	4
III LABORATORY EVALUATION	5
1. Review of Measurement Requirements	5
2. Proximity Probe Evaluation	6
3. Optical Sensor System	32
4. Roller Support Evaluation	46
5. Summary of Laboratory Evaluation	56
IV DESIGN OF BREADBOARD GAGING MODULES	58
1. Capacitance Probe Design	60
2. Radial Measurement Gage	64
3. Axial Measurement Gage	70
4. Contour Measurement Gage	72
V BREADBOARD GAGE EVALUATION	82
1. Test Plan Summary	82
2. Radial/Axial Gage Module Evaluation	83
3. Contour Gage Module Evaluation.	104
VI PROTOTYPE AUTOMATIC GAGE DESIGN	115
1. Cost Effectiveness Study	115
2. Radial/Axial Gage Module	119
3. Contour Gage Module	127
4. Data Acquisition and Machine Control	136
5. Environmental Considerations	145
VII DISCUSSION AND RECOMMENDATIONS	146
REFERENCES	151
APPENDIX A - STATISTICAL EVALUATION OF COMPARABLE INSPECTION DATA	152

TABLE OF CONTENTS (Cont'd)

<u>Section</u>	<u>Page</u>
APPENDIX B - AUTOMATED ROLLER INSPECTION DEMONSTRATION TEST PLAN	160
APPENDIX C - CALCULATION OF ERROR FOR STANDARD CIRCULAR PROBE USED WITH A CYLINDRICAL SURFACE . . .	165
APPENDIX D - RADIAL AXIAL MODULE PROTOTYPE PARTS LIST. .	169
APPENDIX E - CONTOUR GAGE MODULE PROTOTYPE PARTS LIST. .	176

Accession For	
NTIS GRA&I	<input checked="" type="checkbox"/>
DDC TAB	<input type="checkbox"/>
Unannounced	
Justification	
By _____	
Distribution/	
Availability	
Dist	Available for
A	Special

LIST OF ILLUSTRATIONS

<u>Figure</u>	<u>Caption</u>	<u>Page</u>
1	Relative Locations of the Roller Characteristics to be Measured	8
2	Principle of Inductive Proximity Sensor (Eddy Current Type)	9
3	Depth of Penetration of Magnetic Field in Flat Surface Versus Frequency	11
4	Principle of Inductive Probe (Magnetic Reluctance Type). . .	12
5	Miniature Inductance Proximity Probe	14
6	Construction of a Typical Capacitive Sensing Probe	17
7	Effect of Fringe Guard Field Uniformity	19
8	Combined Tip and Fringe Guard Diameter Versus Probe	20
9	Special 0.0014 in. Range Probe Constructed for a Bearing Metrology Program	22
10	Proximity Probe Evaluation Set-up	23
11	Plan View of Line Scan Camera Evaluation Set-Up	34
12	Scan of 19.02mm Diameter Sphere (0.7488 in. dia)	40
13	Horizontal Scan on a 16mm Diameter Roller	41
14	Vertical Scan on a 16mm Diameter Roller	42
15	Results of Test Performed with 16mm Roller Target Oriented at 45° to Camera's Diode Array	44
16	Evaluation Roller Support	47
17	Capacitance Probe Assembly and Details	61
18	Breadboard Gage Module-Miniature Capacitance Probe	62
19	Radial/Axial Gage: Probe Location Diagram	63
20	Radial/Axial Gage Module: Radial Measurement Configuration. .	65
21	Minimum Probe Positioning for Breadboard Gages	67
22	Radial/Axial Breadboard Gage-Lever Systems	68
23	Radial/Axial Breadboard Gage Set-up for 7mm Roller	69
24	Radial/Axial Gage Module Radial Measurement Configuration .	71
25	Roller Positioning in Axial Gage Configuration	73
26	Contour Measuring Gage - Elevation View.	75
27	Contour Measuring Gage - Plan View	76
28	Roller Positions During Contour Measurements	78
29	Contour Gage Module.	80

LIST OF ILLUSTRATIONS

<u>Figure</u>	<u>Caption</u>	<u>Page</u>
30	Contour Gage Module - Gaging Fixture	81
31	Modified Radial/Axial Gage Module.	85
32	Drive Motor Installation; Radial/Axial Gage Module	86
33	Strip Chart - Roller Length Measurement; Repeatability Test	98
34	Modified Contour Gage Module	105
35	Contour Scan - 16mm Dia Roller	109
36	Contour Scan 7mm Roller.	110
37	Radial/Axial Module Automated Roller Inspection Prototype	120
38	Contour Gage Module.	128
39	Mathematical Curves for Roller Contour Calculations. . . .	139
40	Automated Roller Inspection System Block Diagram	140
41	System Chassis Configuration	144
42	Definition of Power of a Statistic Test Given a True Alternate Hypothesis H_1	155
43	Probe to Target Geometry	168

LIST OF TABLES

<u>Number</u>		<u>Page</u>
1	Main Shaft Bearing - Tolerance	7
2	Proximity Probe Used in Evaluation	24
3	Calibration Data CP-1 Capacitance Probe.	25
4	Calibration Data CP-1X Capacitance Probe	26
5	Calibration Data Eddy Current Probe.	27
6	Probe Calibration Least Square Fit	28
7	Probe Calibration Least Square Fit	29
8	Probe Calibration Least Square Fit	30
9	Proximity Probe Calibration Summary.	31
10	Line Scan Camera Evaluation - Test Data.	36
11	Selected Data for Three Point Circle Calculation	35
12	Line Scan Camera Evaluation - Curve Fit Data	38
13	Result of Contacting Probe Measurements.	50
14	Result of Non-Contacting Probe Measurements.	53
15	Roller Dimension Tolerance Gaging.	58
16	Probe Reading Combinations Necessary to Obtain Necessary Measurement Data.	63
17	Tabulated Results Axial/Radial Breadboard Gage Repeatability Evaluation.	90
18	Roller Outer Diameter Measurement Breadboard Gage Evaluation.	91
19	Crown Drop Breadboard Gage Evaluation.	94
20	Tabulated Results Axial/Radial Breadboard Gage Repeatability Evaluation.	100
21	Radial/Axial Roller Dimensions	102
22	Repeatability Evaluation Data Contour Gage Module.	107
23	Roller Contour Measurements.	112
24	Roller Corner Runout Measurements.	113
25	Roller Inspection Costs.	117
A1	Roller Characteristics to be Measured.	164

SECTION I

INTRODUCTION

As operating speeds of turbine engine bearings have increased (>2 million DN), manufacturing tolerances required for the production of reliable roller bearings have become increasingly tighter. At present, a stage has been reached where tolerances are such that their reliable measurement is difficult and often time consuming. There is a need for improvement in both the accuracy and speed of roller inspection techniques to insure both reliable and cost effective production. To satisfy this need, a technique is being developed which will allow automated, or at least semi-automated, inspection of rollers and, at the same time, increase the reliability and accuracy of the measurements being made.

Prior to the inception of the program reported herein, a state-of-the-art survey was conducted by others under Air Force Contract F33615-76-C-2147 to ascertain what precision measurement techniques and equipment were available. The objective of this program was to utilize the results of the survey as a basis for developing a design and constructing a breadboard model of an advanced roller inspection system employing non-contacting sensors. The final breadboard models have been shown to be capable of reliably measuring the tolerances presently required in roller inspection as well as the potential of meeting possible future tightening of these tolerances.

This program, aimed at the development of measuring techniques for automating the inspection of bearing rollers, consists of the following five tasks.

- Task I - Laboratory Evaluation

In this task the measurement sensors and roller support devices were evaluated to establish the best candidates for development into the full scale inspection system.

- Task II - Breadboard Design Development

Using the conclusions of the laboratory evaluation performed in Task I, a detailed design for a breadboard inspection system was developed in this task. This design was used for the construction of a breadboard system.

- Task III - Construction of Breadboard System

Using the detailed design approved in Task II, construction of a breadboard inspection system was the effort in Task III.

- Task IV - Breadboard Capability Demonstration

In this task, the capability of the breadboard system was demonstrated. The demonstration included testing which exhibited the precision, reliability and adaptability of the system to measuring rollers in sizes ranging from 5 mm to 25 mm. Tolerances comparable to those found in use for a high speed (>2.0 million DN) mainshaft bearing design at the time of the demonstration were used as criteria for evaluating the system capability.

- Task V - Prototype Design Specification

Upon completion of the testing of the breadboard inspection system, a design for a prototype inspection system for use in an actual shop environment was developed. This design included all the basic details necessary to construct a prototype system, but does not include actual final machine drawings from which such a system could be constructed. In the development of this prototype design, equal emphasis was given to the minimum production costs and the attainment of performance goals.

The results of this program indicated that a successful inspection system can be developed around non-contacting sensors and that automation to a degree commensurate with industry requirements can be designed.

SECTION II

SUMMARY

The work performed under this contract is described in this report and is broken down into the following four sections:

- Laboratory evaluation of sensors and gaging techniques
- Description of the breadboard gage design
- Evaluation of the breadboard gages
- Design of a prototype automatic gage system

1. Laboratory Evaluation

The laboratory evaluation of position sensors, fully described in the proximity probe evaluation section of this report, investigated both inductive and capacitance-type probes for possible use in an automatic roller gaging system. The conclusion derived from the probe study was that sufficient sensitivity, coupled with the small probe size, could only be met by the capacitance-type probe. The capacitance probe, providing a sensitivity of 1.335×10^{-3} inch/volt as compared to the inductive probe sensitivity of 2.056×10^{-2} inch/volt, also had a linearity nearly an order of magnitude better.

A second study performed during the laboratory evaluation was the investigation of an optical system suitable for making roller contour measurements. The optical sensor system section of this report describes the optical system selected for study, and demonstrates the acceptability of the line scan camera employing a linear array of miniature photo diodes as the primary sensor. This section also describes the lens system requirement necessary to make the camera sensitivity high enough to produce acceptable contour measurements. The evaluation results have a demonstrated sensitivity of 369×10^{-6} inch/count and show a simple method of increasing the sensitivity to 37×10^{-6} inch/count.

The last topic covered in the laboratory evaluation, a comparison of roller support fixtures directed toward the selection of the most suitable design for inclusion in an automated gage, is found in the roller support evaluation section of this report. Three support methods were examined and their use statistically evaluated. It was concluded from this study that a 90° "V" block was the most suitable.

2. Breadboard Gage Design

The pertinent information obtained during the laboratory evaluation was incorporated in the breadboard gage designs described in Section IV of this report. In the capacitance probe design section, the design of the actual capacitance probe to be used in the gages is described; the probe's overall diameter was established at 0.100 in., and had a sensitivity of 1600 volts/inch (6.25×10^{-4} inch/volt).

At the conclusion of the design phase, construction of the gages was initiated and with its completion, evaluation of the gages was begun. To assure stability of the gages, they were mounted on a large granite surface plate weighing 2000 lb. Subsections 2 through 4 of Section IV describe the various gage configurations.

3. Breadboard Evaluation

Each breadboard gage module was evaluated to determine whether it could, in fact, adequately inspect aircraft turbine engine quality bearing rollers. The evaluation was based on the approved test plan found in Appendix C. The initial subtask of the test plan required that a function check be made of the breadboard gages in which the performance of each module was evaluated with respect to roller handling and manipulation. Report subsections 1 and 2 of Section V describe the methods and results of the evaluation, with 1 providing the results of the functional evaluation and 2 the accuracy and repeatability checks of all the modules.

4. Prototype Automatic Gage Design

The successful completion of the breadboard evaluation permitted the design of a prototype automatic gage to proceed. A description of the prototype gage design is found in report section VI. Included as part of the prototype design was a cost-effectiveness evaluation of the inspection process to determine the extent of complexity which should be designed into the gage. The results of this study are found in subsection 1 of section VI. It is concluded that two separate gage modules, one for measuring size and one for measuring contour, would be most appropriate. The remainder of section VI describes the two modules and the electronics required to make them function.

SECTION III

LABORATORY EVALUATION

The initial task of this program was to perform a laboratory evaluation of several inspection techniques to determine which would be the best candidate for development into a full-scale inspection system. The evaluation of the candidate techniques leading to the final recommendation was made on the basis of the following criteria:

- System ability to reliably measure the necessary tolerances
- System ability to operate in a production environment
- System cost effectiveness when fully developed as compared to existing systems
- System ability to be automated to a level commensurate with expected production levels
- System adaptability to different roller sizes and configurations
- System required development and cost
- System ability to be operated and maintained by semi-skilled technicians.

The results of the laboratory evaluation will be a ranking of the investigated systems with regard to the list of criteria. The selected topics for evaluation will be:

- Proximity probes, inductive and capacitive
- Optical system employing a line scan camera
- Roller support method.

1. Review of Measurement Requirements

The current employment of very high-speed roller bearings demands the precise manufacturing of the bearing's rollers in order to minimize dynamic forces and avoid damage or even failure. To assure that finished rollers meet the precision demanded, an extensive roller inspection procedure has been established by bearing manufacturers. With the use of a variety of standard gaging systems, each roller is inspected to determine compliance with drawing requirements. With respect to a typical jet engine main shaft roller bearing, the fourteen

established dimensions and minimum tolerances are those listed in Table 1. Figure 1 illustrates the location of a roller to which each tolerance refers.

Several roller tolerances which are not specifically mentioned in Table 1 must be included in the measurement system design. As an example, the tolerances listed for the cylindrical portion of a roller include a complement diameter variation (0.000025 inch), a 2-point out of roundness (0.000010 inch), a cylindricity (0.000050 inch) and an OD taper (0.000010 inch). Nowhere is the actual diametral size tolerance mentioned. The importance of this exclusion lies in the design of proximity probes for measuring the roller diameter. These probes must provide a measurement accuracy of a few microinches with a range which must extend over the entire envelope of a particular roller nominal diameter tolerance.

The last two characteristics listed in Table 1 cannot be measured by means easily adapted for automation and are, therefore, left to be performed by current practice.

2. Proximity Probe Evaluation

Non-contacting displacement and vibration measurement is developing an increasingly wide range of applications beyond its perhaps traditional key usage by development and testing laboratories. As production gaging demands even greater throughput rates, inspection and classification equipment must be more maintenance-free and offer greater stability of calibration. Tip wear of contacting instrumentation may impose an intolerable situation in this regard along with the effect of the contact on the item being measured.

Several types of non-contacting position sensing instrument systems which may be considered suitable for the inspection system are available commercially. Descriptions of the more common types are presented in the following sections.

Proximity Probes: Inductive Type

- Eddy Current Proximity Probes - The principle of the inductive proximity sensor (eddy-current type) is shown in Figure 2. This

TABLE 1

Main Shaft Bearing - Tolerance

<u>Characteristic</u>	<u>Minimum Tolerance (Presently Known)</u>
Diameter	.000025" Variation/Complement .000010" 2-point O/R
Length	.0002" Variation/Complement
Crown Drop	.0001"
Crown Runout	.000050" FIR
End Parallel	.000050"
End Runout	.000050" FIR
Corner Breakout	.0005"
Corner Runout	.0005" FIR
Flat Length	.039"
Flat Centrality	.030" True Pos.
O.D. Taper	.000010"

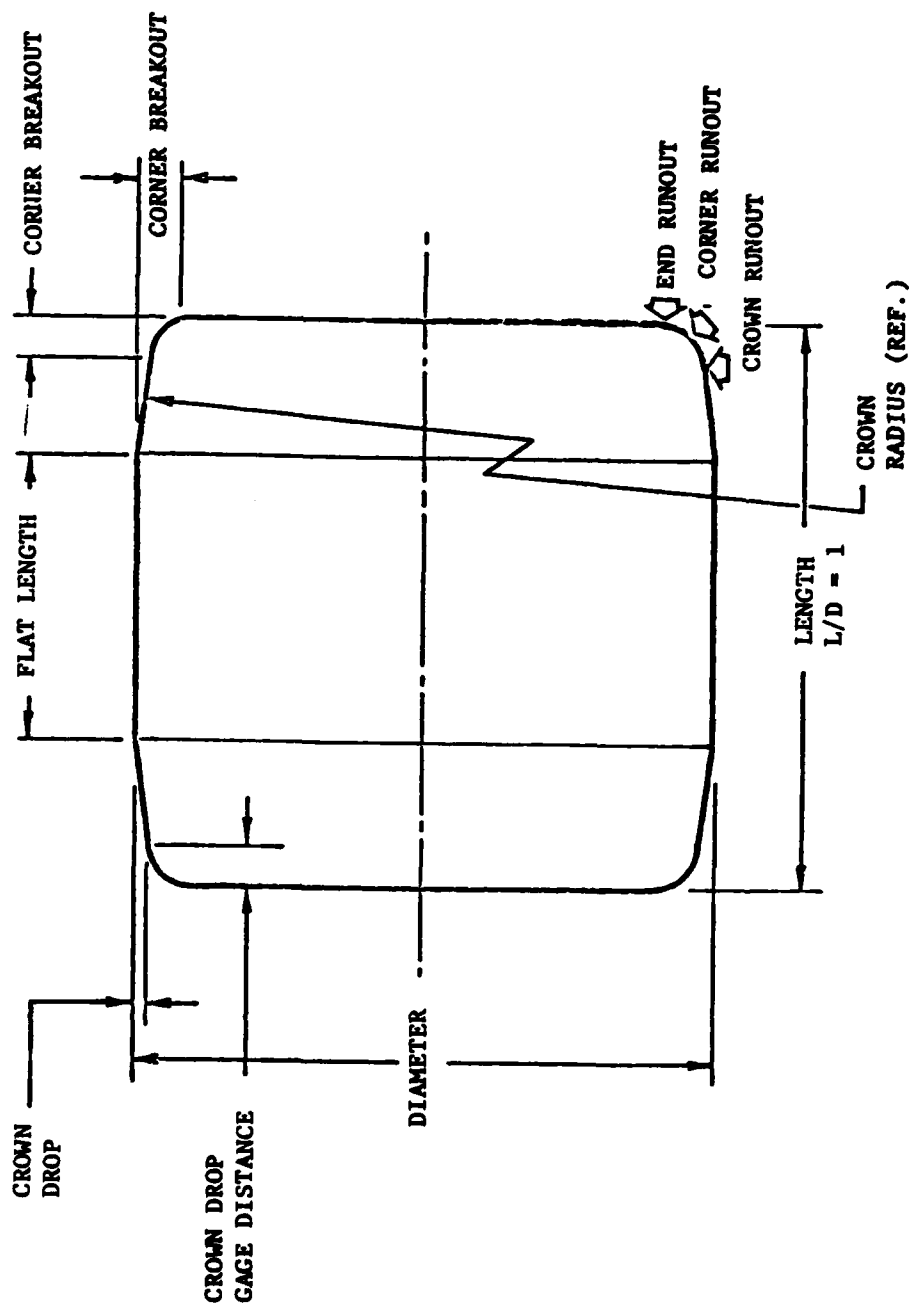


Fig.1 Relative Locations of the Roller Characteristics To be Measured

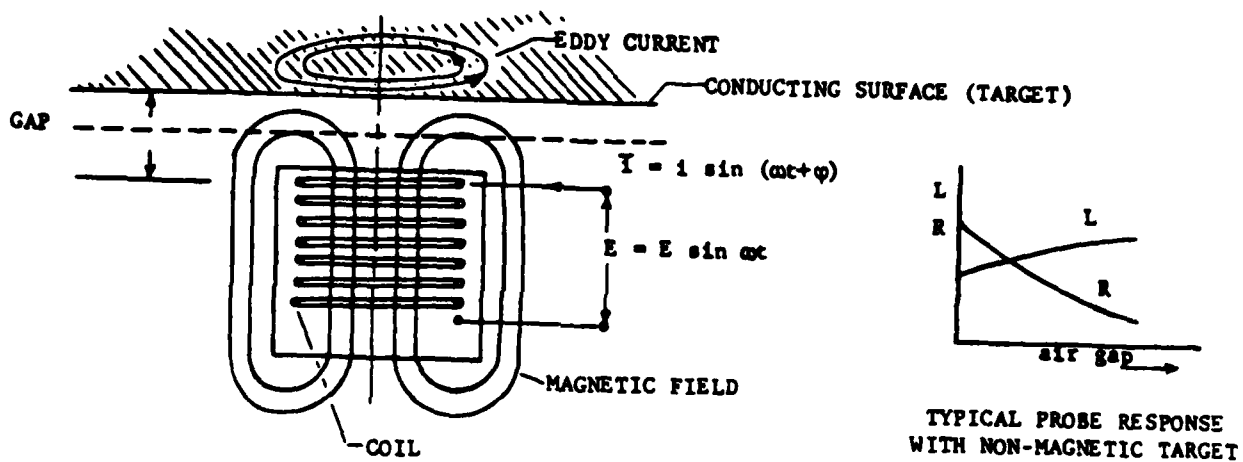


Fig. 2 Principle of Inductive Proximity Sensor
(Eddy Current Type)

792357

sensor consists of a coil powered with alternating current resulting in an alternating magnetic field around the probe. If a conducting (nonmagnetic) surface is brought near the coil, the relationship between \vec{E} and \vec{I} changes. This change is the result of alternating currents (eddy currents) generated in the target by the external field of the probe. The eddy currents, in turn, generate a magnetic field which opposes that of the coil.

The opposing effect of the eddy current's field causes the total field inside the target to become weaker with increasing distance from the surface. The depth at which the intensity is reduced about 60 percent below that on the surface is defined as the depth of penetration.

The effect of the target is to reduce the inductance (L) and to increase the AC series resistance (R).

Three factors which determine the depth of penetration are the electrical conductivity (ρ) and magnetic permeability (μ) of the target material and the frequency (f) of the AC field. These three factors are all of equal importance as is shown by the formulas and graphs in Figure 3.

At a given operating frequency, the depth of penetration can vary two decades between the nonmagnetic resistive material targets and magnetic targets. Figure 3 can be used as a guide in selecting a usable combination of target material, probe envelope material, and operating frequency.

- Magnetic-Reluctance Probe - The principle of this probe is illustrated in Figure 4. The field generated by the alternating current through the coil causes the generation of magnetic flux in the ferro-magnetic core. The flux density when a core is present may be approximately two to three decades higher than without a core.

The alternating current below the surface is:

$$I_x = I_0 e^{-\frac{x}{\delta}}$$

The total current is:

$$I_t = \int_0^\infty I_x dx = \delta I_0$$

I_0 = current at surface

x = distance below surface (.001 inch)

δ = depth of penetration (.001 inch)

$$\delta = 2 \times 10^3 \sqrt{\frac{\rho}{\pi f}} \quad (.001 \text{ inch})$$

ρ = resistivity (ohm)

μ = permeability (vacuum = 1)

f = frequency (Hz)

Note: Depth of penetration is by definition the distance in to the surface at which the current is down to 37% of that on the surface.

at $x = \delta$	$I = .371 I_0$
at $x = 2\delta$	$I = .135 I_0$
at $x = 3\delta$	$I = .05 I_0$
at $x = 4\delta$	$I = .018 I_0$

ρ (ohm)

10^{-5}

2000-5000*

Iron

Cu 1.7×10^{-4}

Al 2.8×10^{-4}

304SS 75×10^{-4}

Nichrome V 100×10^{-4}

Nipercor 27 19×10^{-4}

12 Cr Steel 60×10^{-4}

(416 SS)

Ag 95×10^{-4}

Mn (at 200°F) 10^{-5}

Mn (77°K) 4.1×10^{-5}

* Initial permeability = 200

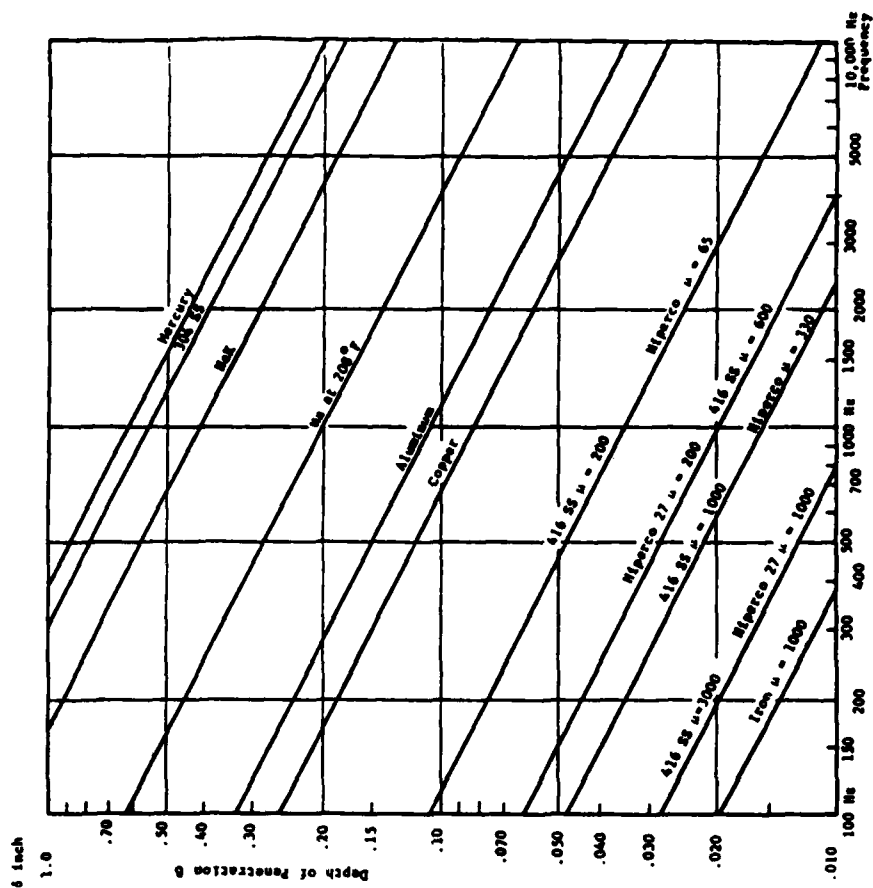


Fig. 3 Depth of Penetration of Magnetic Field in Flat Surface versus Frequency

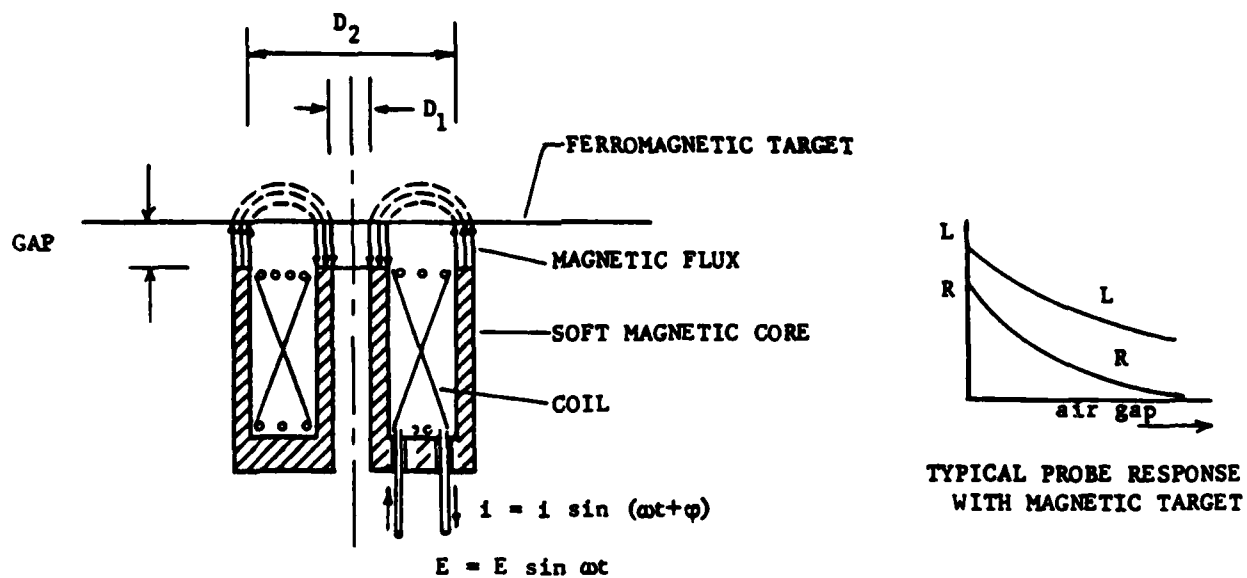


Fig. 4 Principle of Inductive Probe
(Magnetic Reluctance Type)

792363

The generated flux passes from the core through the air gap back into the core with the air gap constituting the major portion of the probe's magnetic reluctance. The typical increase in probe inductance when placing a ferro-magnetic target in contact with the probe is 50 to 100 percent.

The effect of a nonmagnetic target on this probe (Figure 4) is similar to that on the probe in Figure 2. That is, a non-magnetic target causes a decrease in inductance (L) and an increase in the AC series resistance of the probe with the core. When operated with a nonmagnetic target, the probe with a core is an eddy-current probe. When operated with a magnetic target, it is a magnetic-reluctance probe.

Miniaturization of the inductance probe presents no serious obstacle for its use. A photograph of a bi-directional eddy-current probe which was built by MTI as part of a servo positioning loop (shaft positioning) is shown in Figure 5.

A significant and overruling drawback for the use of inductive proximity probes is that, in all cases, their output is affected by subsurface material properties not related to the geometry of the target surface. A hardened steel roller will not be homogeneous enough from both a material and stress viewpoint to permit the inductive probe to deliver sufficiently accurate and sensitive low noise signals. For this reason, the use of inductive type probes is not expected to be satisfactory for use on the proposed inspection effort.

Proximity Probes: Capacitance Type

The electrical capacitance formed between a sensing probe and the test object (target) is used by the measuring electronic instrument to which the probe is connected as a measure of the probe-to-target displacement, based on the well-known relationship for the parallel-plate capacitor:

$$C = K \frac{A}{D}$$

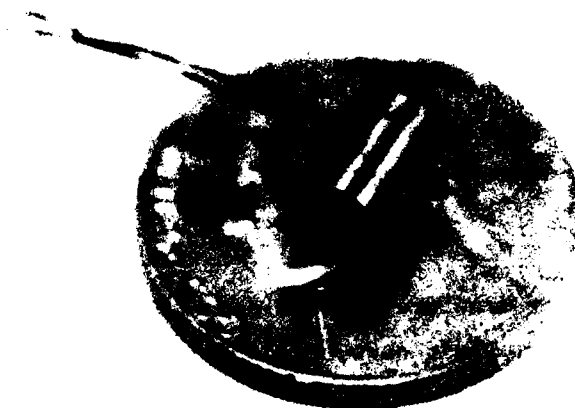


Fig. 5 Miniature Inductance Proximity Probe

where:

C = Capacitance

A = Area of plate

D = Distance between the (parallel) plates

K = Constant (dielectric constant of medium between the plates and proportionality factor for units of measurements).

The electronic instrument converts the change in capacitance into an appropriate analog signal which is available for display, recording or computation. If the target vibrates with respect to the probe, the corresponding change in capacitance can also be interpreted by an appropriate electronic instrument in terms of peak-to-peak vibration amplitude.

This capacitive method of non-contacting displacement and vibration measurement requires that the target material be electrically conductive. Also, the dielectric medium in the gap between the probe and the target must be of a dielectric constant which does not vary with time, temperature, or mechanical stress in order to maintain $K = \text{constant}$ in the basic equation.

A particularly useful feature of the capacitive method is that the measurement is unaffected by the presence of magnetic fields or by any transverse motion between probe and target. Thus the method is not limited to stationary or nonmagnetic targets.

Full-scale ranges of measurement typically lie between 1.0 mil (0.001 inch) and 0.5 inch. This displacement range is covered by a number of probes, each of which is designed to give full-scale output of the measuring instrument for the maximum design range of the probe (a probe-to-target capacitance of 0.35 pf at full scale). For example, a "10-mil probe" allows the electronics to give full output at a displacement of 10 mils; a "500-mil" probe gives full rated output at 500 mils.

When the probes are combined with appropriate electronics, the following can be used as a guide of typical capability:

- Measurements can be made over the range of one percent of full scale to 100 percent of full scale
- Resolution of one part in 50,000
- Accuracy is a direct function of calibration accuracy

Capacitance probes, of the type considered for the automated gaging system, are designed primarily for operation with the type of electronics in which the probe-to-target capacitance acts as the negative feed-back path around a high gain amplifier as in the Wayne Kerr System*.

Figure 6 illustrates construction of a typical capacitive sensing probe. For the majority of applications, cylindrical probe geometries are employed. However, in cases involving nonplanar targets, rectangular- and contoured-face plate geometries have been supplied in order to obtain a more optimum match of probe/target areas and greater field uniformity.

Probe length is relatively independent of range and is determined primarily by the constraints imposed by the mechanical fabrication and assembly of the probe parts, including the electrical coaxial cable connection.

The size of the measuring electrode "plate" (center element) of the probe-to-target capacitance can be very small for probes designed for high gain electronics like the Wayne Kerr since, at maximum probe displacement, the capacitance value is only 0.35 pico-farad; a very small value when compared to the value required in other methods of capacitive sensing. The area of the sensing tip establishes the capacitance of the probe for a given offset (probe gap). The smaller the tip size, the greater the sensitivity. The sensing tip, however, will integrate all the irregularities within its projected area to arrive at a nominal gap. In areas where a nonparallel condition exists, the probe will provide a dimension reading representative of the gap under its axial centerline.

*Wayne Kerr Co. Limited, Surrey, England

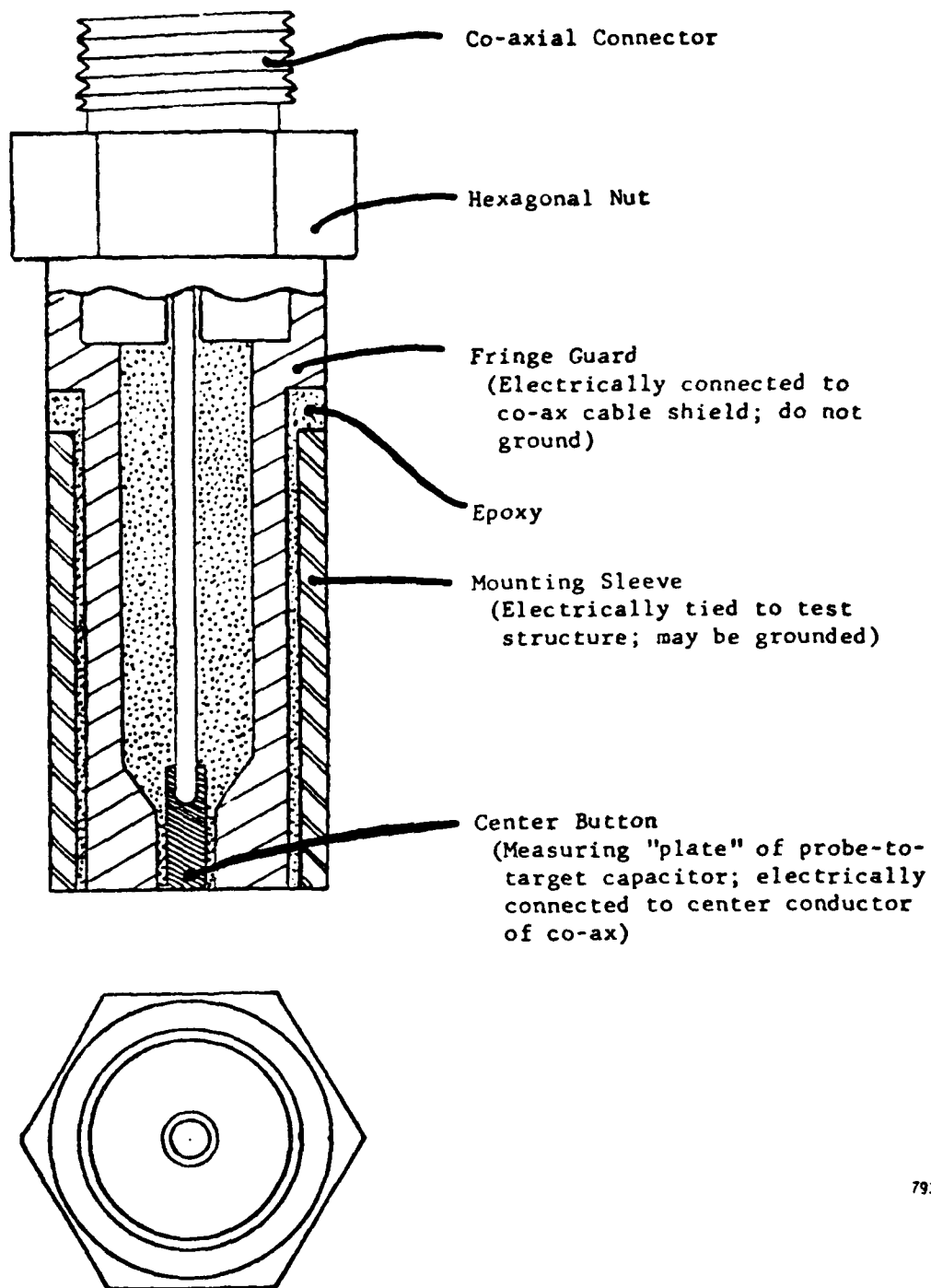


Fig. 6 Construction of a Typical Capacitive Sensing Probe

The center button diameter, however, is usually not the limiting consideration for minimum overall probe diameter. If the field between the probe center button and the target is to be uniform, a fringe guard must be designed to eliminate any fringing effects. As is illustrated in Figure 7, the function of the fringe guard is to keep the field under the center button uniform while allowing fringing only at the end of the fringe guard where its effect does not enter into the measurement. Fringe guard diameters, designed for use with the Wayne Kerr electronics, are known to hold linearity to within one percent over the operating range of the probe. The fringe guard is driven by the electronics so as to maintain a zero potential between it and the center button. The fringe guard, thereby, serves the dual function of neutralizing stray capacitance to the center conductor and of eliminating field fringing at the edge of the center button. The minimum combined sensing tip and fringe guard diameter as a function of probe sensitivity is shown in Figure 8.

The mounting sleeve, made of stainless steel like the other metallic parts of the probe, is required for mechanical support and integrity of the probe structure. It is normally connected electrically to ground potential along with the structure under test and the chassis of the electronics. Its wall thickness and, hence, its contribution to outside probe diameter depend only on mechanical considerations.

A design trade-off exists between probe range, linearity, and probe outside diameter. For a desired increase in range for a given probe, linearity will decrease, or, if linearity is to remain constant, the probe outer diameter must be increased. Conversely, probe outer diameter can be decreased if either (or both) range and linearity are reduced.

This trade-off situation has very practical significance in areas where minimum probe tip diameter is a critical requirement. For a given displacement range (sensitivity), a special probe could have a smaller than optimum fringe guard diameter; the resulting increase in nonlinearity can then be handled by calibrating the system and working with the resulting applicable calibration curve. Furthermore, linearity is also affected by departures in probe-to-target geometry from the case of the infinite coplanar target. If, for example, the probe face is not parallel to the target or if the target area

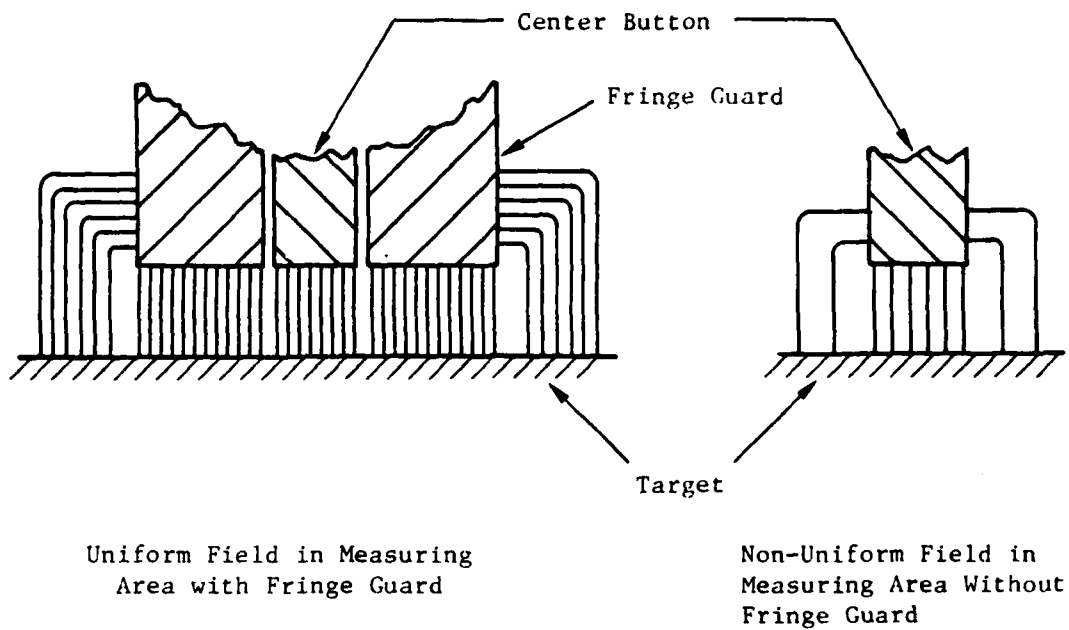


Fig. 7 Effect of Fringe Guard Field Uniformity

793063

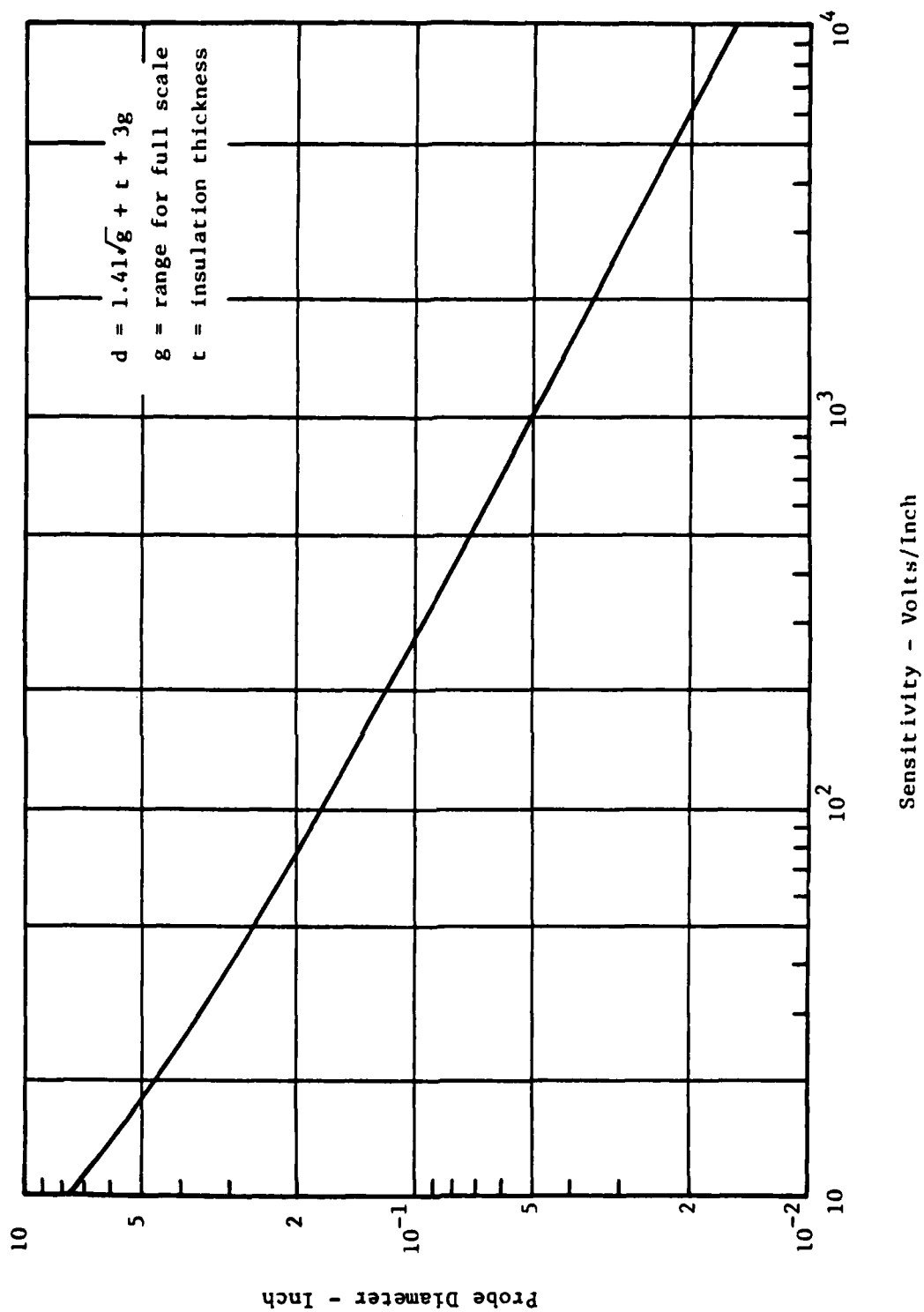


Fig. 3 Combined Tip and Fringe Guard Diameter Versus Probe Sensitivity

792361

is less than that given by the probe's fringe guard diameter, both measurement sensitivity and linearity suffer and special calibration may be required. Maintaining system linearity allows for direct readout and use of the convenient self-calibration feature of the Wayne Kerr electronics. However, in special cases, the user has the option by trading off linearity to modify system performance and obtain a better match for his application requirements. Special probe designs can be obtained to meet special requirements of range, linearity, and target geometry required for the automatic gaging system. Figure 9 shows a photograph of special 0.0014 in. range probe recently constructed for a bearing metrology program.

Proximity Probe Evaluation Results

Three non-contacting sensors were evaluated for sensitivity and linearity. The three sensors investigated were:

- A commercial capacitance probe, MTI's Boice Division Model CP-1 for use in the Wayne Kerr system
- A special purpose capacitance probe, CP-1X for use in the Wayne Kerr system, built under Air Force Contract F33615-77-C-3100. (Figure 9)
- A commercial eddy current probe, Bently Nevada Model 190F.

The capacitance probes designed for use with the Wayne-Kerr system were mounted in a fixture suitable for attachment to a precision micrometer. Figure 10 shows the set-up for this evaluation.

Three sets of calibration data for each probe, using the precision micrometer, were taken over at least the mid-80 percent of the probe range. Reduction of the calibration data shows the probes linearity and the actual sensitivity of the sensor.

As a complement to the capacitance proximity probe evaluation, a commercially available inductance proximity probe of the eddy current type was also evaluated. This evaluation was performed in parallel with that of the capacitance proximity probe and the results are directly comparable.

For reference the three probes studied had the dimensions listed in Table 2.

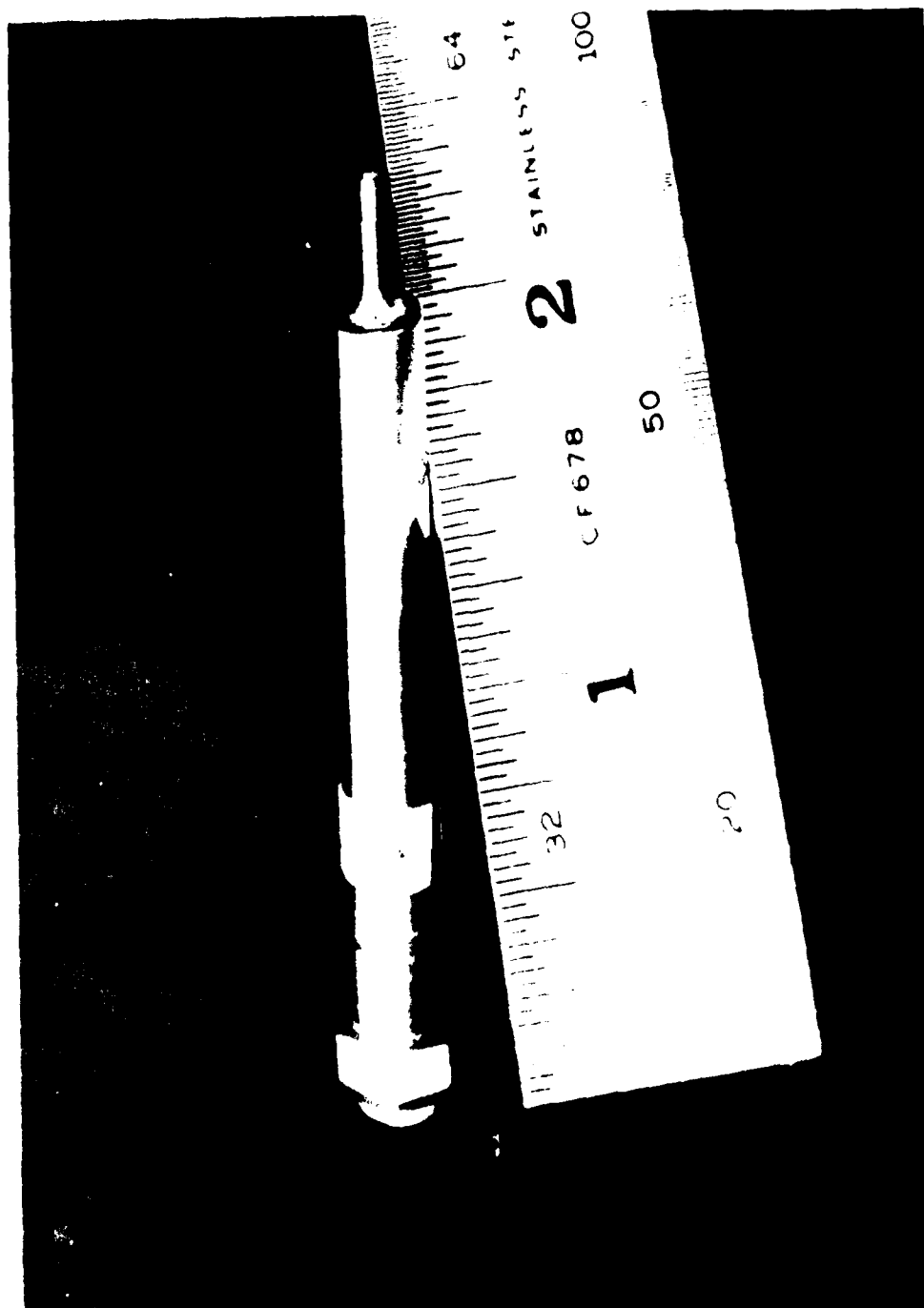


Fig. 9 Special 0.0014 in. Range Probe Constructed for a Bearing Metrology Program

MTI-17515

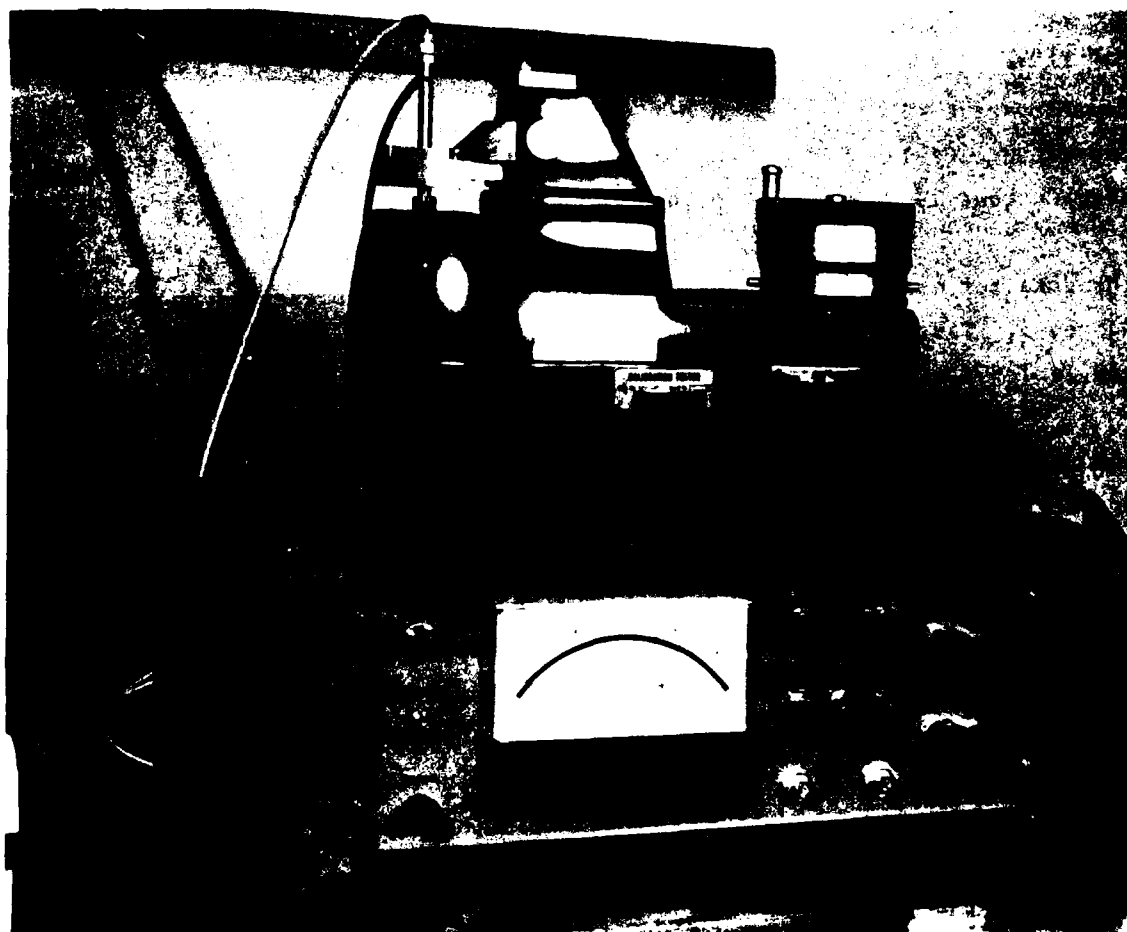


Fig. 10 Proximity Probe Evaluation Set-up

TABLE 2
Proximity Probe Used in Evaluation

<u>Probe</u>	<u>Sensing Tip Diameter</u>	<u>Secondary Shield Diameter</u>	<u>Overall Diameter</u>
Capacitance CP-1	0.041 in.	0.188	0.250
Capacitance CP-1X	0.051	0.063	0.250
Eddy Current 190F	0.190	---	0.250

The data for each of the three probe calibrations are presented in Tables 3, 4, and 5. Table 3 shows the CP-1 probe data, Table 4, the CP-1X probe data and Table 5, the eddy current probe data.

The resulting calibrations, based on both a linear and second order polynomial curve fit calculation, are shown in Tables 6, 7, and 8 and summarized in Table 9.

The calibration results show that sufficient sensitivity is available from either capacitance probe to successfully measure the roller characteristics listed on Table 1. As an example, the CP-1X capacitance probe showing a linear calibration sensitivity of 1.335×10^{-3} inch/volt, when installed in a system capable of discerning 1.0×10^{-4} volts, will register readings down to 1.335×10^{-7} inch; almost two orders of magnitude smaller than the minimum tolerance listed for high DN bearing rollers.

Conversely, the eddy current probe used with the same readout system would only register 2.056×10^{-6} inch, which is not sufficiently accurate for the precise measurement requirements mentioned previously.

In addition, the linearity of the capacitance probes is significantly better than the eddy current probe. This is evident by the lower dimensions listed in the "variation" columns for the capacitance probes, than for the eddy current probes (Tables 6, 7, and 8) (less than 10×10^{-6} in. as compared to approximately 100×10^{-6} in.).

TABLE 3

Calibration Data CP-1 Capacitance Probe

DISTANCE		AMPLITUDE		AMPLITUDE
RELATIVE	MEASURED	MEASURED	MEASURED	MEASURED
(INCHES)	(INCHES)	(VOLTS)	(VOLTS)	(VOLTS)
0.000000	0.000000	.2011	.2013	.2005
.000020	.000020	.2180	.2308	.2150
.000040	.000040	.2439	.2487	.2451
.000060	.000060	.2708	.2753	.2675
.000080	.000080	.2896	.3086	.2901
.000100	.000100	.3129	.3258	.3136
.000120	.000120	.3367	.3498	.3383
.000140	.000140	.3645	.3758	.3643
.000160	.000160	.3847	.3988	.3858
.000180	.000180	.4102	.4149	.4091
.000200	.000200	.4368	.4389	.4345
.000220	.000220	.4595	.4628	.4579
.000240	.000240	.4819	.4890	.4806
.000260	.000260	.5122	.5089	.5104
.000280	.000280	.5277	.5291	.5235
.000300	.000300	.5495	.5538	.5461
.000320	.000320	.5779	.5785	.5741
.000340	.000340	.6006	.6036	.5933
.000360	.000360	.6224	.6219	.6266
.000380	.000380	.6444	.6437	.6413
.000400	.000400	.6639	.6679	.6695
.000420	.000420	.6807	.6996	.6845
.000440	.000440	.7095	.7122	.7062
.000460	.000460	.7209	.7368	.7234
.000480	.000480	.7569	.7512	.7533
.000500	.000500	.7685	.7806	.7697
.000520	.000520	.7987	.7933	.7967
.000540	.000540	.8214	.8145	.8221
.000560	.000560	.8360	.8405	.8363
.000580	.000580	.8593	.8602	.8590
.000600	.000600	.8822	.8810	.8813

TABLE 4

Calibration Data CP-1X Capacitance Probe

DISTANCE		AMPLITUDE	AMPLITUDE	AMPLITUDE
RELATIVE	MEASURED	MEASURED	MEASURED	MEASURED
(INCHES)	(INCHES)	(VOLTS)	(VOLTS)	(VOLTS)
0.000000	0.000000	.8099	.8094	.8088
.000100	.000100	.7419	.7392	.7379
.000200	.000200	.6687	.6662	.6663
.000300	.000300	.5967	.5940	.5949
.000400	.000400	.5237	.5203	.5213
.000500	.000500	.4498	.4466	.4470
.000600	.000600	.3747	.3699	.3724
.000700	.000700	.2968	.2931	.2948
.000800	.000800	.2180	.2151	.2157
.000900	.000900	.1356	.1309	.1328

TABLE 5

Calibration Data Eddy Current Probe

DISTANCE		AMPLITUDE	AMPLITUDE	AMPLITUDE
RELATIVE	MEASURED	MEASURED	MEASURED	MEASURED
(INCHES)	(INCHES)	(VOLTS)	(VOLTS)	(VOLTS)
0.000000	.160000	7.902	7.908	7.905
.001000	.161000	7.949	7.954	7.951
.002000	.162000	7.996	8.005	7.997
.003000	.163000	8.042	8.046	8.043
.004000	.164000	8.088	8.093	8.090
.005000	.165000	8.135	8.140	8.136
.006000	.166000	8.180	8.186	8.183
.007000	.167000	8.228	8.233	8.231
.008000	.168000	8.276	8.280	8.277
.009000	.169000	8.322	8.328	8.324
.010000	.170000	8.370	8.374	8.371

TABLE 6

Probe Calibration Least Square FitPN0032CDC 6600CP-1 Capacitance Probe-Average

STATIC CALIBRATION RESULTS			.000878 INCHES/VOLT	
DISTANCE		AMPLITUDE	VARIATION	
RELATIVE (INCHES)	MEASURED (INCHES)	MEASURED (VOLTS)	MEASURED-FITTED (VOLTS)	(INCHES)
0.000000	0.000000	.2010	-.00534	.000005
.000020	.000020	.2213	-.00782	.000007
.000040	.000040	.2459	-.00599	.000005
.000060	.000060	.2712	-.00346	.000003
.000080	.000080	.2941	-.00134	.000001
.000100	.000100	.3174	-.00281	.000002
.000120	.000120	.3413	-.00169	.000001
.000140	.000140	.3682	.00244	-.000002
.000160	.000160	.3898	.00127	-.000001
.000180	.000180	.4114	.00009	-.000000
.000200	.000200	.4367	.00262	-.000002
.000220	.000220	.4601	.00324	-.000003
.000240	.000240	.4838	.00417	-.000004
.000260	.000260	.5105	.00810	-.000007
.000280	.000280	.5268	.00162	-.000001
.000300	.000300	.5498	.00185	-.000002
.000320	.000320	.5768	.00607	-.000005
.000340	.000340	.5992	.00570	-.000005
.000360	.000360	.6236	.00733	-.000006
.000380	.000380	.6431	.00405	-.000004
.000400	.000400	.6671	.00528	-.000005
.000420	.000420	.6883	.00370	-.000003
.000440	.000440	.7093	.00193	-.000002
.000460	.000460	.7270	-.00314	.000003
.000480	.000480	.7538	.00088	-.000001
.000500	.000500	.7729	-.00279	.000002
.000520	.000520	.7962	-.00226	.000002
.000540	.000540	.8193	-.00194	.000002
.000560	.000560	.8376	-.00641	.000006
.000580	.000580	.8595	-.00729	.000006
.000600	.000600	.8815	-.00806	.000007

CALIBRATION RESULTS .000878 INCHES/VOLT
 VARIATION + OR - .000067

EQUATION OF CURVE

X = DISTANCE
 Y = VOLTAGE

$$Y = -.000156 + .000771 X + .000098 X^2$$

TABLE 7

Probe Calibration

Least Square Fit

PN0032

CDC 6600

CP-1X Capacitance Probe-Average

STATIC CALIBRATION RESULTS -.001336 INCHES/VOLT

DISTANCE		AMPLITUDE		VARIATION	
RELATIVE	MEASURED	MEASURED	MEASURED	MEASURED-FITTED	
(INCHES)	(INCHES)	(VOLTS)	(VOLTS)	(INCHES)	
0.000000	0.000000	.8094	-.00718	-.000010	
.000100	.000100	.7393	-.00242	-.000003	
.000200	.000200	.6671	.00024	.000000	
.000300	.000300	.5952	.00319	.000004	
.000400	.000400	.5218	.00465	.000006	
.000500	.000500	.4478	.00551	.000007	
.000600	.000600	.3723	.00487	.000006	
.000700	.000700	.2949	.00232	.000003	
.000800	.000800	.2163	-.00142	-.000002	
.000900	.000900	.1331	-.00976	-.000013	

CALIBRATION RESULTS -.001335 INCHES/VOLT
VARIATION + OR - .000108

EQUATION OF CURVE

X = DISTANCE
Y = VOLTAGE

$$X = .001062 + -.001184 Y + -.000159 Y^2$$

DISTANCE		AMPLITUDE		SLOPE	
(INCHES)	(VOLTS)	(INCHES/VOLT)	NORMALIZED		
0.000000	.8094	-.001442	1.080922		
.000100	.7393	-.001420	1.064067		
.000200	.6671	-.001397	1.046810		
.000300	.5952	-.001374	1.029625		
.000400	.5218	-.001351	1.012082		
.000500	.4478	-.001327	.994395		
.000600	.3723	-.001303	.976350		
.000700	.2949	-.001278	.957850		
.000800	.2163	-.001253	.939064		
.000900	.1331	-.001227	.919178		

TABLE 8

Probe Calibration

Least Square Fit

PN0032

CDC 6600

Eddy Current Probe-Averages

STATIC CALIBRATION RESULTS		.020739 INCHES/VOLT		
RELATIVE (INCHES)	DISTANCE MEASURED (INCHES)	AMPLITUDE MEASURED (VOLTS)	VARIATION MEASURED-FITTED (VOLTS)	(INCHES)
0.000000	0.000000	7.9050	.01455	-.000302
.001000	.001000	7.9510	.01233	-.000256
.002000	.002000	7.9360	-.05089	.001055
.003000	.003000	8.0440	.00889	-.000184
.004000	.004000	8.0900	.00667	-.000138
.005000	.005000	8.1370	.00545	-.000113
.006000	.006000	8.1830	.00324	-.000067
.007000	.007000	8.2310	.00302	-.000063
.008000	.008000	8.2780	.00180	-.000037
.009000	.009000	8.3200	-.00442	.000092
.010000	.010000	8.3720	-.00064	.000013

CALIBRATION RESULTS .020556 INCHES/VOLT
VARIATION * OR * .001859

EQUATION OF CURVE

X = DISTANCE
Y = VOLTAGE

$$X = .101354 + -.044222 Y + .003980 Y^2$$

DISTANCE (INCHES)	AMPLITUDE (VOLTS)	SLOPE (INCHES/VOLT)	NORMALIZED
0.000000	7.9050	.018697	.909585
.001000	7.9510	.019063	.927397
.002000	7.9360	.018944	.921589
.003000	8.0440	.019803	.963408
.004000	8.0900	.020170	.981220
.005000	8.1370	.020544	.999419
.006000	8.1830	.020910	1.017231
.007000	8.2310	.021292	1.035817
.008000	8.2780	.021666	1.054016
.009000	8.3200	.022000	1.070279
.010000	8.3720	.022414	1.090415

8 in./volt
0 in./volt
0 in./volt

[illegible][illegible]

TABLE 9	
Probe Calibration Summary	
Linear Fit	
0.000878 in./vol	
0.001335 in./vol	
0.020556 in./vol	

Pro
Sensit
001
0014
225

Type	Identification
Capacitance	CP-I
Capacitance	CP-IX
Y Current	190F

Proximity Probe Calibration Summary			
Type	Identification	Nominal Sensitivity	Linear Fit
Capacitance	CP-1	0.001 in./volt	0.000878 in./volt
Capacitance	CP-1X	0.0014 in./volt	0.001335 in./volt
Eddy Current	190F	0.025 in./volt	0.020556 in./volt

A particularly useful feature of the capacitive method is that the measurement is unaffected by the presence of magnetic fields or by any transverse motion between probe and target. Thus the method is not limited to stationary or nonmagnetic targets.

Based on the calibration results and other features previously discussed, the capacitance probe was selected for use on this program.

3. Optical Sensor System

Optical means for obtaining dimensional data have been an accepted part of gage room procedures for a considerable length of time. The significant drawback for using optics as a measuring technique is that the usual optical inspection systems require visual observation for measurement interpretation.

An automated inspection system cannot rely on visual interpretation but must depend on some type of optical-electrical signal conversion for data interpretation. Commercially available optical measurement systems which include the use of photo sensitive detectors provide sufficient sensitivity combined with adequate data retrieval capability to make them suitable for automated inspection systems. The actual incorporation of such a system hinges on the ability to interface the many subsystem components into a viable cost-effective inspection tool.

The optical system which was selected for use in this program is a line-scan camera combined with a scanning slide, a magnifying lens system, and an illuminator.

The illuminator which provides the gaging light that is most applicable to roller measurement is the spot illuminator which provides a source of light for back illumination of selected portions of the roller contour. Back illumination is a desirable technique where size or position is to be measured and clear edges exist. The shadow-type object provides good contrast and eliminates any problems associated with surface reflectance variations. A typical spot illuminator usually consists of a quartz iodine lamp with a built-in reflector. The lamp is normally used in a reduced voltage mode which

significantly increases the life of the lamp. A small vane axial fan, usually included, is mounted at the rear of the lamp to provide cooling.

The lens system associated with the complete optical measuring system would include an imaging lens, required to focus the desired information on the photodiode array, and a collimating lens for providing a parallel ray light beam. The lens systems were commercially available and provided no procurement difficulties.

Line Scan Camera

In this phase of the laboratory investigation the suitability of using a line scan camera for measuring roller contours was evaluated. The ability of the line scan camera to make contour measurements depends on several qualities, including:

- Adequate sensitivity and reliability
- Ability to be automated
- Reasonable cost relative to present techniques

An experimental program utilizing a commercial line scan camera was initiated in order to establish actual sensitivity and repeatability of this measurement device.

The line scan camera employed for these studies was a Reticon* Model LC1004. This camera is normally used for taking non-contacting measurements in automatic inspection machinery**.

The sensing portion of the line scan camera consists of an array of high resolution solid state image sensors designed specifically for facsimile and related applications. The monolithic silicon*integrated circuits contain a row of 1728 photodiodes, 16 μ m wide, located on 15 μ m centers, together with shift register scanning circuits for sequential readout.

*Reticon, 910 Senicia Ave., Sunnyvale, California 94033

**Reticon, Model RS833 Roller Inspection System

The line scan camera is used in conjunction with an RS600 series controller, which is designed to interface with a line scan camera to provide a complete non-contact measurement or inspection system. Through a connecting cable, the controller supplies power to the camera and accepts the camera output for processing and display. The controller gives an indication that the light level is adequate, provides for pattern selection within the camera field of view which is to be measured and give both a digital display of the measurement and a corresponding BCD output for further processing. The light source for the line scan camera includes a quartz-iodide lamp, a lamp cooling fan and collimating lens; when installed with an autotransformer in the lamp circuit, an adjustable intensity light beam 1-1/2 inches in diameter is provided.

For the laboratory demonstration the camera was set up in a clean area, as illustrated in Figure 11.

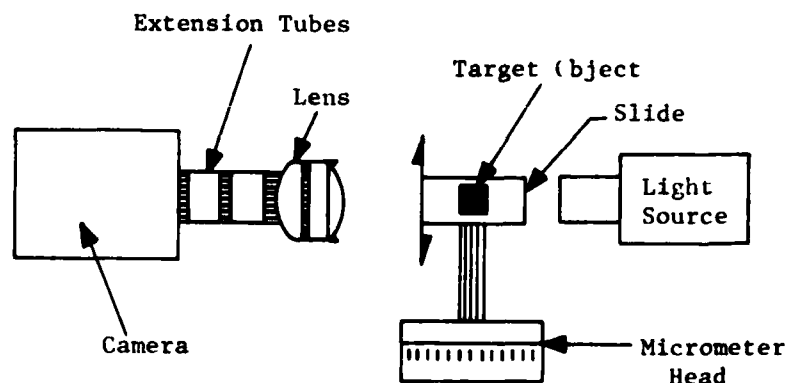


Fig. 11 Plan View of Line Scan Camera Evaluation Set-Up

This set-up was the simplest arrangement for quickly determining the camera's ability to measure contour precisely. Specifically, the camera was installed with a 50 mm 1.8 f lens on a 68 mm extension tube, so that its diode array was perpendicular to the motion direction of the micrometer. The lens was set back 2.2 inches from the target mid-plane, thereby providing a total calculated magnification factor of 9.375 μ per diode count.

Line Scan Camera Evaluation Results

For initial evaluation purposes, a 3/4-inch diameter ball bearing ball was positioned on the micrometer slide in the line scan camera field of view. At 250 μ increments, as measured at the micrometer head, the number of dark camera elements was recorded. These data are shown in Table 10. To obtain the actual vertical dimension sensed by the diodes, the diode count is multiplied by the magnification factor.

From these data, two calculations were made to determine the measured contour's match to the circular shadow cast by the sphere. Both calculations use the basic equation of a circle with its center at some arbitrary location given as:

$$R^2 = (x-a)^2 + (y-b)^2$$

The first calculation was performed by selecting three data points and then by substitution, solving a set of three simultaneous equations for a, b and R. The selected points are shown in Table 11 and includes the conversion from diode reading to linear dimension.

TABLE 11

Selected Data for Three Point Circle Calculation

<u>Point No.</u>	<u>x Micrometer (Microns)</u>	<u>y Diode Count</u>	<u>y Diode (Microns)</u>
1	5,000	1,260	11,812
2	9,000	1,390	13,031
3	13,000	1,331	12,478

Calculated results show that:

$$a = 9.720 \text{ mm}$$

$$b = 3.495 \text{ mm}$$

$$R = 9.563 \text{ mm}$$

TABLE 10

Line Scan Camera Evaluation - Test Data

Camera S/N: LC100U1728/300-77244

Target: .7488 in. Dia Sphere

Micrometer: Brown and Sharp

Extension Tube: 68mm

Lens: 50mm 1:1.8

MICROMETER SETTING	DIODE READING	MICROMETER SETTING	DIODE READING
0	0	9750	1393
250	299	10000	1392
500	552	10250	1391
750	716	10500	1389
1000	788	10750	1387
1250	843	11000	1384
1500	892	11250	1380
1750	934	11500	1375
2000	937	11750	1370
2250	1008	12000	1363
2500	1041	12250	1356
2750	1070	12500	1350
3000	1098	12750	1340
3250	1124	13000	1331
3500	1147	13250	1320
3750	1168	13500	1310
4000	1189	13750	1298
4250	1208	14000	1285
4500	1227	14250	1271
4750	1244	14500	1256
5000	1260	14750	1239
5250	1274	15000	1222
5500	1288	15250	1204
5750	1301	15500	1183
6000	1313	15750	1162
6250	1324	16000	1139
6500	1334	16250	1115
6750	1343	16500	1089
7000	1351	16750	1062
7250	1360	17000	1030
7500	1365	17250	997
7750	1371	17500	961
8000	1376	17750	921
8250	1381	18000	877
8500	1384	18250	827
8750	1388	18500	771
9000	1390	18750	651
9250	1392	19000	468
9500	1393	19250	59
		19500	0

A second calculation, employing all the data points from a micrometer reading of 3000 μ through 15,000 μ , was performed using a least square circle fit computer program. From this calculation, the three constants were calculated to be:

$$a = 9.717 \text{ mm}$$

$$b = 3.535 \text{ mm}$$

$$R = 9.525 \text{ mm}$$

Each set of constants was then used to calculate values of the y dimension, based on the micrometer reading. Table 12 shows the test data and the results of all the calculations.

The target radius determined by the least square circle fit to the experimental data was:

$$R = 9.525 \text{ mm}$$

The actual target radius was:

$$R = 9.510 \text{ mm}$$

Indicating the actual system magnification was:

$$M = 9.375 \text{ } \mu/\text{count} \times \frac{9.510}{9.525}$$

$$M = 9.360 \text{ } \mu/\text{count}$$

The radius calculated for the three point fit was slightly larger than that calculated from the least square fit and deviates somewhat more from the measured sphere diameter.

Deviations of the multipoint test data from a least square fit circle show a mean value of $0.094 \times 10^{-6} \text{ m}$ with a standard deviation of $5.05 \times 10^{-6} \text{ m}$. A mean deviation value of $-1.92 \times 10^{-6} \text{ m}$ with a standard deviation of $6.41 \times 10^{-6} \text{ m}$ was obtained for the 3 point fit. The correlation between the test and calculated data points is sufficient to state that over an angular extent of at least $\pm 60^\circ$, when measured from the diode array axis, the camera scan output does plot a true circle.

TABLE 12

Line Scan Camera Evaluation - Curve Fit Data

"x" Dimension 10 ⁻⁶ m	"y" Dimension 10 ⁻⁶ m	"y" Dimension 3 Point Calc. 10 ⁻⁶ m	Y Dimension Least Square 10 ⁻⁶ m	X Dimension 10 ⁻⁶ m	Y Dimension 10 ⁻⁶ m	Y Dimension 3 Point Calc. 10 ⁻⁶ m	Y Dimension Least Square 10 ⁻⁶ m
3,000	10,294	10,300	10,289	11,250	12,938		12,936
3,250	10,538		10,528	11,500	12,891		12,892
3,500	10,753		10,752	11,750	12,844		12,841
3,753	10,950		10,960	12,000	12,778	12,782	12,782
4,000	11,147	11,159	11,154	12,250	12,712		12,717
4,250	11,325		11,355	12,500	12,656		12,644
4,500	11,503		11,504	12,750	12,562		12,564
4,750	11,662		11,633	13,000	12,478	12,478	12,476
5,000	11,812	11,825	11,810	13,250	12,375		12,381
5,250	11,935		11,948	13,500	12,281		12,277
5,500	12,075		12,076	13,750	12,169		12,164
5,750	12,197		12,195	14,000	12,047	12,047	12,043
6,000	12,309	12,305	12,305	14,250	11,916		11,912
6,250	12,412		12,407	14,500	11,775		11,772
6,500	12,506		12,501	14,750	11,616		11,622
6,750	12,591		12,586	15,000	11,456	11,468	11,461
7,000	12,666	12,663	12,664				
7,250	12,750		12,735				
7,500	12,797		12,800				
7,750	12,853		12,855				
8,000	12,900	12,902	12,904				
8,250	12,947		12,947				
8,500	12,975		12,982				
8,750	13,012		13,011				
9,000	13,031	13,031	13,033				
9,250	13,050		13,049				
9,500	13,059		13,058				
9,750	13,059		13,060				
10,000	13,050	13,054	13,056				
10,250	13,041		13,045				
10,500	13,022		13,028				
10,750	13,003		13,004				
11,000	12,975	12,972	12,973				

A graph showing the spherical test data is presented in Figure 12. Two areas of related measurement uncertainty exist. Upon examination of the test data, these are:

1. The actual axial dimension "zero" position; the circle center is located beyond the calculated radius.
2. The contour data close to the 90° before or after top dead center is inaccurate.

These uncertainties can be attributed to the following reasons.

At the magnification employed during these tests, the apparent camera aperture (width of target seen by the diode array) was $9.375 \mu\text{m}$ (369×10^{-6} inch).

If the angle at which the target shadow crosses the diode array, as measured from the diode array axis, is large, then good resolution is obtained since the switching of diodes will occur after large translations of the target. If the target angle is small or approaches zero, however, an uncertainty of at least the aperture width will occur. Examples of both these situations are seen on Figure 12 and from the results of the scan taken of an actual 16 mm roller from a high DN roller bearing, shown in Figures 13 and 14.

Figures 13 and 14 show the results of a scan taken with the roller parallel to the micrometer axis and perpendicular to the camera diode array axis. The locations on this figure, indicated by the asterisks, are where a one (1) diode count change was registered. The scan data for the crown portion of the roller would, therefore, be a series of steps followed by lengths of uniform diameter data. The true contour would be defined by the axial coordinate of the step location and the radius of the mean value of the step height. This technique would only use a small number of the data points obtained and would not be a satisfactory method of establishing contour dimensions. The corner breakout location presents a different problem with regard to its definition.

According to detailed roller drawing dimensions, the corner and crown of rollers are true circles which intersect at the corner breakout location. It is obvious from the roller measurement data on Figures 13 and 14 that the corner is not circular but some other curve shape possibly resulting from the

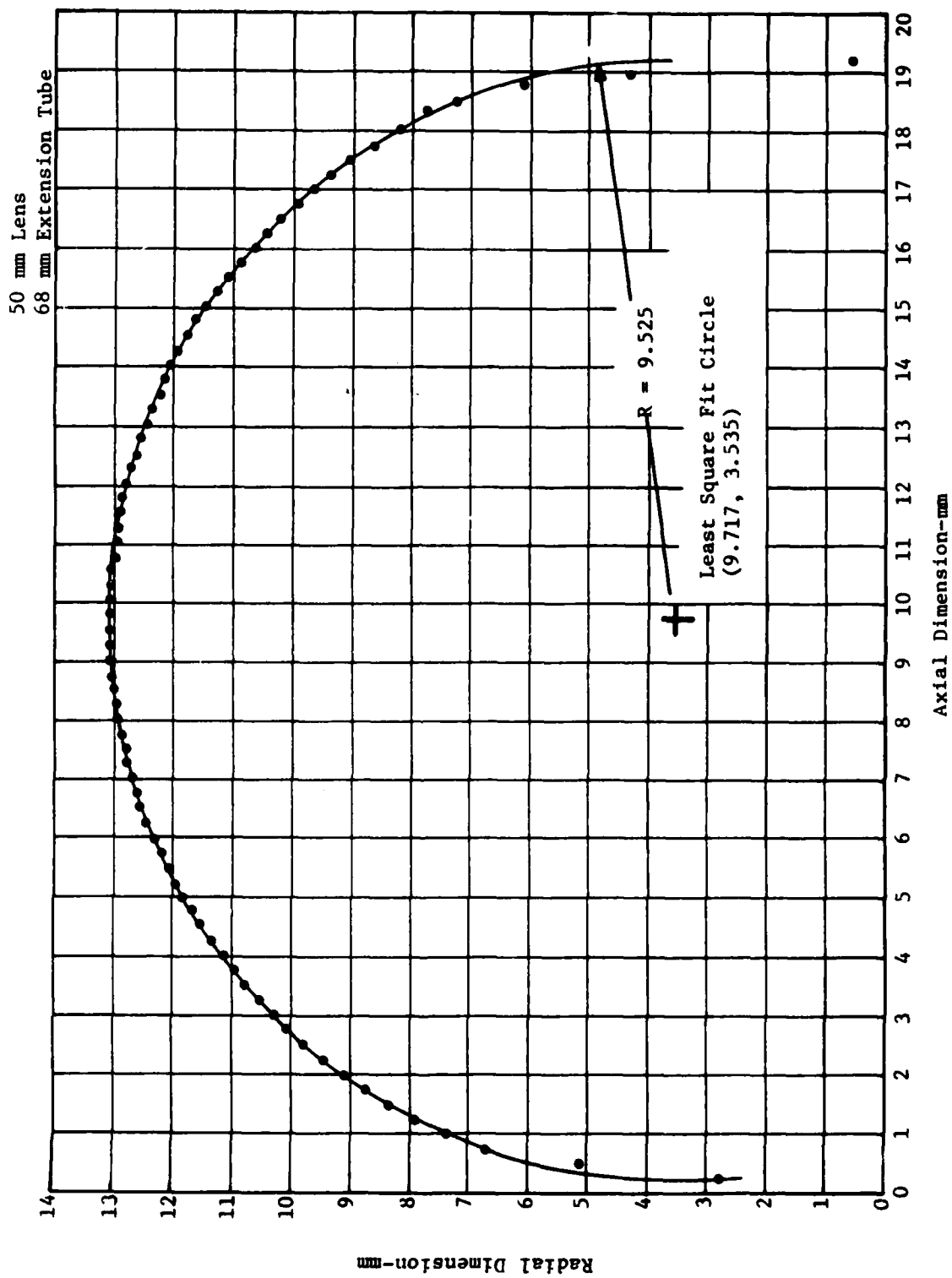


Fig. 12 Scan of 19.02 mm Diameter Sphere (0.7488 in. dia)

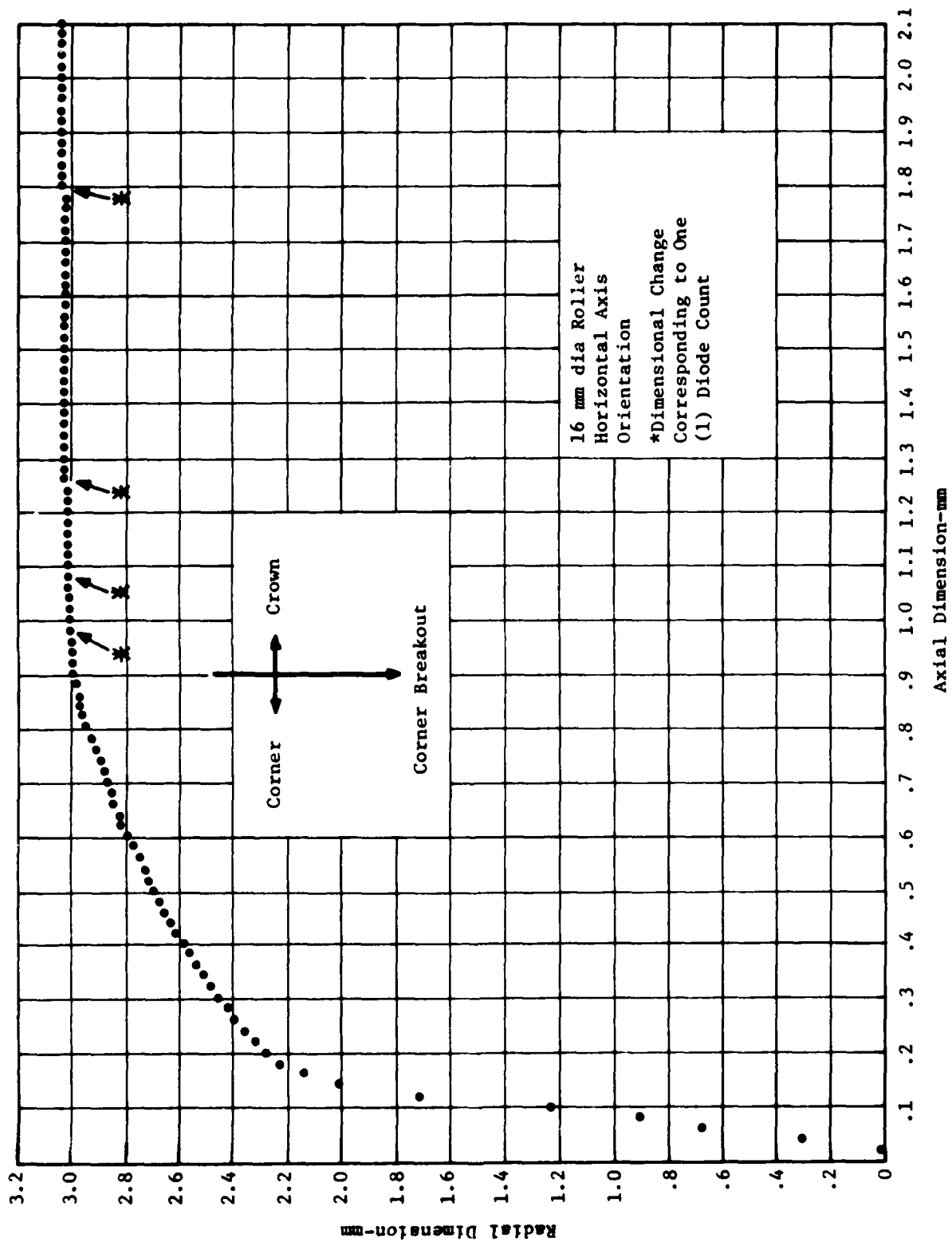


Fig. 13 Horizontal Scan on a 16 mm Diameter Roller

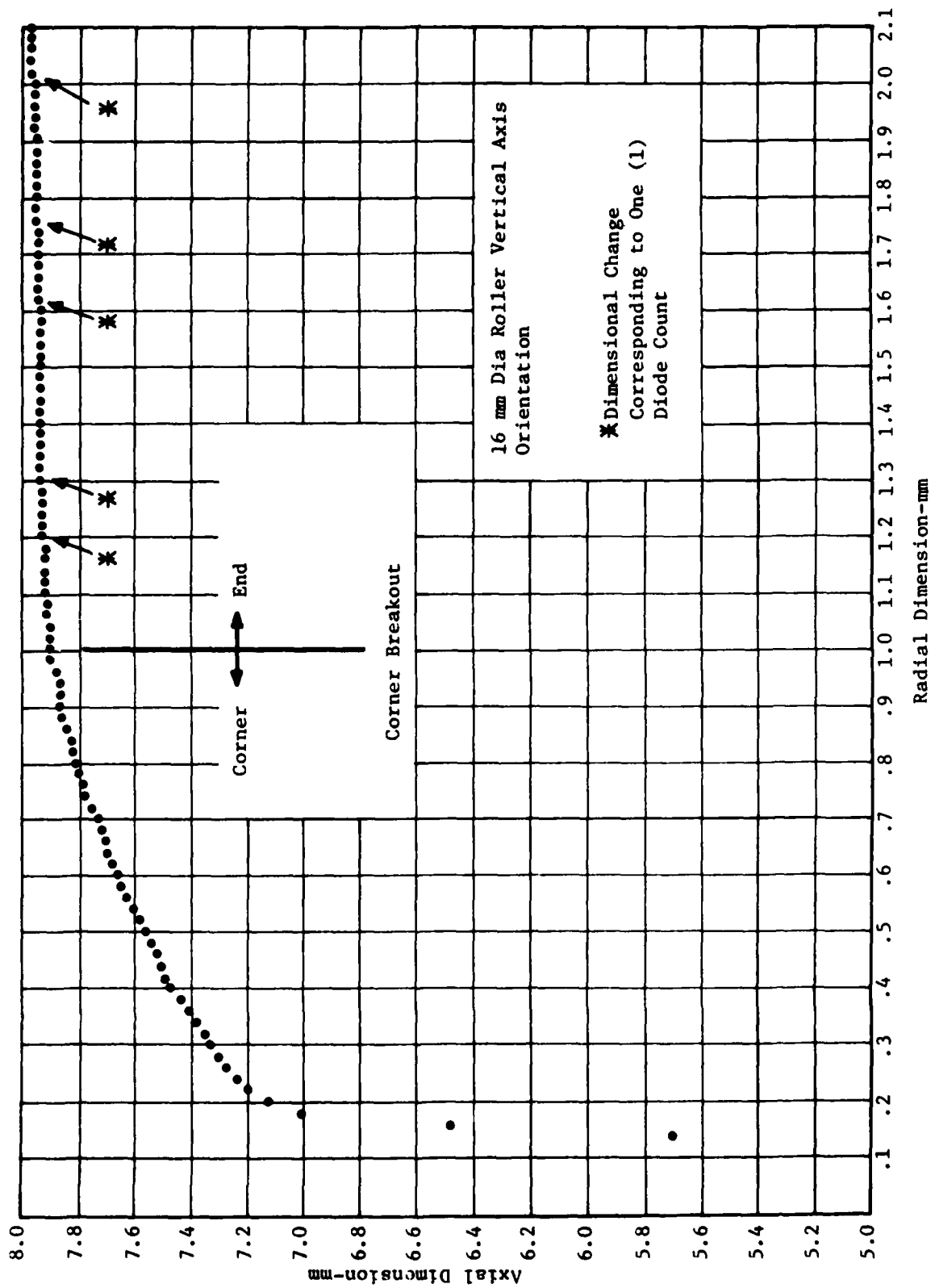


Fig. 14 Vertical Scan on a 16 mm Diameter Roller

blending process used to remove the intersection line between crown and corner during manufacture. Any computation system which uses the camera and slide output data to compute the breakout location will require a curve fitting routine. In addition to the curve fit requirement, at the portion of the scan data where the target shadow crosses the camera diodes at a small angle, the resulting indeterminate location of the radial dimension with respect to axial position produces the distorted corner data shown on Figures 13 and 14 at the initial axial scan position.

The line scan camera evaluation was continued to determine whether the inability of the line scan camera to accurately measure contour when the angle of incident between the object shadow and camera's diode array was small could be overcome. A test was performed with a 16 mm roller target oriented at 45° to the camera's diode array with the results of this test being shown in Figure 15.

On this figure the data points shown are only 20 percent of the actual number of points taken. With even the reduced number of data points shown, all the corner geometry is visible. From the data taken, a computer could perform a least square fit calculation to arrive at the roller end contour given by $y = mx + b_1$, the corner contour by $(x - b_2)^2 + (y - b_3)^2 + R_2^2$, and the crown contour by $(x - b_4)^2 + (y - b_5)^2 = R_1^2$.

If the slopes of the intersecting curves are equal at identical coordinates, then the intersection points for the three curves could be obtained.

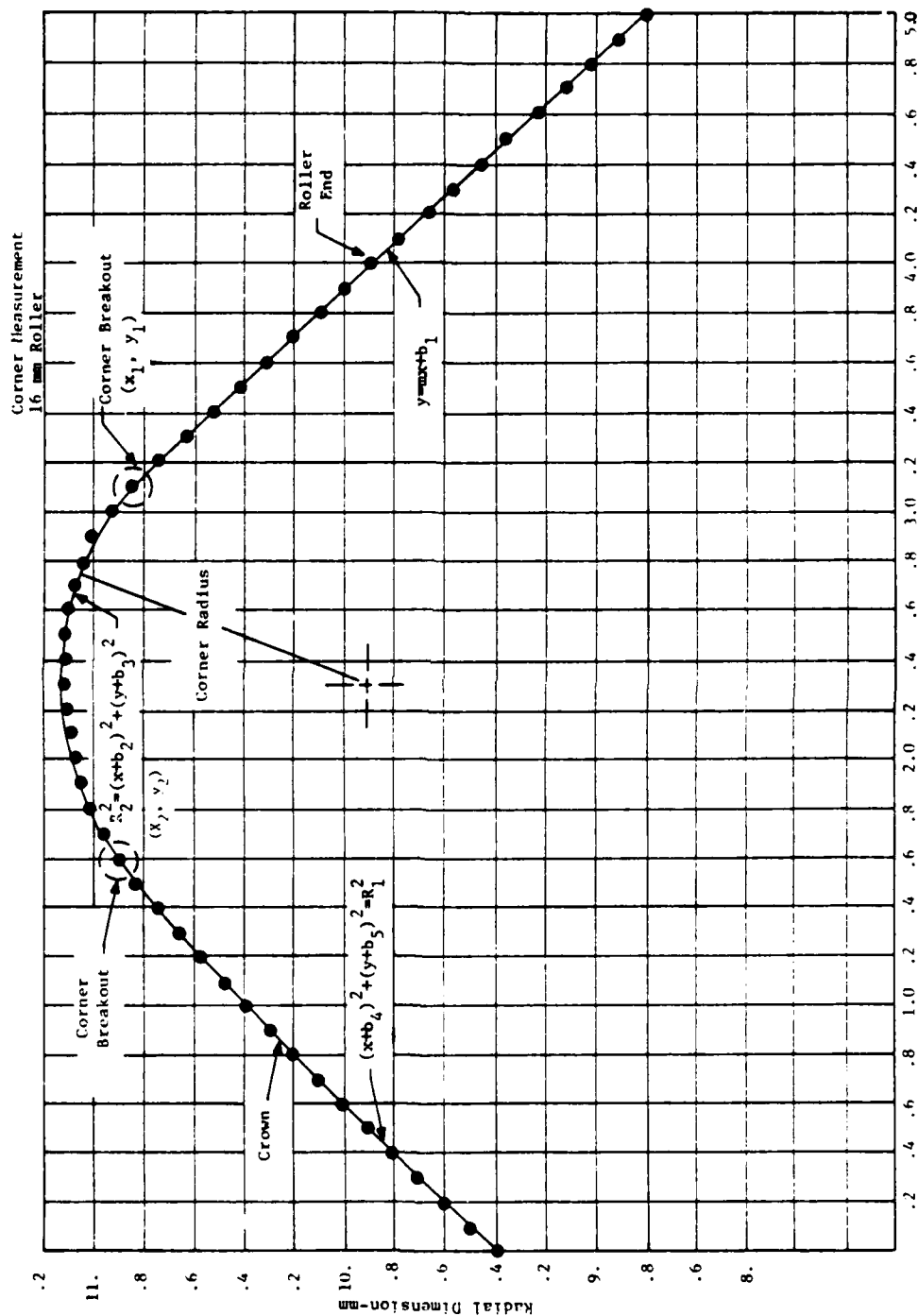


Fig. 15 Results of Test Performed with 16 mm Roller Target Oriented at 45° to Camera's Diode Array

When the previous conditions are met, the corner breakout location, relative to the roller end is calculated from the slope of the roller end and the dimensions x and y are calculated by establishing the length of the line having a slope of m which passes through x_1, y_1 and intersects $y = mx + b_1$. A similar calculation would be made for the corner breakout location relative to the flat central portion of the roller.

An added feature of this measurement technique is the determination of the true contour of the roller corner. If future measurements determine that the corner is not a true arc segment, then a polynomial curve fit could be used with the same effectiveness.

Discussion of the Line Scan Camera Test Results

The mean deviation between the least square fit circle calculation fit and the test data, when using a sufficiently large number of data points, is only 9.4×10^{-8} m or less than 4×10^{-6} inch. This indicates that the mean value of data, taken when the line scan camera is installed for these tests, is well within the required accuracy for roller contour measurements. The standard deviation, however, either from the least square (5.05×10^{-6} m) or three point fit (6.41×10^{-6} m) circles, is of the same magnitude as the camera sensitivity and is close to a plus or minus one diode count measurement error.

For the laboratory study, the combined magnification resulting from the camera lens set-back distance, the lens size and the extension tube length provided a calculated camera sensitivity of:

$$S = 9.375 \mu/\text{count} \quad (369 \times 10^{-6} \text{ in./count})$$

The sensitivity of the laboratory study is not high enough to produce sufficiently accurate roller contour measurements. This deficiency can be corrected by the addition of an extension tube length of 610 mm (24 inch) and the repositioning of the camera to an approximate 1.0 inch set-back. This change would increase the camera sensitivity to:

$$S = 9.375 \times \frac{68}{678} \frac{.4}{.85}$$

$$S = 0.4427 \mu/\text{count} \quad (37.0 \times 10^{-6} \text{ in./count})$$

At this level of sensitivity the camera is capable of measuring roller contours to the proper accuracy. The only restriction placed on the system is the limit on the angle that the target shadow makes on the camera's diode array. The orientation of the roller axis at 45° to the axis of the diode array as shown in Figure 15 provides the method of eliminating the shallow angle distortion problem.

4. Roller Support Evaluation

Along with the need to establish the type of sensors suitable for use in an automated inspection system, a method of holding a roller in the position necessary for obtaining good measurement data is equally important. To establish the most suitable roller support method, three mounting types were investigated: a kinematic mount (Reference 2) and a 90° and a 120° "V" block.

Figure 16 illustrates the three selected mounting blocks and indicates the orientation in which they were evaluated. Each mounting block was assessed for ease of use, suitability for inclusion in an automated gaging system, as well as for the production of repeatable measurements.

Determination of the first characteristic is subjective and was based on operator judgement. The second characteristic was judged by relying on the past experience of automatic machine designs, and the third characteristic by comparing the mean and standard deviations of a series of 100 measurements taken on each block. The measurements were obtained using both a contacting and a non-contacting gage. A 16 mm roller from a high DN aircraft turbine engine roller bearing was used as the gaged member.

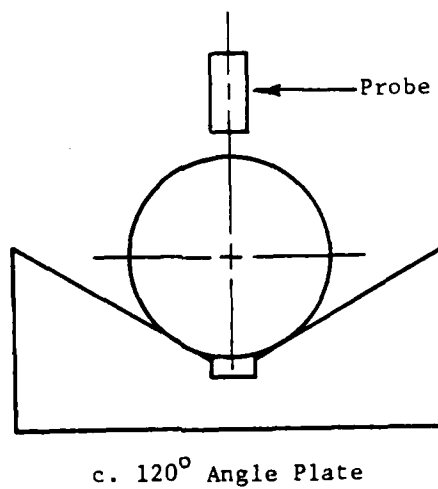
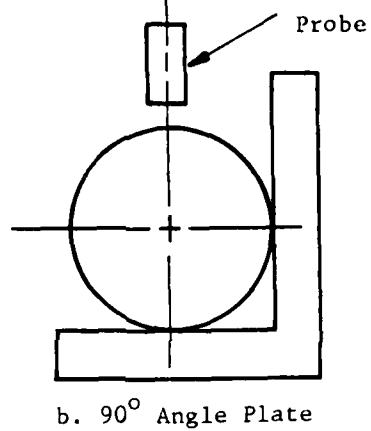
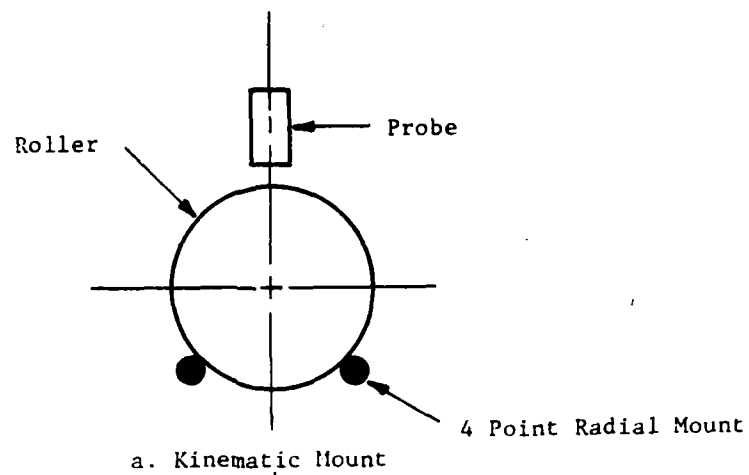


Fig. 16 Evaluation Roller Support

792362

Prior to construction, a calculation of Hertzian stresses generated by the kinematic mount was made. The support spacing for the mount is based on the support width (L) to bearing diameter (D) ratio of

$$L/D = 0.99.$$

The maximum Hertzian stress for a 16 mm diameter x 16 mm long roller at that spacing ratio under its own weight is:

$$\sigma_c = 2.74 \times 10^5 \text{ lb/in.}^2.$$

This level of stress, although high, should not produce roller damage, providing no additional gaging loads are imposed.

Roller Support Evaluation Results

The results of the roller support evaluation produced the following.

- The mounting block providing for the easier insertion and retrieval of the roller under the sensing elements is the 90° block since a straight entrance can be made without sliding the roller. The ranking of the mounting blocks was judged to be:

90° block	1
120° block	2
Kinematic Mount	3

- Production costs for the mounting blocks in an actual inspection machine, based on procurement costs for the laboratory devices, are rated as follows:

90° block	1
120° block	1
Kinematic Mount	2

- The ranking of the mounting blocks based on the ability to adapt to different roller sizes is judged to be:

90° block	2
120° block	1
Kinematic Mount	4

- The ranking of the three roller support blocks, based on the ability to perform the required measurement, was obtained by testing the hypothesis about "differences" in the means* of the collected roller measurement data. The measurements were obtained using both a contacting and a non-contacting gage. A 16 mm roller from a high DN aircraft turbine engine roller bearing was used as the gaged member. For each mounting block, 100 measurements of the roller diameter were taken by repeatedly inserting the roller, in the same orientation, into the mounting block.

The instrumentation used for this evaluation were:

Height Gage	- Cleveland IND-AC Model BT-1A S/N 380936 (contacting probe)
Capacitance Probe	- 1 mil range (CP-1)
Wayne Kerr	- Model DM100B, S/N 388
Multimeter	- Digitec Model 2120

For all tests the sensing probe and roller support blades were fixed in position and not moved, the roller was inserted, removed and reinserted into the support block for each reading. The roller orientation relative to the probe location was held constant throughout the tests to eliminate out-of-roundness or other geometric irregularity from interfering with the data.

The previously identified computer program was used to evaluate the test data and test the hypothesis about differences in means. Table 13 shows the recorded data and the calculated results for the contacting probe measurements, Table 14 the result of the non-contacting probe measurements.

The calculation of differences in means for the three mounting blocks indicates the ranking as:

90° block	2
120° block	2
Kinematic Mount	1

This ranking is based on the mean and standard deviations obtained from the evaluation data.

*See Appendix A

TABLE 13 - RESULT OF CONTACTING PROBE MEASUREMENTS

SPECIMEN RANK ORDER	ROLLER MOUNT EVALUATION		
	I 90VEE	II 120VEE	III KINEMATIC
1	-.12		
2	-.15	-.02	.05
3		-.05	.04
4	-.12		
5	-.04	-.02	.02
6	-.18		.04
7	-.12	-.02	.03
8	-.15	-.01	.03
9	-.10	-.03	.03
10	-.10	-.02	.06
11	-.08	-.03	.07
12	-.10		
13	.01	-.05	.09
14	.02	-.01	.05
15	.03	-.05	.06
16	-.02	-.01	.05
17		-.02	.02
18		-.02	.04
19		-.04	.02
20	.01	-.02	.03
21	.01	-.01	.02
22		-.02	.02
23	.01	-.02	.02
24		-.03	.03
25		-.03	.05
26	.02	-.02	.05
27	.01	-.05	.01
28	-.01	-.02	.03
29		-.03	.04
30	-.05	-.03	.03
31	-.02	-.02	.03
32	-.03	-.02	.01
33	-.06	-.02	.01
34	-.08	-.04	
35	.02	-.02	.01
36		-.02	.02
37	-.01	-.03	.03
38	.04	-.02	.01
39	.10	-.02	.01
40	.07	-.03	.02
41	.10	-.01	.02
42	.06	-.04	.05
43	.07	-.02	
44	-.50	-.02	.05
45	-.02	-.02	.02
46	-.04	-.04	.03
47	.05	-.04	.02
48	-.06	-.03	
49	-.01	-.03	.03
50	-.11	-.03	.03

TABLE 13 - RESULT OF CONTACTING PROBE MEASUREMENTS (cont'd)

51	-.10	-.03	-.01
52	.02	-.02	
53	-.11	-.01	.03
54	.08	-.04	
55	-.10	-.03	.01
56	-.10	-.02	.02
57	.05	-.04	
58		-.05	.02
59	.02	-.04	.04
60	.08	-.05	
61	.10	-.04	
62	.03	-.03	.04
63		-.03	
64		-.04	.02
65	-.02	-.02	-.02
66	-.01	-.03	.03
67	-.01	-.03	
69		-.02	.01
70	-.02	-.05	
71	-.01	-.02	-.01
72	-.04	-.01	
73	-.02	-.02	
74	-.01	-.02	
75	-.02		.03
76	-.02	-.03	-.01
77		-.04	.01
78	-.01	-.03	
79			.02
80	-.10		.02
81	.01		
82	.01	-.01	.02
83	-.01	-.02	
84		-.01	
85	-.02	-.01	.01
86	-.02	-.01	-.01
87	-.01	-.02	
88	-.01	-.01	
89		-.02	.04
90	-.02		.01
91	-.01		-.01
92	-.02	.01	-.01
93	-.02		.01
94		-.01	
95	-.03		
96	-.01	-.04	.02
97	-.01		.03
98			-.03
99	-.02	.01	
100	-.02	-.01	-.02
MEAN	-2.1300E-02	-2.1400E-02	1.7650E-02
STD DEV	-7.2549E-02	-1.4906E-02	-2.2152E-02

TABLE 13 - RESULT OF CONTACTING PROBE MEASUREMENTS (Cont'd)

STATISTICAL TEST OF DIFFERENCE IN MEANS OF PROCESSES II AND III:

STD DEV OF DIFF IN MEANS	= 2.6710E-03	
T-RATIO AND ALPHA	= 1.4620E+01	2.5969E-33
95% CONFIDENCE LIMITS	= 3.3783E-02	4.4317E-02
	= -157.864	2207.090% FOR FIRST MEAN
STRENGTH OF ASSOCIATION	= 5.1545E-01	
F-RATIO AND [1-P(F)]	= 2.1375E+02	1.4211E-14

STATISTICAL TEST OF DIFFERENCE IN MEANS OF PROCESSES I AND II:

STD DEV OF DIFF IN MEANS	= 7.4065E-03	
T-RATIO AND ALPHA	= 5.4006E-02	9.5698E-01
95% CONFIDENCE LIMITS	= -1.4206E-02	1.5006E-02
	= 65.164	-68.834% FOR FIRST MEAN
STRENGTH OF ASSOCIATION	= 0.	
F-RATIO AND [1-P(F)]	= 2.9167E-03	9.5698E-01

STATISTICAL TEST OF DIFFERENCE IN MEANS OF PROCESSES I AND III:

STD DEV OF DIFF IN MEANS	= 7.5859E-03	
T-RATIO AND ALPHA	= 5.2005E+00	4.9398E-07
95% CONFIDENCE LIMITS	= 2.4491E-02	5.4409E-02
	= -112.342	-249.585% FOR FIRST MEAN
STRENGTH OF ASSOCIATION	= 1.1522E-01	
F-RATIO AND [1-P(F)]	= 2.7045E+01	4.9398E-07

TABLE 14 - RESULT OF NON-CONTACTING PROBE MEASUREMENTS

SPECIMEN RANK ORDER	ROLLER MOUNT EVALUATION		
	I 90VEE	II 120VEE	III KINEMATIC
1	.634	.635	.445
2	.636	.630	.516
3	.630	.613	.524
4	.643	.637	.493
5	.640	.631	.519
6	.647	.626	.492
7	.642	.635	.508
8	.638	.631	.518
9	.647	.637	.538
10	.644	.634	.535
11	.640	.634	.532
12	.644	.635	.524
13	.646	.631	.504
14	.646	.639	.502
15	.636	.630	.494
16	.641	.632	.536
17	.644	.634	.518
18	.650	.630	.520
19	.636	.632	.490
20	.653	.631	.526
21	.657	.627	.519
22	.652	.625	.522
23	.657	.629	.499
24	.647	.636	.490
25	.650	.629	.532
26	.651	.632	.526
27	.657	.632	.509
28	.654	.640	.500
29	.651	.624	.510
30	.650	.636	.505
31	.653	.633	.525
32	.655	.631	.518
33	.659	.638	.497
34	.662	.640	.490
35	.661	.636	.510
36	.655	.631	.500
37	.658	.631	.499
38	.660	.632	.485
39	.662	.632	.503
40	.658	.629	.494
41	.649	.631	.505
42	.656	.632	.499
43	.659	.635	.492
44	.658	.633	.508
45	.642	.631	.508
46	.651	.638	.515
47	.641	.633	.500
48	.642	.635	.528
49	.635	.635	.502
50	.637	.640	.492

TABLE 14 - RESULT OF NON-CONTACTING PROBE MEASUREMENTS (cont'd)

51	.635	.635	.508
52	.644	.633	.509
53	.635	.632	.506
54	.649	.629	.511
55	.639	.640	.502
56	.645	.630	.508
57	.645	.629	.495
58	.649	.639	.494
59	.645	.633	.472
60	.643	.640	.451
61	.655	.630	.454
62	.650	.636	.455
63	.655	.637	.494
64	.656	.637	.497
65	.642	.639	.511
66	.664	.641	.515
67	.667	.635	.496
68	.659	.639	.506
69	.659	.636	.519
70	.655	.631	.529
71	.630	.627	.513
72	.647	.642	.519
73	.644	.639	.512
74	.652	.643	.527
75	.655	.642	.520
76	.652	.640	.520
77	.653	.636	.514
78	.653	.642	.525
79	.649	.634	.494
80	.641	.633	.496
81	.664	.640	.480
82	.635	.636	.515
83	.637	.632	.502
84	.643	.641	.490
85	.631	.635	.506
86	.650	.632	.490
87	.635	.633	.501
88	.642	.635	.493
89	.642	.635	.485
90	.627	.632	.510
91	.631	.637	.481
92	.646	.640	.487
93	.625	.635	.506
94	.625	.643	.485
95	.632	.634	.491
96	.627	.635	.472
97	.633	.634	.482
98	.645	.632	.487
99	.636	.626	.455
100	.647	.635	.481

MEAN 6.4712E-01 6.3433E-01 5.0411E-01
 STD DEV 1.0443E-02 4.7504E-03 1.6429E-02

TABLE 14 - RESULT OF NON-CONTACTING PROBE MEASUREMENTS (cont'd)

STATISTICAL TEST OF DIFFERENCE IN MEANS OF PROCESSES II AND III:

STD DEV OF DIFF IN MEANS	=	1.7102E-03	
T-RATIO AND ALPHA	=	-7.6142E+01	1.3311-148
95% CONFIDENCE LIMITS	=	-1.3359E-01	-1.2685E-01
	=	-21.060	-19.997% FOR FIRST MEAN
STRENGTH OF ASSOCIATION	=	9.6665E-01	
F-RATIO AND [1-P(F)]	=	5.7977E+03	1.4211E-14

STATISTICAL TEST OF DIFFERENCE IN MEANS OF PROCESSES I AND II:

STD DEV OF DIFF IN MEANS	=	1.1477E-03	
T-RATIO AND ALPHA	=	-1.1144E+01	1.0564E-22
95% CONFIDENCE LIMITS	=	-1.5053E-02	-1.0527E-02
	=	-2.326	-1.627% FOR FIRST MEAN
STRENGTH OF ASSOCIATION	=	3.8116E-01	
F-RATIO AND [1-P(F)]	=	1.2419E+02	1.4211E-14

STATISTICAL TEST OF DIFFERENCE IN MEANS OF PROCESSES I AND III:

STD DEV OF DIFF IN MEANS	=	1.9470E-03	
T-RATIO AND ALPHA	=	-7.3452E+01	1.2948-145
95% CONFIDENCE LIMITS	=	-1.4685E-01	-1.3917E-01
	=	-22.693	-21.506% FO FIRST MEAN
STRENGTH OF ASSOCIATION	=	9.6425E-01	
F-RATIO AND [1-P(F)]	=	5.3952E+03	7.1054E-15

The net ranking of the three mounting block designs is obtained by adding the individual ranking values with the lowest total indicating the preferred design. The net rankings are:

90° block	6
120° block	6
Kinematic Mount	10

Although the 90° and 120° blocks are equally ranked, the selection of the 90° block for application in the automatic measurement system is made on the basis of the ease in which it can be applied and used in the final system design.

5. Summary of Laboratory Evaluation

The laboratory evaluation study has investigated both non-contacting sensors which would be directly applicable to an automated gaging system and the method by which a precision roller would be supported in such a system.

The conclusions reached as a result of the evaluations performed are summarized below:

1. Inductive-type proximity probes lack the linearity and in practical sizes, the sensitivity, to be used for taking precision measurements in an automated roller gage system.
2. The capacitance probe in the high sensitivity design demonstrates both the necessary sensitivity and linearity to be successfully used in a precision roller inspection system.
3. The video line scan camera has demonstrated its ability to measure the less precise roller contour characteristics with sufficient accuracy and repeatability to be directly applicable to the automated gage system.
4. The 90° "V" block has been shown to provide the required reliability and ease of use to be used as the method for

positioning a roller to be inspected in the proper orientation relative to the sensing probes.

An additional conclusion drawn from the laboratory study is that the roller characteristic to be measured in an automatic gaging system should be grouped according to the capability of the sensors used. From this conclusion, therefore, the measurements to be made in the breadboard version of the automated inspection system will be grouped as follows:

- High Sensitivity Requirements - Diameter
(capacitance probes)
 - Length
 - Crown Drop and Runout
 - End Parallel and Runout
 - OD Taper
- Low Sensitivity Requirements - Corner Breakout
(video line scan camera)
 - Corner Runout
 - Flat Length
 - Flat Centrality

SECTION IV

DESIGN OF BREADBOARD GAGING MODULES

The main thrust of this program is to demonstrate the features of an automated roller inspection device rather than to build a completely automated inspection system. For this reason, the development effort concentrated on the successful design and demonstration of two related gaging stations. Table 15 identifies the gage stations and the tolerance types which can be evaluated at each. The gaging stations were used to evaluate measuring techniques and to obtain the information needed to prepare the basic design of the automated system. For this reason, no attempt was made in the experimental phases of this program to provide automated transfer mechanisms, self-contained environmental controls for temperature or humidity, automatic sorting logic, or automatic roller clean- and re-oiling features. Rather, the design effort was directed toward features which will require a minimum of redesign when the gage heads are incorporated into the final automated gage configuration.

TABLE 15

Roller Dimension Tolerance Gaging

Gage #1	{	Radial Dimensions	{	Diameter	}	Two Radial Probes Along Flat Length
				OD OR		
				OD Taper		
	{	Axial Dimensions	{	Crown Drop	}	Radial Probe Each End Gage Location
				Crown OR		
				{		
End Runout						
Gage #2	{	Contour Dimensions	{		Corner Breakout	}
				Contour Dimensions	Corner Runout	
	{	Contour Dimensions		Flat Length		
				Flat Centrality		

Another reason for not emphasizing transfer mechanisms in this program is to retain the flexibility of including a greater or lesser degree of automation based on the economic and technical cost effectiveness factors. For example, small production rates may be handled better with more manual operations and without automated roller transport, while large production rates will obviously benefit from a greater degree of automation. With this philosophy, the gage modules will provide a minimum base capability from which various degrees of multiple gaging performance can be generated.

Material presented in this section only describes the configuration of the gages and briefly, their use. A detailed description of their operation and capabilities is presented in the following sections.

Manual gaging methods and instruments currently used contain numerous design features developed through experience. Some design features adapted for use in the breadboard gaging modules are:

- The gaging loads set by springs or counter weights in the manual gages will be retained for applying gaging loads in the automatic machine.
- Belt drives for rotating the rollers during roundness measurements will be replaced with a rubber covered wheel.
- The angle plate type of mount used in the manual gage will be retained on the automatic gage because point contact mounting for rollers may induce unnecessary damage during roller manipulation.

During the breadboard evaluation, each of the gaging modules will be assembled and evaluated for these principal capabilities:

- Measurement of accuracy and repeatability
- Manual throughput rate
- Interchangeability for varying roller sizes
- Adaptability for automatic transfer

1. Capacitance Probe Design

The initial task in the development of the breadboard gages was the design and construction of the smallest practical capacitance probes. The final probe design is illustrated in Figure 17 (Dwg. 10B000397). The actual sensing tip (center element) has a diameter of 0.031 in., however, for linearity requirements the fringe shield increases the active probe diameter to 0.072 in. It is this diameter which determines the true probe envelope.

The new probe is designed to provide a full scale reading at an offset of 0.0005 inch in order to produce a small sensing diameter. Range extension circuitry in the associated probe electronics will decrease the probe sensitivity to that of a 0.001 inch probe thereby increasing the space available between the probe and the roller target. The larger probe to target spacing permitted greater flexibility in introducing and retracting rollers from the gage module.

Figure 18 shows a finished probe and two preliminary calibration curves. Calibration "a" was taken with the probe electronics in their normal configuration. Calibration "b" was taken with the probe range extension circuitry added to the electronics. The range extension substantially increased the probe sensitivity, from 636 volts/inch to 1600 volts/inch without sacrificing linearity. Positions of the capacitance probes for measuring roller characteristics are illustrated in Figure 19. The probes are identified as probes A through E. The combinations of probe readings necessary to obtain the necessary measurement data are listed on Table 16.

The successful design of the miniature capacitance probes established the envelope of the sensing elements and permitted the design of the gaging module to proceed. The first module for which a firm design was completed was the combined radial/axial gage which can be easily converted from making radial to axial measurements. In the evaluation phase of this program, it was determined that the gage could function properly in a combined form. Presently, it is better to show the functions separately.

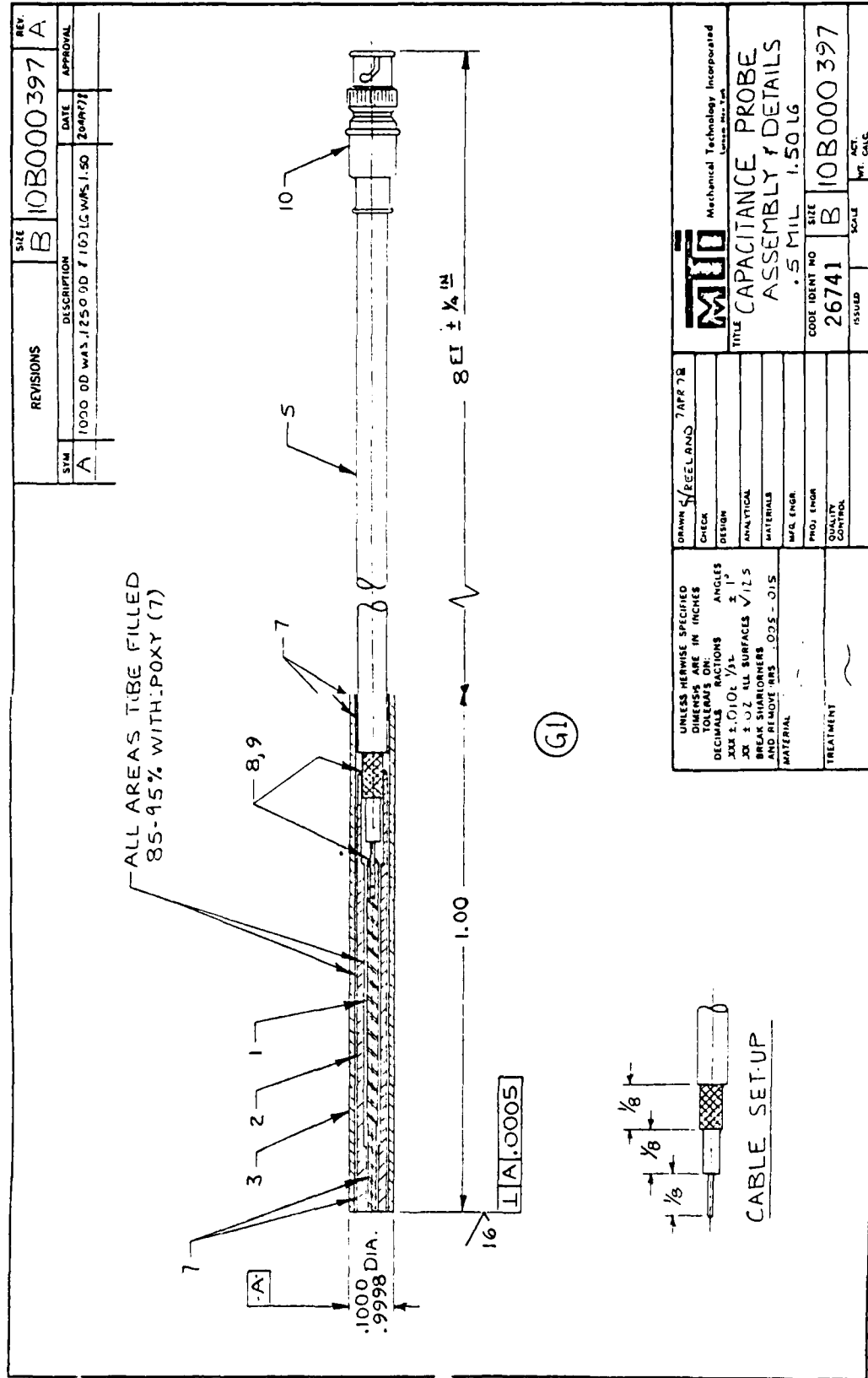


Figure 17

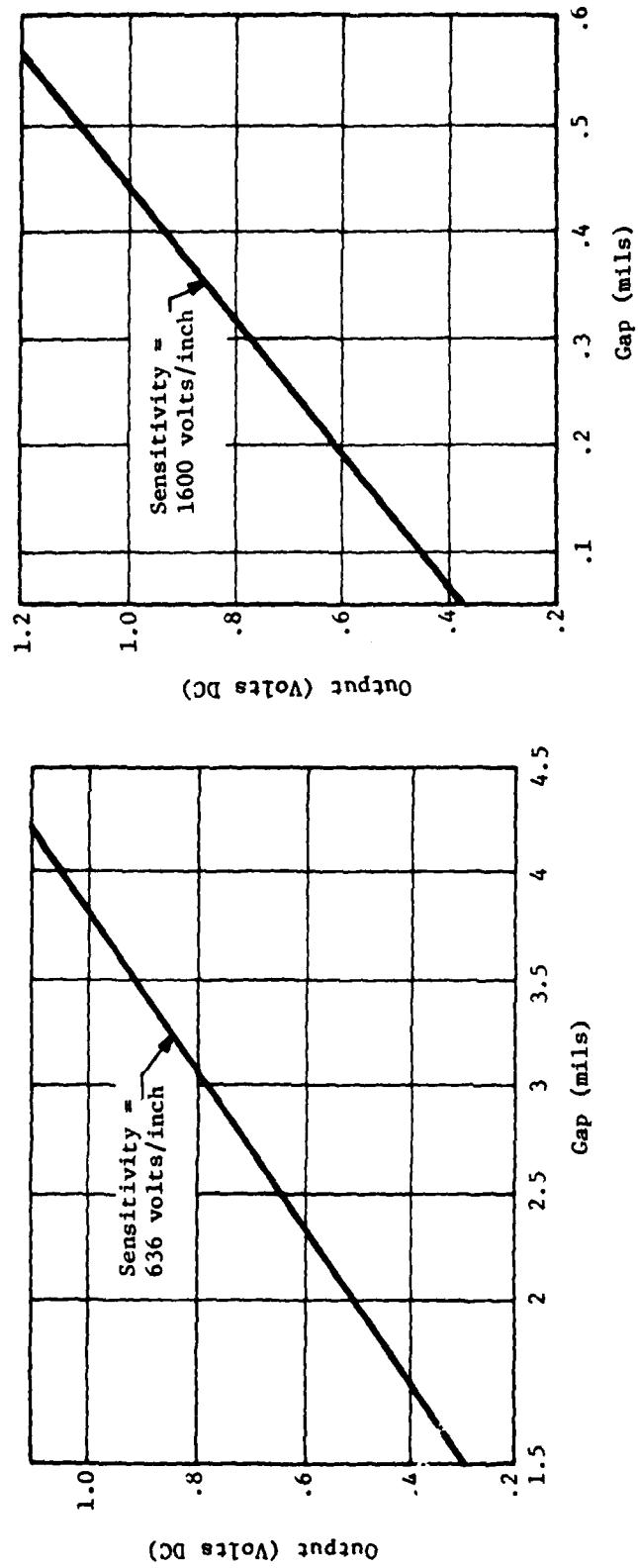
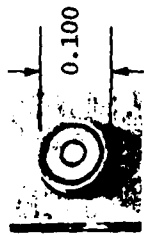


Fig. 18 Breadboard Gage Module-Miniature Capacitance Probe

792371

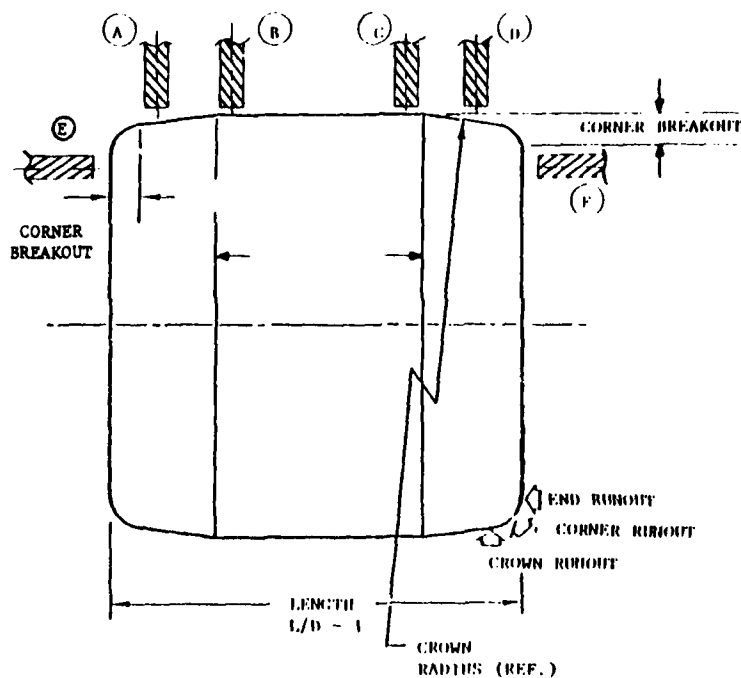


Fig. 19. Radial/Axial Gage: Probe Location Diagram

TABLE 16

Probe Reading Combinations Necessary to
Obtain Necessary Measurement Data

<u>Characteristic</u>	<u>Probe used to Obtain Characteristic Value</u>
Diameter	B&C
Length	E&F
Crown Drop	B-A and C-D
Crown Runout	B-A and C-D continuous
End Parallel	E-F
End Runout	E&F
Corner Breakout	NA
Corner Runout	
Flat Length	
Flat Centrality	
OD Taper	B-C

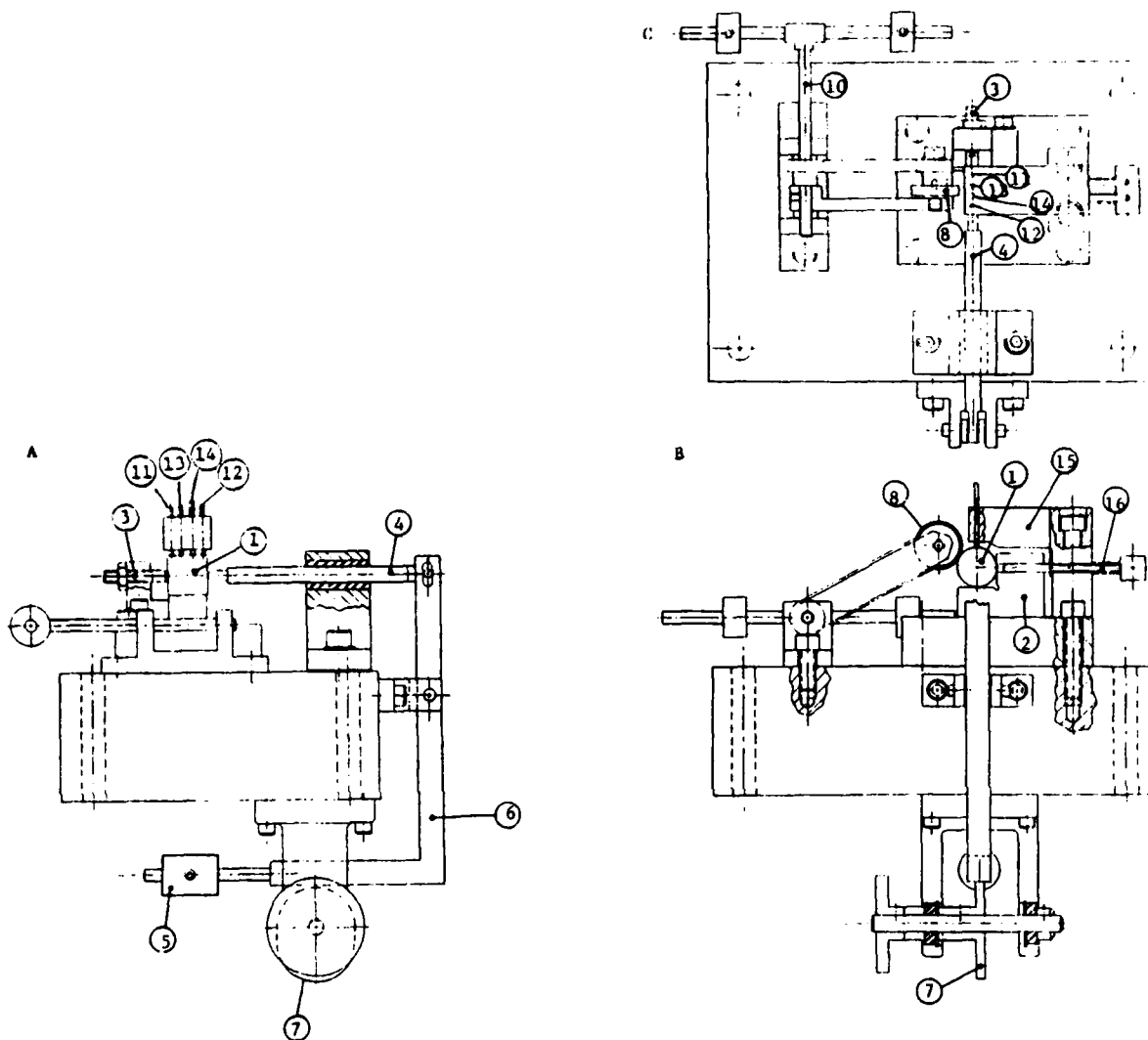
In the following designs, all gaging functions are performed manually, but in a manner such that the manual operations duplicate functions which could easily be automated. Following is a description of gage usage.

2. Radial Measurement Gage

The radial gage configuration is shown in Figure 20. In this figure, a roller undergoing measurement (1) is shown inserted onto a tungsten carbide faced 90° angle plate anvil (2). The roller is secured axially by an adjustable carbide tipped position pin stop (3), and a clamping level (4). The fixed axial stop is set so that the roller is properly oriented in the axial direction with respect to the position sensing probes. The clamping lever (4) includes a counter-balance weight (5) to provide an axial clamping load via the clamping lever (6). The axial clamping load is actuated by a rotating cam (7). Placement of the counterbalance weight along the clamping lever will determine the amount of clamping load. A rotating rubber covered wheel (8) is positioned against the roller to provide both a clamping load to hold the roller against the anvil and a torque to rotate the roller during a measurement sequence. Adjustment of the clamping load provided by the wheel is achieved by a movable counterbalance (9) mounted on a lever system (10). Roller measurements will be made using four capacitance probes. Two probes (11) and (12) will measure the diameter, two point out of roundness and OD taper simultaneously. Two additional probes, (13) and (14), oriented in the fixture at the appropriate crown drop gage locations are used to measure both crown drop and crown runout simultaneously. The four probes are positioned over the roller using a precision mounting block (15).

The positioning of the non-contacting capacitance probes in the radial and axial gage modules is critical to both the successful measurement of all necessary roller characteristics and to the acceptance of these measurements by the manufacturers and users of high precision roller bearings. Each roller design has specific locations where such measurements as crown drop, corner breakout and central flat length are taken. In order to place the sensors obtaining such dimensions as crown drop, diameter and taper of the central flat and roller end characteristics in their proper locations the geometry of the probes becomes important.

The probe diameter established for the breadboard gages is $D = 0.100$ inch; the active portion of the probe, however, is only $D = 0.075$ inch. Since the entire



192375

Fig. 20 Radial/Axial Gage Module: Radial Measurement Configuration

active portion of the probe must view the probe's target, if sensitivity and linearity are to be maintained, positioning the probe relative to roller contour discontinuities, such as corner breakout, are critical. Because groupings of probes require finite space, either longitudinally along a roller's axis to obtain radial measurements or circumferentially placed perpendicular to the roller's axis; to obtain axial measurements the probe dimensions govern the minimum roller size which can be accommodated in the breadboard gages.

To illustrate the development of minimum probe spacing refer to Figure 19. Assuming a probe separation of 0.010 inch longitudinally and a 0.050 clearance circle for the circumferentially positioned probes, Figure 21 shows the minimum longitudinal spacing for the breadboard probes to be 0.185 inch, which is significantly greater than the roller flat length found on 7 mm rollers (approximately 0.160). The conclusion drawn from this is that radial dimensions on small rollers can only be measured at one end at a time, and that a central flat length greater than 0.185 in. must exist before all four radial probes can be employed. Along with the radial probe orientation, a minimum gaging circle of 0.225 inch results from a circumferential orientation of probes as illustrated by Figure 22. The 0.225 inch diameter is less than the diameter defined by the difference between the outside diameter and the corner breakout dimension for the 7 mm roller (approximately 0.230) but would be greater than the same dimension for smaller rollers.

Although the breadboard probe design, because they are required to be removable, presents some restrictions on their use with very small rollers, the difficulty can be somewhat relieved in the final automated design by eliminating the outer probe sheath. The probe outer sheath is used as a fixturing device to permit probe clamping and in the automated gage version these probes can be epoxied directly into holding fixtures. Since an insulation layer of approximately 0.004 in. must be maintained between the probe and its holder, for the same minimum probe spacing of 0.010 inch, the new longitudinal and circumferential spacings would reduce to 0.168 in. and 0.200 in., respectively. Even at this spacing, however, the full compliment of axial and radial probes is barely adequate for use with the 7 mm rollers and would have to be evaluated at the time of construction.

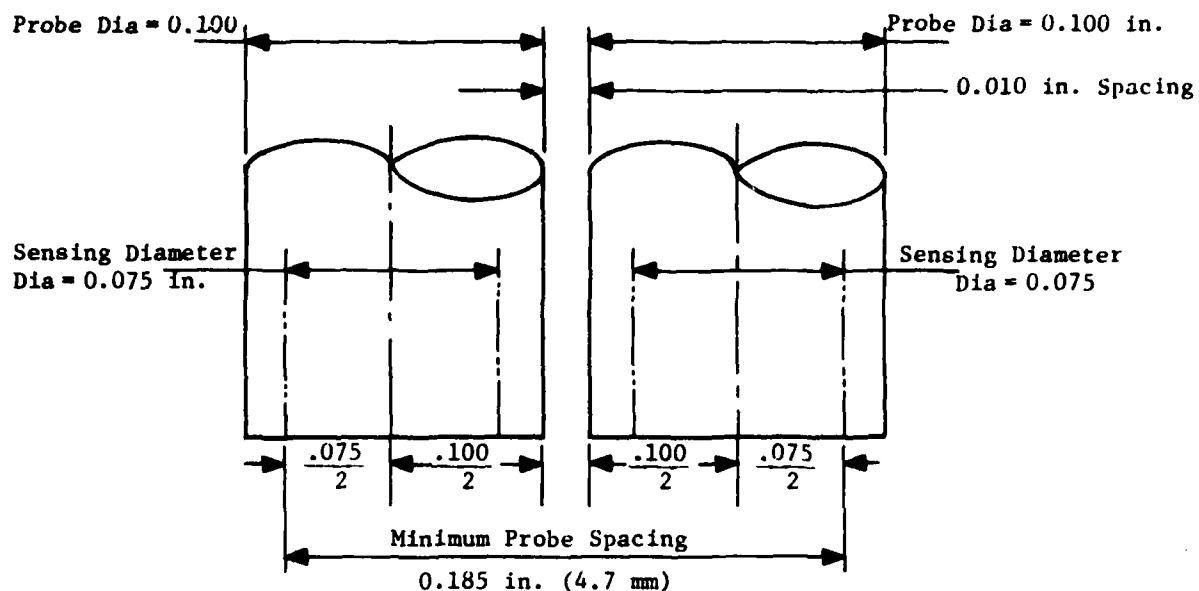


Fig. 21a Longitudinal Probe Spacing

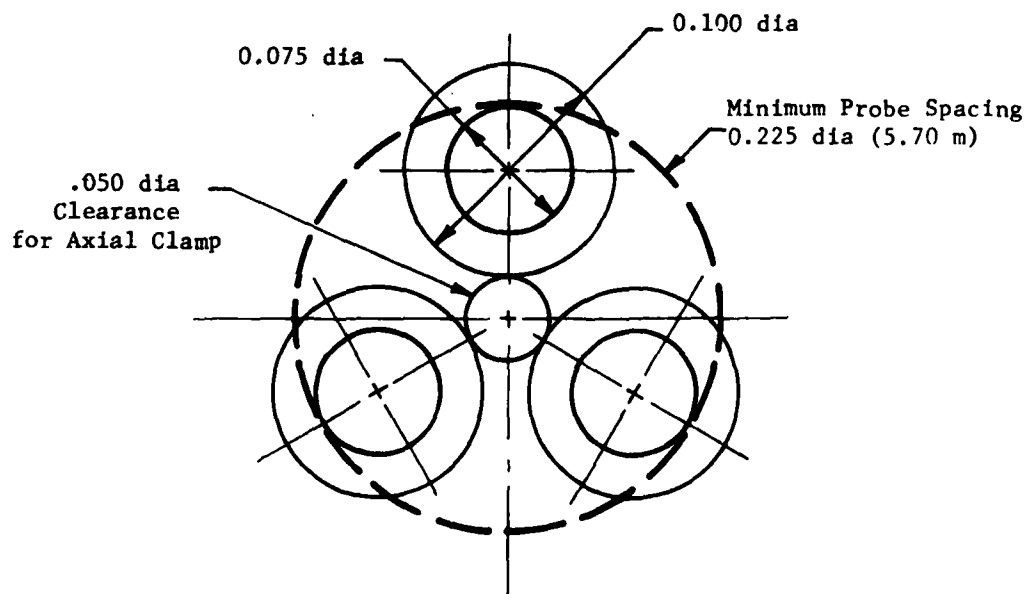


Fig. 21b Circumferential Probe Spacing

Fig. 21 Minimum Probe Positioning for Breadboard Gages

In the breadboard version of the gaging head, a manual stripper mechanism (16) is included for the removal of a measured roller, but a manual operation will be required to complete the removal function as well as to insert a roller into the gaging head.

In the final automated version of the gaging head, the roller entrance into the fixture will have to be guided to assure that no contact is made with the axial stop during roller insertion.

The completed radial gage module is shown on the photographs identified as Figure 22 and 23. Figure 22 illustrates the levers and loading lever locations. Figure 23 shows the positioning of the sample roller, the probes and probe holders and the roller rotating wheel for the 7 mm roller inspection.

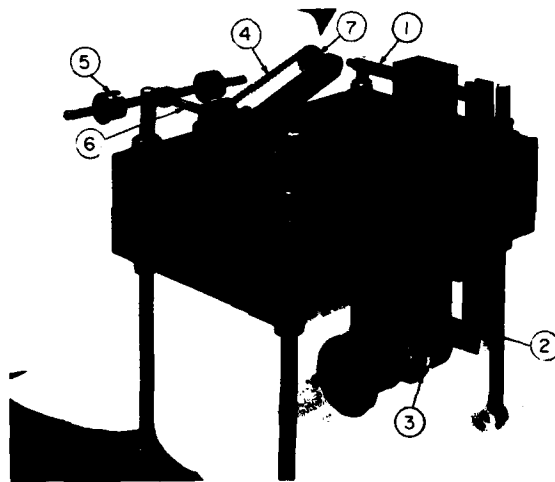


Fig. 22 Radial/Axial Breadboard Gage-Lever Systems

The major components identified on Figure 22 are the roller axial clamp rod (1) and lever (2) and their actuating cam (3). The roller clamp lever assembly includes the belt for rotating the roller (4) and the cantilevered loading weights (5). The pulley which drives the belt (4) is free to turn on the counter weight shaft (6) but the loading are (7) which carries the roller rotating wheel is not. The addition of the 90° 'V' block, the roller position stop and the sensing probes to the assembly shown in Figure 22 forms a complete gage module.

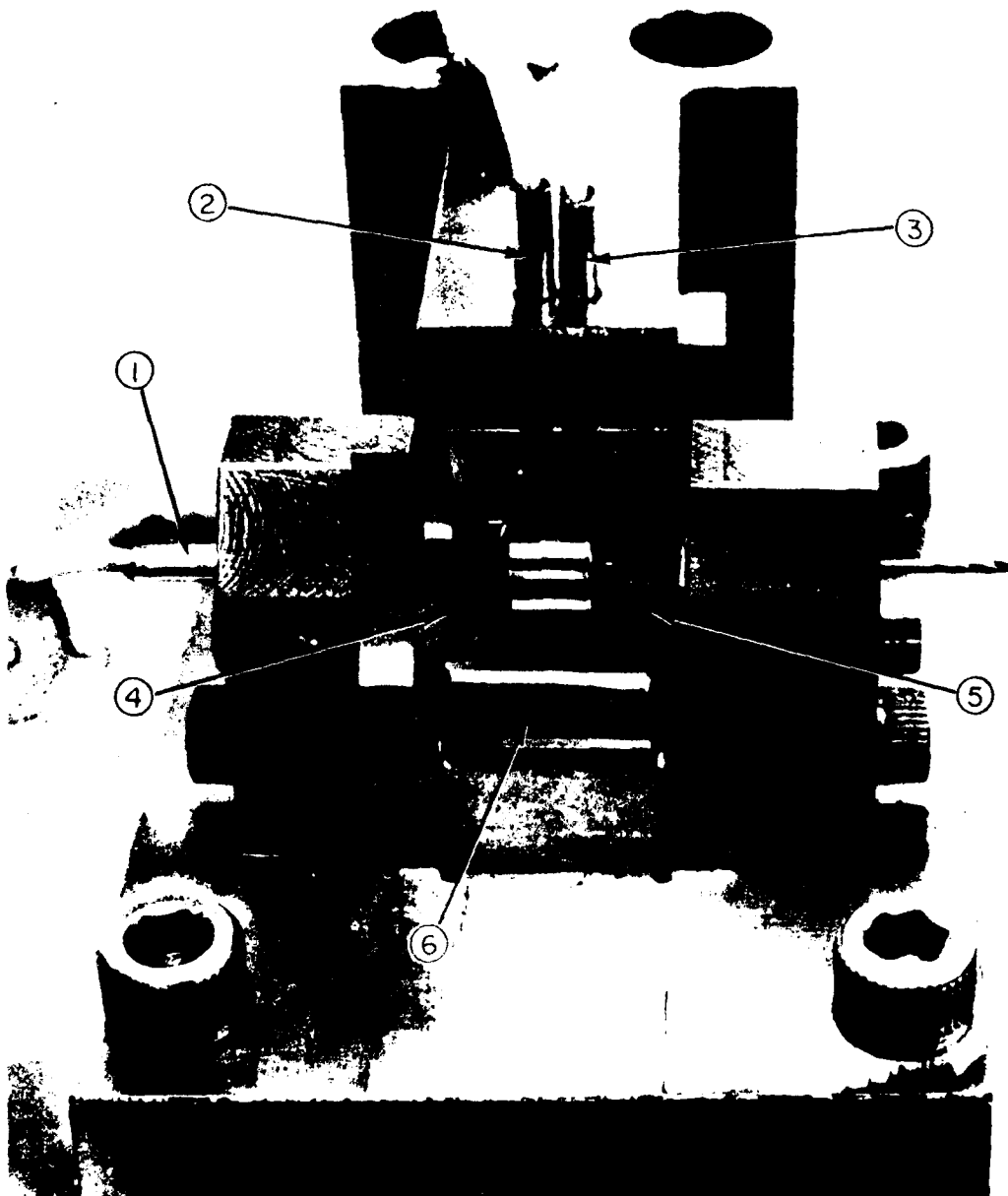


Fig. 23 Radial/Axial Breadboard Gage Set-up for 7 mm Roller

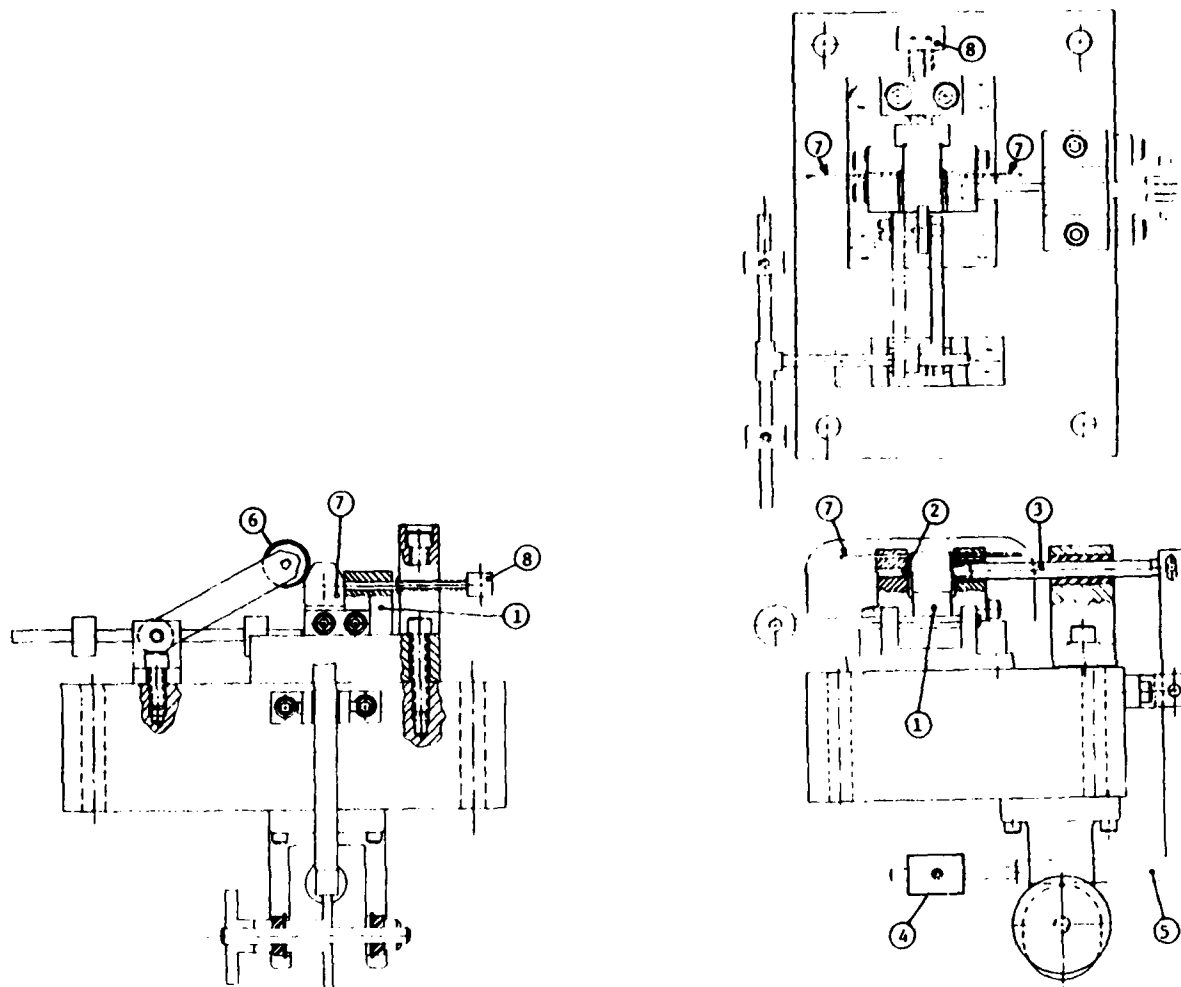
In Figure 23 the 7 mm roller is shown installed in the gage fixture with one axial probe (1) and two radial probes (2) and (3). Plastic guides (4) and (5) are positioned on the 'V' block (6) to serve as roller installation guides.

3. Axial Measurement Gage

The axial gaging assembly shown in Figure 24 is constructed from the radial gage and in this configuration will gage all the axial dimensions listed in Tables 1 and 15. This gage head is similar to the radial measurement head but differs in the placement of the capacitive gage sensors; the conversion from a radial to an axial gage configuration is simply performed by replacing only the probe holding brackets.

In the axial measurement configuration, an individual roller is also inserted into an angle plate anvil (1) and is clamped against an axial stop (2) by a clamping lever (3). The clamping lever includes a slideable counterweight (4) for the adjustment of axial load; a cam operated lever (5) is used to engage and disengage the load lever. The roller is loaded against the 90° angle plate anvil by a counterweighted belt driven wheel (6) which provides both a gaging load and a means for rotating the roller for runout evaluation.

Axial roller measurements are made using two (2) capacitance probes (7) oriented parallel to the roller axis with one positioned at each roller end. The probes are positioned so that their fringe shields lie within the corner breakout gage diameter. The average reading difference between the two probes will define the roller length. The variation of the probe readings will establish end runout, the variation in their output difference will define end parallelism.



792174

Fig. 24 Radial/Axial Gage Module Radial Measurement Configuration

In the breadboard model of the axial gage, rollers are inserted manually and a manually operated stripper mechanism (8) ejects rollers from the gaging fixture. In the automated version of the fixture, roller stripping will be included as part of the automated mechanism, as will the insertion of rollers into the gage. Special lead-in devices will have to be included in the automated gaging head to assure proper positioning of the roller between the axial probes. However, range extension circuitry is included as part of the probe design to increase probe to roller clearances.

An enlarged view of the roller positioning within the axial gage assembly is shown in Figure 25. This view of the roller as it is set into the gage is used to illustrate the closeness to which the probe must be placed between the axially oriented probes.

The initial design intent of the radial/axial gage modules was to provide separate gage entities for radial and axial measurements arrived at by adding or removing fixturing and probe holders. As the assembly of the module progressed the decision was made to combine both axial and radial measurement capabilities and perform all the necessary measurements simultaneously. Figure 23 included in the radial measurement gage section illustrates how the two systems were easily combined. In final form, the axial measurement gage fixturing is included with the radial gage fixturing rather than assembled as a separate item.

4. Contour Measurement Gage

The second breadboard gage module design, which completed the breadboard design phase of the program, was the contour measurement gage. This gage is used to establish all the roller contour measurements as described in Table 1.

In the contour measurement gage, the shadow cast by the interruption of a collimated light beam by a roller being measured is interpreted by a linear array of photo sensitive diodes in the line scan camera and a numerical display of the number of shadowed diodes is presented. The set-up used in the laboratory evaluation study consisted of a 50 mm, 1.8,^f lens installed with a

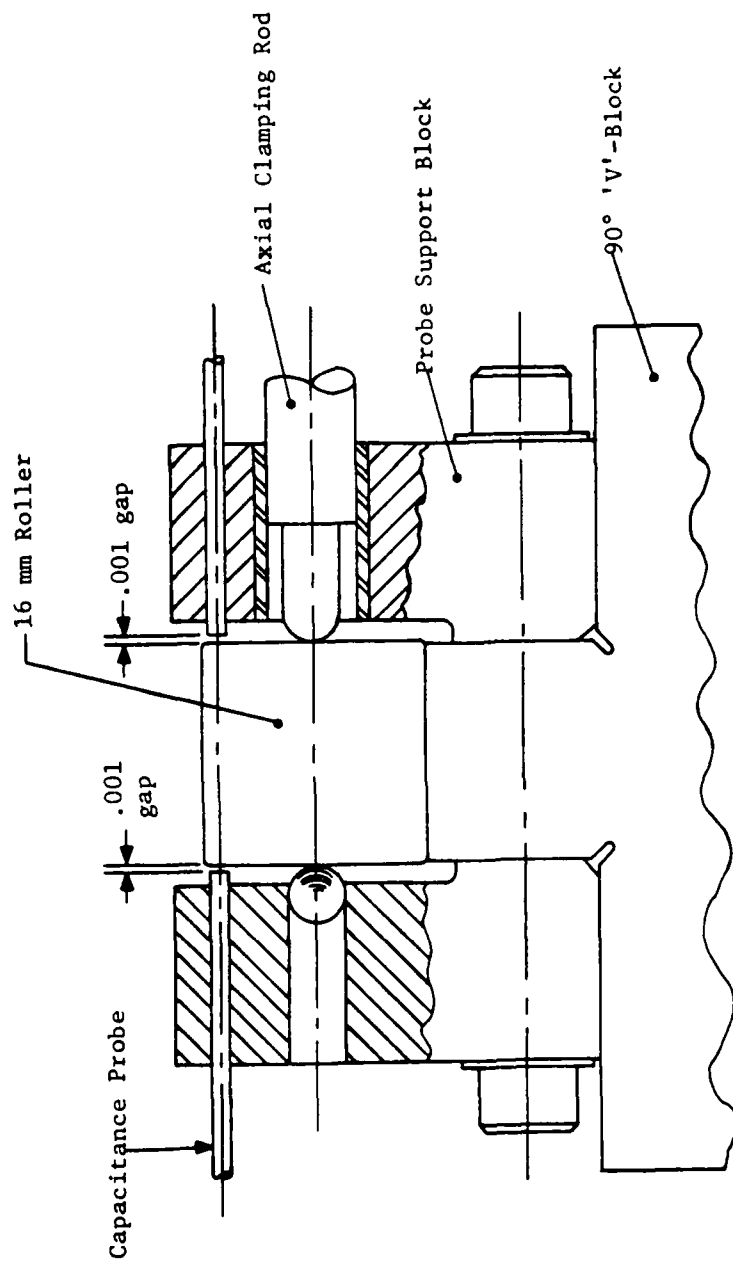


Fig. 25 Roller Positioning in Axial Gage Configuration

792370

65 mm extension tube. This arrangement provided a total system sensitivity of 369×10^{-6} in./diode count. At this sensitivity the optical system was not suitable for measuring roller contour. The addition of a 24 in. extension tube and repositioning of the lens closer to the test roller, however improved the sensitivity by an order of magnitude. The final configuration of the optical scanning gage, including the 24 in. extension tube and the positioning of the target roller's primary axis at 45° , is shown in Figures 26 and 27. Figure 26 presents an elevation view of the gage looking along the camera axis and Figure 27 a plan view illustrating the general arrangement of the system.

In Figure 26, test roller (1) is shown positioned in a 45° mounting 'V'-block (2). The roller's position along the 'V' axis is maintained by a precision micrometer (3) which is used to adjust the axial position of the roller within the vision field of the line scan camera so that appropriate portions of the roller can be scanned.

A tungsten carbide ball (4), attached to the end of the micrometer shaft, is used to support the roller. The position of the ball is accurately maintained along the centerline of the roller to minimize extraneous motions caused by a possible axial offset.

In order to obtain corner runout measurements of a roller, it is necessary to rotate the roller while maintaining a constant pressure against it. A roller rotating mechanism similar in design to that used on the radial/axial gage is also incorporated in the optical gage design. A rubber covered wheel (5), mounted in a counterbalanced spindle (6) contacts the target roller on its central land location. A hand wheel (7) is used to facilitate roller rotation.

In order to accomodate other roller sizes and to assure that the wheel always contacts rollers on their central land, the spindle shaft is machined with a series of concentric grooves. These grooves communicate with a positioning pin (8) in the spindle housing. When a repositioning of the wheel is required, a different groove is engaged with the positioning pin.

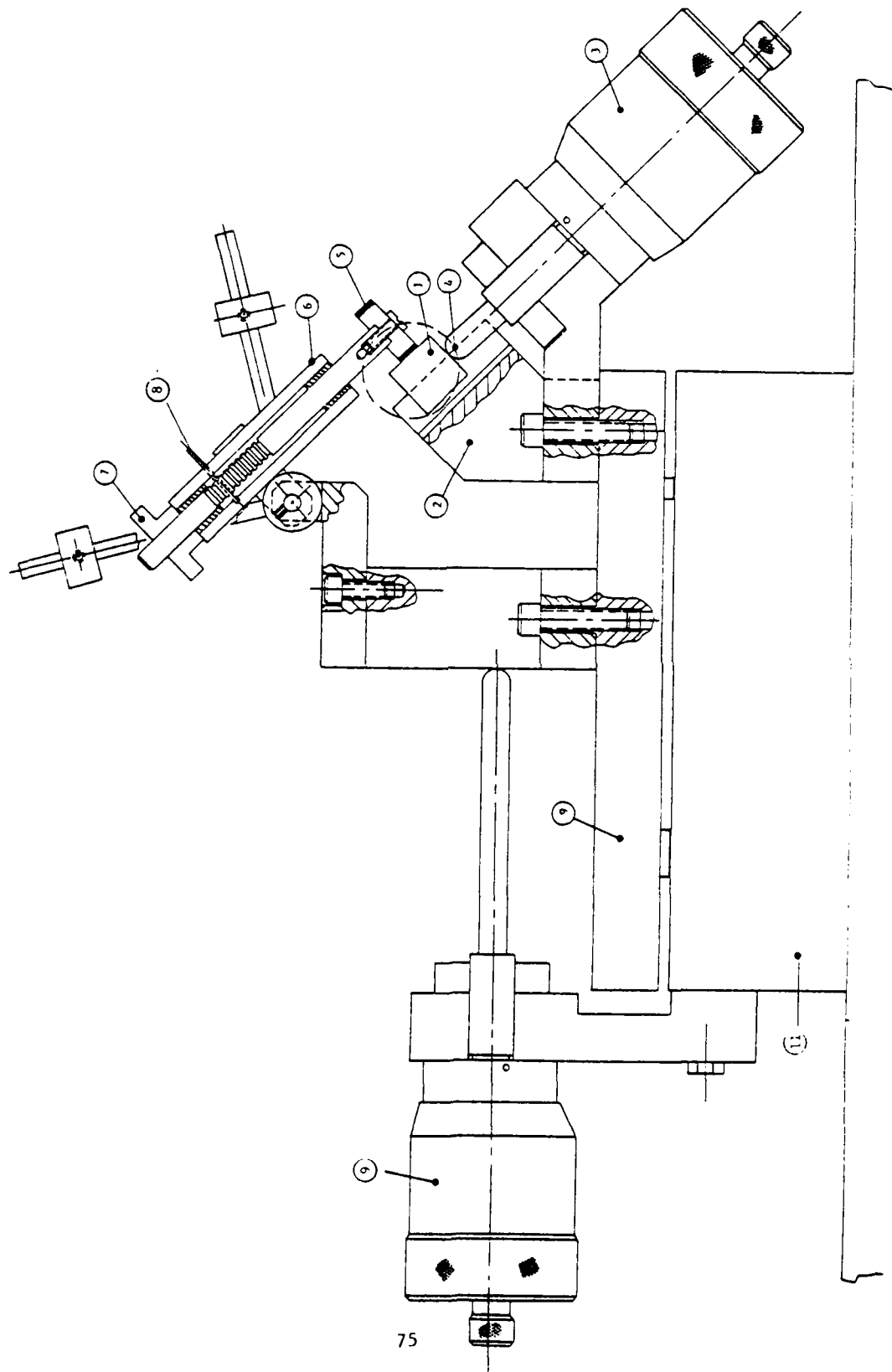


Fig. 26 Contour Measuring Gage - Elevation View

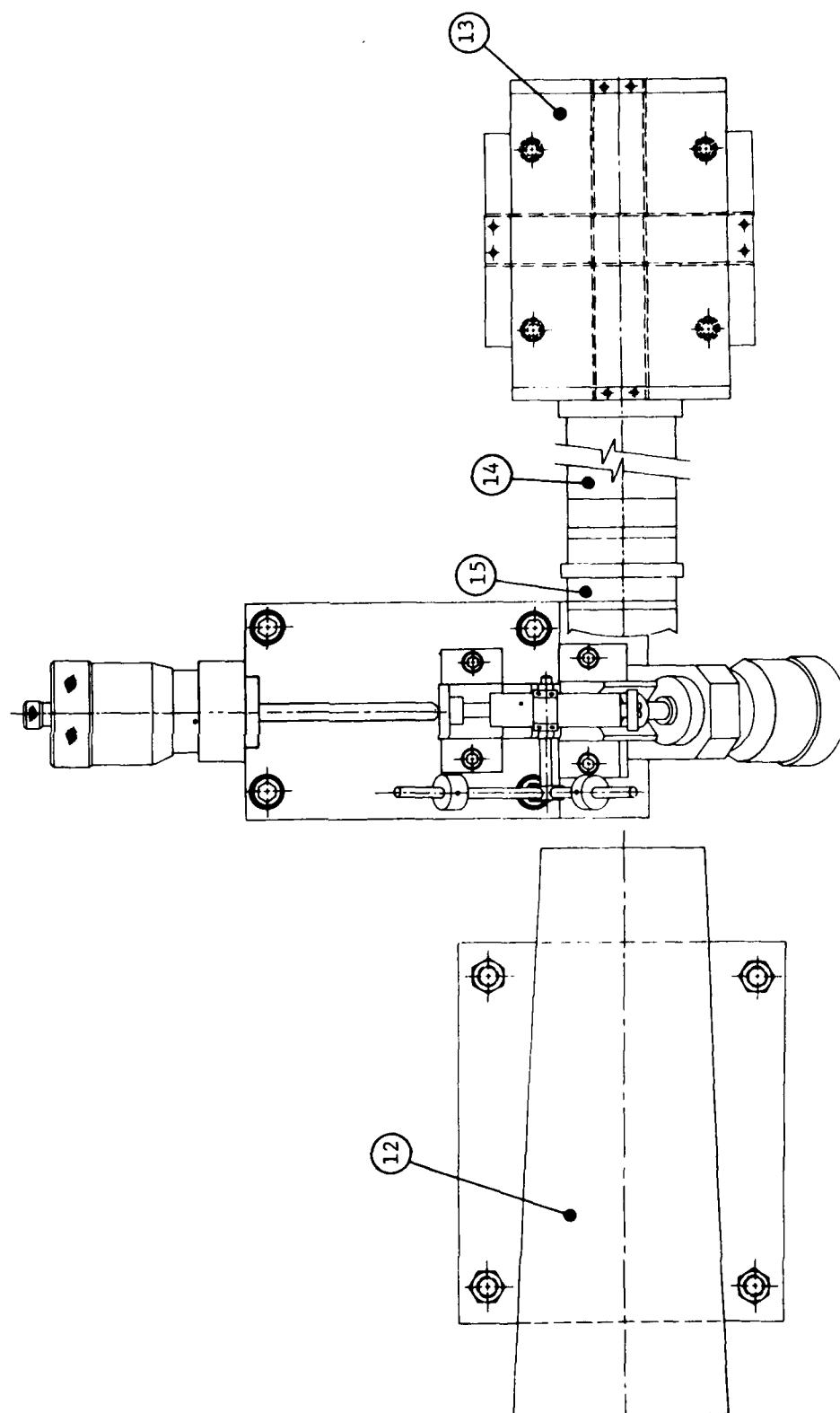


Fig. 27 Contour Measuring Gage - Plan View

One additional axis of motion is required to fully position the roller within the line scan camera field of vision. With the vertical position of the roller established by the axially oriented micrometer and the circumferential roller position maintained by the rubber covered wheel, a second micrometer (9) provides the horizontal roller position. This micrometer is used to traverse a roller across the line scan camera field of view.

Accurate traversing of the roller is critical to contour measuring since any vertical mispositioning of the roller will be interpreted by the camera as a change of contour.

To reduce the tracking error to a minimum, the entire roller support assembly, including the axial micrometer and the circumferential rolling wheel, is mounted on a precision frictionless gas bearing slide (10). The tracking accuracy of this support bearing is 0.2×10^{-6} inch; entirely adequate for the level of accuracy required for the contour measurements. The axial micrometer (9) attached to the same base (11) as the gas bearing slide can now easily position the roller and its mounting block anywhere within the required camera field.

In the plan view, Figure 27, the positioning of the collimating light source (12), and the line scan camera (13) with its extension tubes (14) and lens (15) is shown.

To measure a roller contour the sample roller is placed in the "V"-block. The circumferential rolling wheel is positioned and both micrometers are adjusted so that the maximum high point of the roller's corner radius blocks light from at least 95 percent of the total diodes in the array. At this roller location the roller corner runout is measured by rotating the rubber covered wheel. The relationship between the roller and the photodiode array at this time is shown as position (A) on Figure 28.

When the corner runout measurement is completed, the horizontal micrometer (Item 9 on Figure 26) is backed off until position (B) in Figure 28 is reached. The diode count at this point should lie between 1 and 30. At this time the horizontal micrometer is indexed in small increments and the diode count is noted at each incremental step until the roller position (C) is reached where again the diode count lies between 1 and 30. On small rollers the single scan

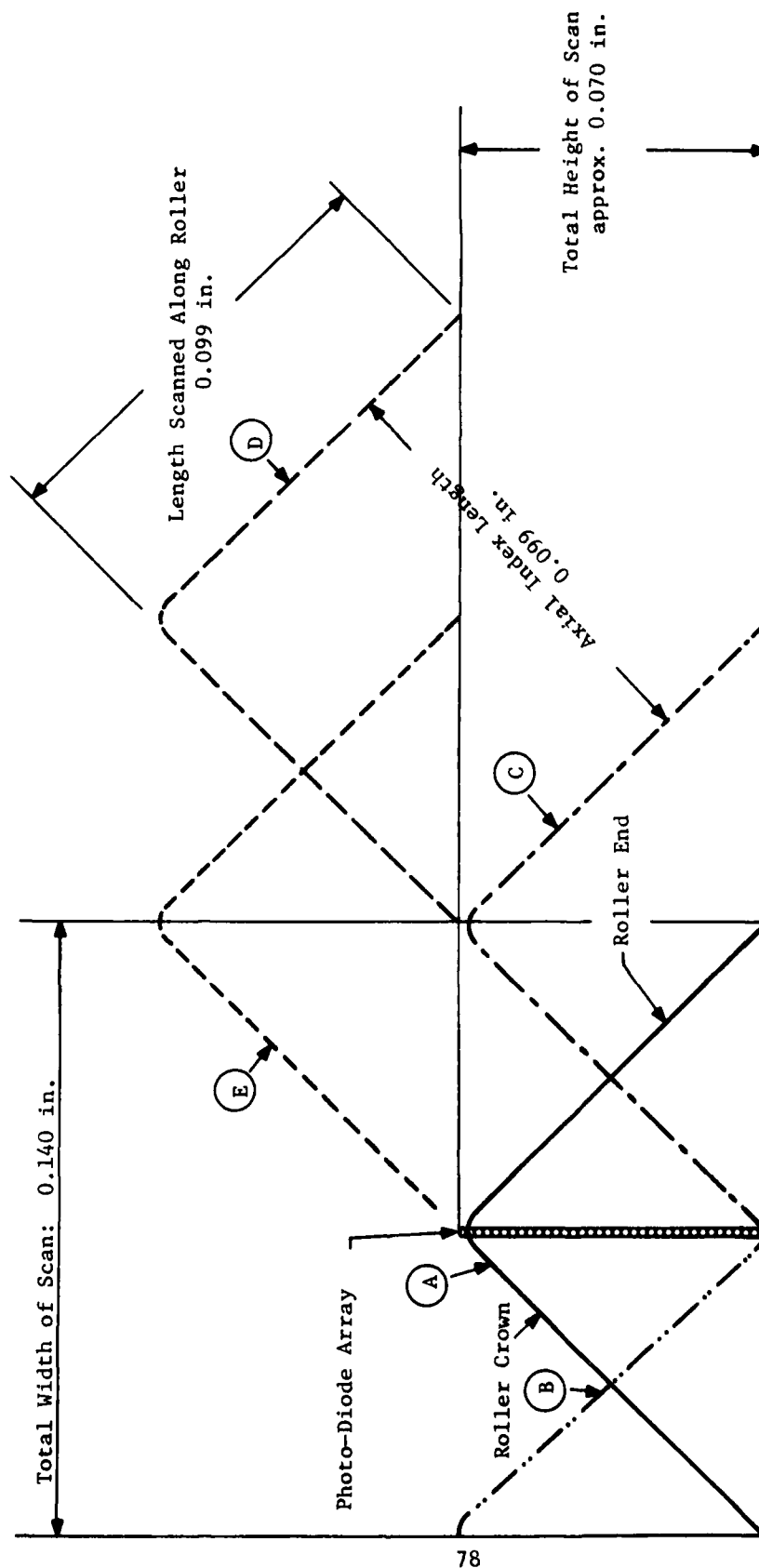


Fig. 28 Roller Positions During Contour Measurements

described above should provide sufficient data to determine all the roller contour characteristics required for that roller end. If this is the case, the roller can be reversed in the "V" block and the entire procedure repeated. The criterion for this condition is that the scan must include at least one-third ($1/3$) of the central flat length. If the roller is too large to meet this requirement, the remainder of the roller inspection must be obtained by completing the following procedure until the one-third ($1/3$) criterion is achieved.

When the target roller reaches position (C) on Figure 28, and its inspection is not complete, the axial micrometer (item (3) on Figure 26) is employed to reposition the roller to location (D) on Figure 27. The horizontal micrometer is then backed-off placing the roller in position (E) to start the second scan. The back-off position is necessary to eliminate back-lash in the micrometer screw from introducing measurement errors.

Incremental indexing of the horizontal micrometer is then repeated until roller position (D) is again reached. The above procedure is repeated until the roller inspection is completed. It should be noted that for these additional steps it is not necessary to provide data for the roller end but only for the roller crown, sufficient data were obtained from the first scan to define the roller end contour. The compilation of a complete roller contour is made by relating the micrometer readings at the beginning and end of each scan to generate a montage of the roller profile. The determination of the roller contour characteristics is then computed according to the method described in the roller support evaluation section of this report.

Central flat centrality is established by relating the crown to the central flat location measured from both roller ends to the roller length measured by the axial measurement gage described in the axial measurement gage section.

Acquisition and reduction of the breadboard gage data were manual. In the automated system, the entire data acquisition and reduction function will be computer controlled and processed. The line scan camera is already designed for that type of system, a replacement of both micrometers with motor driven indexing devices and position encoders will permit the entire scan sequence to be performed without operator interference.

The assembled contour measurement gage is shown installed on a granite surface plate in Figure 29.

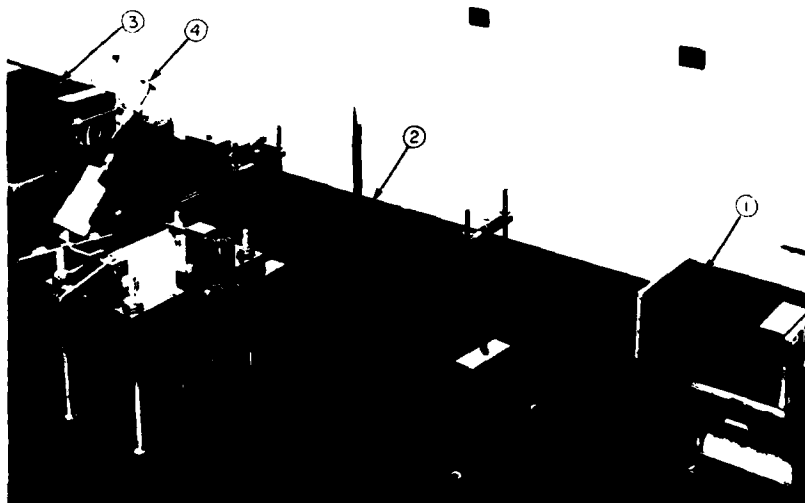


Fig. 29 Contour Gage Module

Identified on this photograph is the line scan camera (1), the extension tube and lens assembly (2), the collimated light source (3) and the contour gage fixture (4). A more detailed picture of the gage fixture is shown in Figure 30. Figure 30a shows the gage as it would be when a roller is being installed or retrieved from the gage.

In Figure 30a the roller rotating wheel assembly (1) is shown in its retracted position and a roller (2) in its gaging position in the 90° 'V'-block (3). The orientation of the counterbalance weights (4) holds the wheel in its disengaged position. Also visible in this photograph are the axial and horizontal micro-meters (5) and (6), the gas bearing slide (7), the illuminating light source (8) and the line scan camera lens (9). Figure 30b, is presented to illustrate the position of the roller rotating wheel assembly (1) when inspection data are taken.

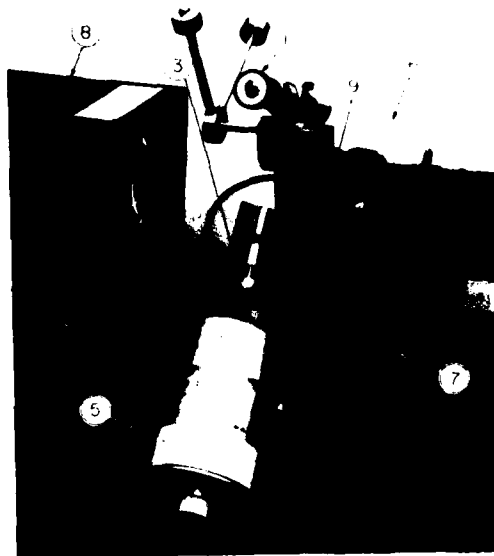


Fig. 30 Contour Gage Module - Gaging Fixture

SECTION V
BREADBOARD GAGE EVALUATION

Two basic breadboard gages were constructed to evaluate the gaging concepts incorporated in their design. One of the two gages contained several change-over components which permitted conversion from a gage making radial measurements to one making axial measurements, the second gage was devoted to making only contour measurements. Each of the gage modules was evaluated for performance with regard to usability and function according to an approved test plan. Evaluation results generated through completion of the test plan were then compared to similar evaluations conducted at roller manufacturer facilities using existing gaging equipment and techniques accepted as standard for the industry. Statistical methods were used to compare the two gaging methods in order to estimate the adequacy of roller inspections performed by the breadboard modules.

1. Test Plan Summary

The approved test plan found in Appendix B provided for three evaluation steps which are summarized as follows. The first step in the implementation of the test plan was to evaluate the functionality of each module. To perform this evaluation, each module was assembled and a roller put through an inspection process. The results of this test were to determine how the gage handled the roller; not necessarily how well the measurements were performed. When each module had been examined in this manner, the second step in the evaluation was performed.

In the second evaluation step, 100 consecutive readings of the 16 mm roller characteristics measured on the breadboard gages were compared to similar, conventionally taken measurements that were supplied by roller manufactures. The data were compared statistically to determine the mean as well as the standard deviations of the data. This step in the evaluation was primarily concerned with repeatability. In order to investigate the ability of the gage to make valid measurements on rollers of different sizes, a third step in the evaluation test plan is required.

The third test plan step involved the inspection of two roller lots consisting of 25 rollers each, one lot having 16 mm diameter rollers, the second lot

made up of 7 mm diameter rollers. A direct comparison of measured quantities was intended to indicate breadboard gage adequacy. Results of the test plan implementation are shown in the following report sections.

2. Radial/Axial Gage Module Evaluation

As previously mentioned, the initial intent of the breadboard gage design was to provide independent modules to measure radial and axial roller characteristics. It became apparent during the gage assembly that the two functions could be combined and performed concurrently, and it was in this configuration that the approved test plan was initiated. The application of the test plan provided the following results.

Functional Check

The functional check of the radial gage module was performed by installing a sample roller in its proper gaging position and proceeding through the necessary motions to fully measure the roller. Initially, the roller is statically measured for diameter, taper and crown drop (taken without roller rotation). The roller is then rotated to obtain the dynamic measurements of crown concentricity and two point out-of-roundness.

The static measuring function appeared entirely satisfactory but difficulty was experienced as an attempt to obtain the dynamic measurement was made.

As the rubber covered wheel rotated the sample roller, several malfunctions were noted. One malfunction resulted from small particles of rubber that rubbed off the wheel and were drawn under the roller thereby causing very erratic roller motion. A second more serious problem was caused by the tungsten carbide plasma sprayed wear surface coatings on the 90° "V" block. Even though the surfaces were lapped to at least an 8 μ finish, the porous nature of the surface resulted in severe scoring of the rollers flat cylindrical area.

Two less serious functional problems with the radial gage module were also identified during this portion of the evaluation test. One difficulty was the inability to provide a constant rotating force on the rollers when the roller rotating wheel was hand operated. A second difficulty resulted from a less than ideal location of the wheel tangent point of the sample bearing roller. When the roller rotating assembly was in its operating position stick-slip rotation of the roller resulted.

All the difficulties with the functional performance of the gage were easily remedied as indicated by the following list of corrective procedures.

- The rubber covered wheel, used to rotate the roller undergoing inspection was replaced by a wheel employing a silicon rubber O-ring. This change improved the roller wheel traction and eliminated rubber particles from interfering with the inspection process.
- The tungsten carbide plasma sprayed wear surfaces on the 90° "V" gaging block were repaired by removing the plasma spray and replacing it with sintered tungsten carbide blocks. These blocks were then ground and lapped flat to 8 μ rms. After the rework of the gaging block, damage to the roller no longer occurred.
- A clock motor was added to the roller rotating mechanism to eliminate the erratic rotation caused by hand operation.
- The roller rotating mechanism support bracket mounting holes were elongated to permit position adjustment.

A photograph of the modified radial/axial gage module is shown as Figure 31. Identified in the photograph is the new silicone rubber O-ring driving wheel and a new driving belt along with a reduction gear for the drive motor. A second photograph, Figure 32, shows the installation of the drive motor.

A functional check was performed on the radial/axial gage assembly after the modifications were completed. No apparent malfunctions of the gage were noted; the corrective procedures had eliminated all the previously noted difficulties. The satisfactory completion of the function check permitted the initiation of the repeatability portion of the gage evaluation.

Repeatability Check

In the evaluation of breadboard gage repeatability, more emphasis is placed on the standard deviation of the measurement data than on the mean value obtained. The reasoning behind this concentration on the standard deviation is based on the following argument. When making precision measurements, more confidence can be placed on the measurement results if the repeatability of the gage is established since the operator can be assured the readings taken at one time will be duplicated by data taken at a later time.

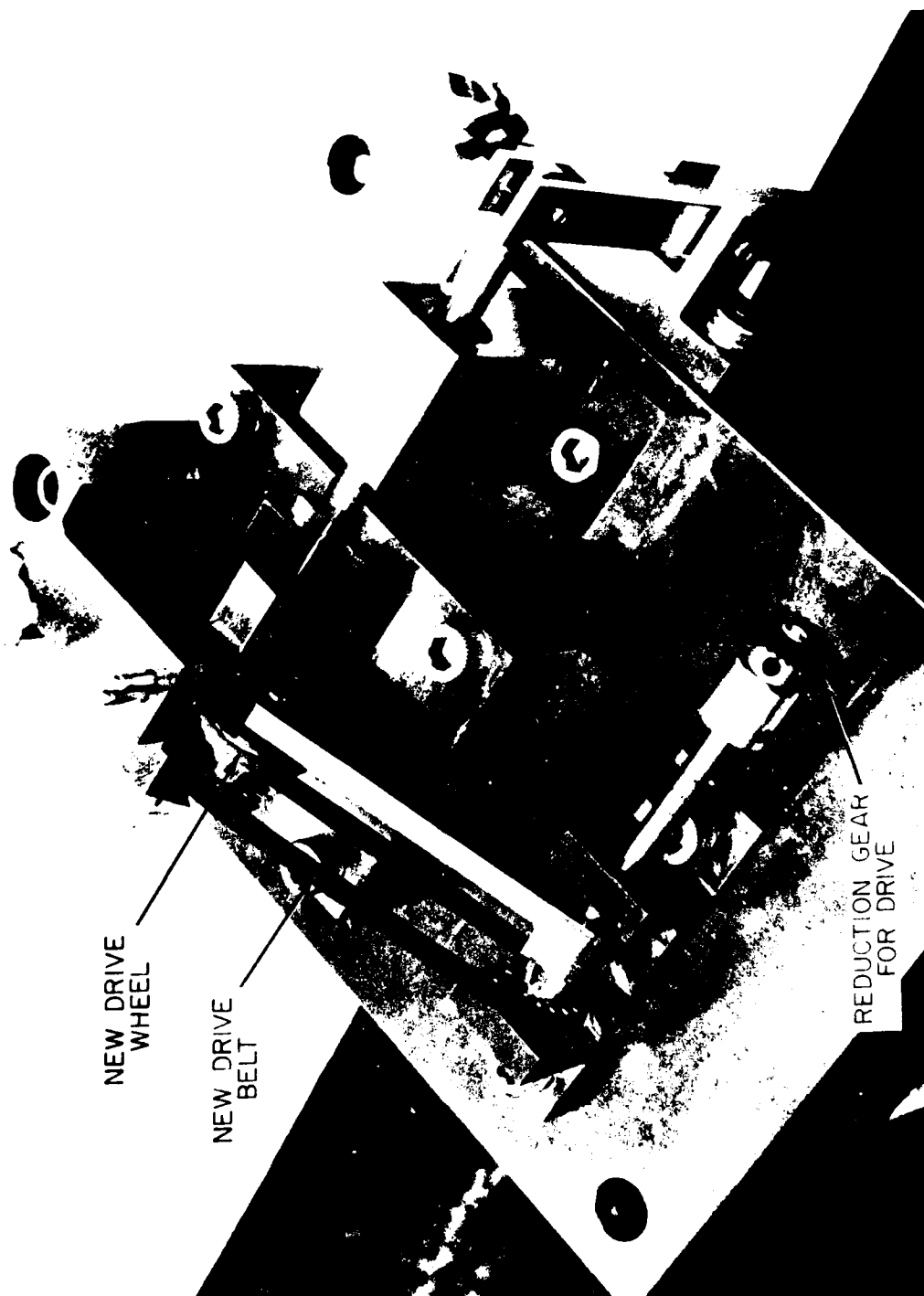


Fig. 31 Modified Radial/Axial Gage Module

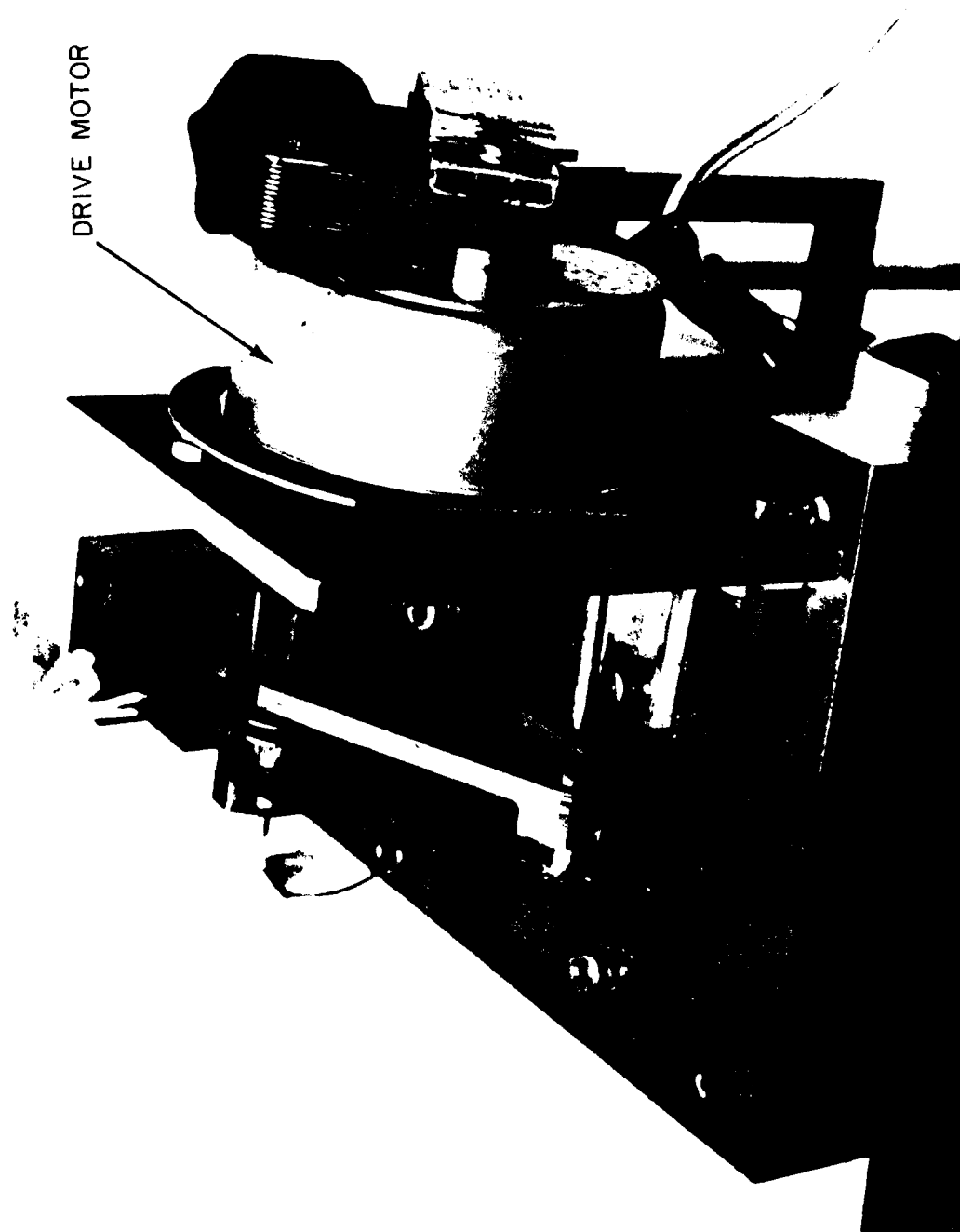


Fig. 32 Drive Motor Installation; Radial/Axial Gage Module

The absolute accuracy of the gage, however, depends primarily on the ability to establish an accurate calibration technique, which once set can be repeated with confidence. In the course of the functional checks it became apparent that the absolute calibration of the gages would be difficult since special, high-quality gaging rollers of exact diameter would be required. Rather than have the program delayed because of gage roller procurement, commonly available gage blocks were used for in-place calibration.

The first data taken on the radial configuration of the radial/axial module were what will be referred to as static measurements, i.e., those measurements taken without the need to rotate the roller. These data include:

- Diameter
- Crown drop
- OD Taper
- Length

For the static measurements extreme care was taken to assure that the roller was identically placed in the gage.

The second set of data taken will be referred to as dynamic data; i.e., that data which must be taken while the roller is being rotated in the gage.

These data include:

- 2 point out-of-roundness
- Crown Concentricity
- End Parallelism
- End Runout

In all evaluation tests the comparison will be made between data taken on the breadboard with data taken with conventional gages by a military aircraft turbine engine bearing manufacturer.

Only evaluation data for the roller diameter and crown drop measurements are tabulated and included in this report. The evaluation of all the other characteristics has been performed but only the results will be presented. The data will remain on file and can be provided as required.

The repeatability evaluation of the radial/axial breadboard gage required that it be compared with the manual gaging. Proof of repeatability will consist of obtaining the same reading on each set of rollers as obtained by conventional gaging methods. Since the conventional gage and the breadboard gage will be similarly set-up mechanically, it would seem that comparison of a set of measurements would be sufficient.

Unfortunately, the situation is not that simple. It is well known that successive readings on the manual gage do not usually give the same result. Theoretically, the dimensions of a single roller are fixed. The measured dimensions vary from this value for a number reasons, such as:

- Small local roller variations
- Variations in operator handling
- Inability to set the roller at the true gaging position for each measurement.
- Temperature

For these reasons, measurements on a single roller vary from reading to reading and have a statistical behavior. If a large number of readings are taken, there will be a mean value, M , and a standard deviation from the mean, σ , representing the spread of the data that can be calculated.

In view of this statistical behavior of roller measurements, where σ may be significant, successive readings are likely to differ. Consequently, comparison between the breadboard gage and the presently used gages based on a single set of readings cannot be expected to be meaningful as proof of the performance of the automatic gage.

A meaningful comparison can be made by making a large number of measurements, N , on both the manual and breadboard gages from which the following can be calculated:

$M_P \quad \sigma_P$ for the manual gage

$M_B \quad \sigma_B$ for the automatic gage

AD-A085 740

MECHANICAL TECHNOLOGY INC LATHAM N Y

F/G 13/9

THE DEVELOPMENT OF AN AUTOMATED ROLLER INSPECTION SYSTEM USING --ETC(U)

NOV 79 M # EUSEPI

F33615-77-C-3142

UNCLASSIFIED

MTI-79TR60

AFAL-TR-79-2076

NL

2 of 2

AD-A085 740



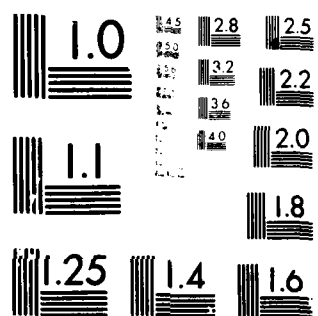
END

DATE

FILED

7-80

DTIC



MICROCOPY RESOLUTION TEST CHART
NATIONAL BUREAU OF STANDARDS-1963-A

If the two measurement systems are identical, then M_B will be almost identical to M_P , differing only by the amount that can be expected to result from two samples of size N taken from the same distribution with a standard deviation σ . This is given by:

$$(M_B - M_P) < 2 \frac{\sigma}{\sqrt{N}} t(0.025, N-1)$$

with 95 percent probability. Similarly, the standard deviations will also be almost identical, differing only by:

$$(\sigma_B^2 - \sigma_P^2) < (N-1) \sigma^2 \left[\frac{1}{\chi^2_{(N-1, 975)}} - \frac{1}{\chi^2_{(N-1, 0.025)}} \right]$$

with 95 percent probability. Here t and χ^2 are the variables from the standard t and χ^2 distributions.

If M_B is significantly different than M_P , then one would look for errors in the breadboard gage. For example, are the sensor calibrations accurate? If σ_B is significantly larger than σ_P , greater variability of the breadboard gage would be indicated.

For the repeatability determination, 100 measurements of a single roller for each characteristic listed on Table 1 were obtained on presently used gages. The mean thus obtained will be within 0.45σ of the true mean with a 95% probability. In this way, the intrinsic statistical behavior of a roller in the conventional gages will be determined.

For evaluation in the breadboard gage the identical procedure was followed. Comparisons were then made using the analysis found in Appendix A.

The results for the static roller measurements are shown in Table 17, with tabulated data for the roller diameter and crown drop shown on Tables 18 and 19. The differences in mean values found by examining Tables 18 and 19 are to be expected since each data set was taken with a different roller. A different roller was used because the one used for conventional measurements

TABLE 17

TABULATED RESULTS
AXIAL/RADIAL BREADBOARD GAGE
REPEATABILITY EVALUATION

"Static" Measurements

Number of Samples: 100

Mean Value: Within 0.45σ of True Mean with
a Probability of 95%

Characteristic	Standard Deviation	
	Breadboard	Conventional
Diameter	3.9×10^{-6}	9.6×10^{-6}
Crown Drop	6.7×10^{-6}	6.0×10^{-6}
Length	13.0×10^{-6}	4.8×10^{-6}
O.D Taper	5.7×10^{-6}	5.6×10^{-6}

TABLE 18

ROLLER OUTER DIAMETER MEASUREMENT

BREADBOARD GAGE EVALUATION

SPECIMEN RANK ORDER	I	II
	CONVENTIONAL	BREADBOARD
1	.629980E+00	.629677E+00
2	.629990E+00	.629679E+00
3	.629980E+00	.629680E+00
4	.629990E+00	.629675E+00
5	.630000E+00	.629680E+00
6	.629980E+00	.629677E+00
7	.629980E+00	.629673E+00
8	.630000E+00	.629685E+00
9	.629990E+00	.629676E+00
10	.630000E+00	.629679E+00
11	.630000E+00	.629679E+00
12	.629990E+00	.629675E+00
13	.630000E+00	.629679E+00
14	.629990E+00	.629679E+00
15	.629980E+00	.629676E+00
16	.629980E+00	.629678E+00
17	.629980E+00	.629676E+00
18	.629990E+00	.629674E+00
19	.629990E+00	.629674E+00
20	.629980E+00	.629675E+00
21	.629980E+00	.629676E+00
22	.629990E+00	.629671E+00
23	.629980E+00	.629673E+00
24	.629990E+00	.629677E+00
25	.629990E+00	.629674E+00
26	.630000E+00	.629677E+00
27	.629990E+00	.629675E+00
28	.630000E+00	.629674E+00
29	.629990E+00	.629674E+00
30	.630000E+00	.629673E+00
31	.629990E+00	.629673E+00
32	.629990E+00	.629677E+00
33	.629990E+00	.629672E+00
34	.629990E+00	.629673E+00
35	.629990E+00	.629673E+00

TABLE 18 cont'd.

36	.629970E+00	.629679E+00
37	.629980E+00	.629673E+00
38	.629980E+00	.629672E+00
39	.629980E+00	.629672E+00
40	.629990E+00	.629680E+00
41	.629980E+00	.629674E+00
42	.629990E+00	.629674E+00
43	.629990E+00	.629672E+00
44	.630000E+00	.629671E+00
45	.630000E+00	.629671E+00
46	.629990E+00	.629672E+00
47	.629970E+00	.629674E+00
48	.629970E+00	.629674E+00
49	.629980E+00	.629673E+00
50	.629980E+00	.629671E+00
51	.630000E+00	.629675E+00
52	.629980E+00	.629671E+00
53	.629980E+00	.629674E+00
54	.629980E+00	.629673E+00
55	.629980E+00	.629672E+00
56	.629980E+00	.629672E+00
57	.629980E+00	.629669E+00
58	.629990E+00	.629673E+00
59	.629990E+00	.629674E+00
60	.629990E+00	.629674E+00
61	.629990E+00	.629670E+00
62	.629970E+00	.629671E+00
63	.629980E+00	.629671E+00
64	.629990E+00	.629673E+00
65	.630000E+00	.629672E+00
66	.629990E+00	.629673E+00
67	.630000E+00	.629672E+00
68	.629990E+00	.629673E+00
69	.629990E+00	.629670E+00
70	.629990E+00	.629671E+00
71	.629960E+00	.629672E+00
72	.629965E+00	.629671E+00
73	.629980E+00	.629670E+00
74	.629965E+00	.629672E+00
75	.629965E+00	.629671E+00
76	.629965E+00	.629671E+00
77	.629970E+00	.629671E+00
78	.629980E+00	.629670E+00
79	.629970E+00	.629676E+00
80	.629975E+00	.629669E+00
81	.629970E+00	.629673E+00
82	.629970E+00	.629677E+00
83	.629975E+00	.629677E+00
84	.629970E+00	.629680E+00
85	.629985E+00	.629679E+00
86	.629985E+00	.629683E+00

TABLE 18 cont.

87	.629975E+00	.629682E+00
88	.629985E+00	.629681E+00
89	.629985E+00	.629677E+00
90	.629980E+00	.629679E+00
91	.629985E+00	.629689E+00
92	.629980E+00	.629688E+00
93	.629985E+00	.629682E+00
94	.629985E+00	.629678E+00
95	.629990E+00	.629674E+00
96	.629980E+00	.629674E+00
97	.629985E+00	.629673E+00
98	.629980E+00	.629673E+00
99	.629990E+00	.629673E+00
100	.629995E+00	.629674E+00
MEAN	6.2998E-01	6.2967E-01
STD DEV	9.5795E-06	3.8799E-06

TABLE 19

CROWN DROP

BREADBOARD GAGE EVALUATION

SPECIMEN RANK ORDER	I	II
	CONVENTIONAL	BREADBOARD
1	.1415000E-02	-.1654335E-02
2	.1415000E-02	-.1647711E-02
3	.1410000E-02	-.1645630E-02
4	.1400000E-02	-.1656283E-02
5	.1400000E-02	-.1647008E-02
6	.1410000E-02	-.1646822E-02
7	.1400000E-02	-.1655658E-02
8	.1400000E-02	-.1637322E-02
9	.1400000E-02	-.1648787E-02
10	.1400000E-02	-.1649982E-02
11	.1400000E-02	-.1647952E-02
12	.1410000E-02	-.1655631E-02
13	.1400000E-02	-.1650849E-02
14	.1400000E-02	-.1655803E-02
15	.1405000E-02	-.1649642E-02
16	.1410000E-02	-.1650303E-02
17	.1390000E-02	-.1654614E-02
18	.1390000E-02	-.1654666E-02
19	.1400000E-02	-.1652555E-02
20	.1400000E-02	-.1652351E-02
21	.1400000E-02	-.1657636E-02
22	.1400000E-02	-.1660191E-02
23	.1400000E-02	-.1652606E-02
24	.1400000E-02	-.1654120E-02
25	.1400000E-02	-.1653922E-02
26	.1400000E-02	-.1651640E-02
27	.1400000E-02	-.1650954E-02
28	.1400000E-02	-.1655804E-02
29	.1390000E-02	-.1653657E-02

TABLE 19 (cont'd)

30	.1400000E-02	-.1653523E-02
31	.1400000E-02	-.1658236E-02
32	.1400000E-02	-.1652089E-02
33	.1400000E-02	-.1650798E-02
34	.1410000E-02	-.1652835E-02
35	.1410000E-02	-.1651456E-02
36	.1410000E-02	-.1644254E-02
37	.1410000E-02	-.1649155E-02
38	.1410000E-02	-.1657211E-02
39	.1410000E-02	-.1652257E-02
40	.1410000E-02	-.1644215E-02
41	.1410000E-02	-.1652838E-02
42	.1410000E-02	-.1652728E-02
43	.1410000E-02	-.1657333E-02
44	.1410000E-02	-.1664246E-02
45	.1412500E-02	-.1655618E-02
46	.1412500E-02	-.1657426E-02
47	.1412500E-02	-.1655706E-02
48	.1410000E-02	-.1657534E-02
49	.1410000E-02	-.1649560E-02
50	.1410000E-02	-.1667501E-02
51	.1410000E-02	-.1654917E-02
52	.1410000E-02	-.1655046E-02
53	.1410000E-02	-.1657176E-02
54	.1410000E-02	-.1650896E-02
55	.1410000E-02	-.1650307E-02
56	.1410000E-02	-.1649845E-02
57	.1410000E-02	-.1661658E-02
58	.1410000E-02	-.1655899E-02
59	.1410000E-02	-.1649620E-02
60	.1410000E-02	-.1647774E-02
61	.1410000E-02	-.1657958E-02
62	.1410000E-02	-.1654221E-02
63	.1410000E-02	-.1654117E-02
64	.1410000E-02	-.1651653E-02
65	.1410000E-02	-.1654922E-02
66	.1410000E-02	-.1648440E-02
67	.1410000E-02	-.1656860E-02
68	.1400000E-02	-.1653406E-02
69	.1400000E-02	-.1655915E-02

TABLE 19 (Cont'd)

70	.1390000E-02	-.1654013E-02
71	.1400000E-02	-.1650947E-02
72	.1395000E-02	-.1653909E-02
73	.1400000E-02	-.1658100E-02
74	.1395000E-02	-.1656029E-02
75	.1400000E-02	-.1653004E-02
76	.1400000E-02	-.1650517E-02
77	.1400000E-02	-.1652456E-02
78	.1400000E-02	-.1657940E-02
79	.1400000E-02	-.1644898E-02
80	.1400000E-02	-.1656870E-02
81	.1400000E-02	-.1651849E-02
82	.1400000E-02	-.1651732E-02
83	.1400000E-02	-.1644029E-02
84	.1400000E-02	-.1640387E-02
85	.1400000E-02	-.1636864E-02
86	.1400000E-02	-.1631620E-02
87	.1400000E-02	-.1633012E-02
88	.1400000E-02	-.1636903E-02
89	.1400000E-02	-.1641192E-02
90	.1400000E-02	-.1637885E-02
91	.1400000E-02	-.1636097E-02
92	.1400000E-02	-.1629698E-02
93	.1400000E-02	-.1638851E-02
94	.1400000E-02	-.1645504E-02
95	.1400000E-02	-.1650992E-02
96	.1400000E-02	-.1648599E-02
97	.1400000E-02	-.1650471E-02
98	.1400000E-02	-.1650084E-02
99	.1400000E-02	-.1647425E-02
100	.1400000E-02	-.1644642E-02

MEAN 1.4037E-03 -1.6510E-03
STD DEV 5.9511E-06 -6.7077E-06

was not available for use with the breadboard gages. The important parameter to consider, however, is the standard deviation σ which is an indication of the gage repeatability. The data from the breadboard gage for roller diameter shows a considerably lower standard deviation of $\sigma=3.9 \times 10^{-6}$ inch as compared to $\sigma=9.6 \times 10^{-6}$ inch for the conventional gage. This indicates that a very repeatable roller diameter measurement can be made on the breadboard gage concept.

The next data examined were for determining the repeatability of the crown drop measurement. The breadboard evaluation data were obtained from the difference in the readings of probes A & B of Figure 19.

For these data the breadboard gage performed almost as well as the conventional gage; the breadboard data having a σ of 6.7×10^{-6} as compared to the conventional gage data's σ of 6.0×10^{-6} . The difference in σ values is exceedingly small however, so that the ability of the breadboard gage to provide repeatable crown drop data must be considered satisfactory.

The third roller characteristic measured and evaluated was the roller outer diameter taper. The measurement was taken by recording the difference between the two adjacent diameter reading probes (probes B & C on Figure 19).

For these tests the breadboard gage data showed a standard deviation of 5.7×10^{-6} compared to a conventional gage standard deviation of 5.6×10^{-6} which is a favorable comparison.

The fourth and last static measurement taken on the axial/radial breadboard gage was that of roller length. For these data, a strip chart recording was taken while dynamic data were also being recorded. The chart calibration of 0.0001 in/div was used. A sample of the typical data is shown in Figure 33. The standard deviation of the length measurement data was a high 13×10^{-6} inch, compared to the conventionally obtained roller length data of 4.8×10^{-6} inch. The larger deviation of the breadboard results for the roller length measurement is in part the result of strip charting recording with little pen damping. The measurement results, however, are still within acceptable limits of the required measurement tolerance of 200×10^{-6} inch.

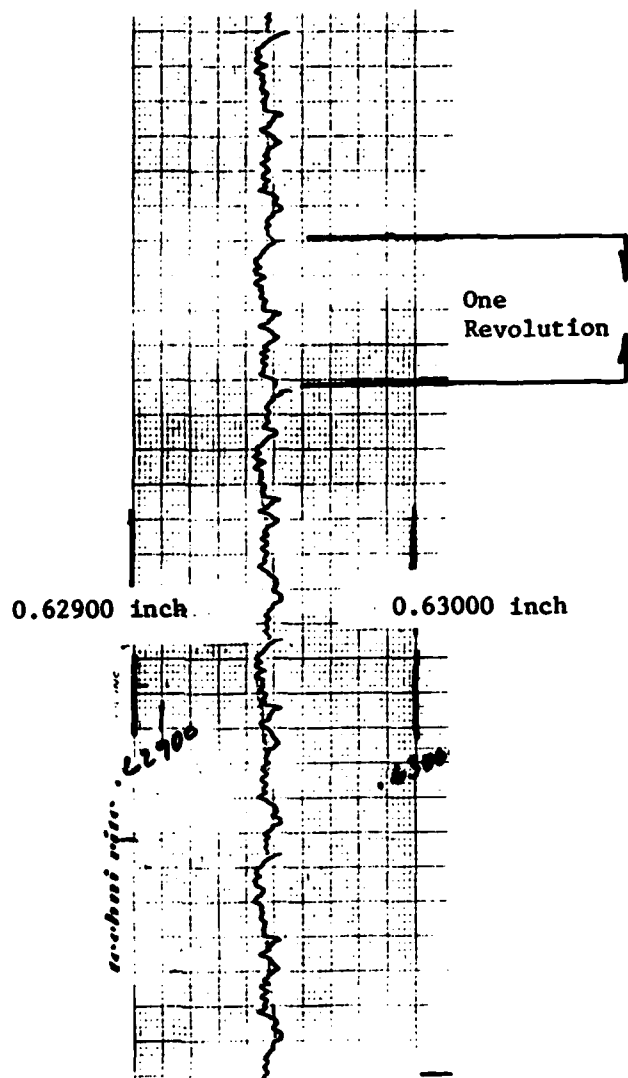


Fig. 33 Strip Chart - Roller Length Measurement;
Repeatability Test

Repeatability measurements of the four roller characteristics comprising the "dynamic" roller characteristics are listed in Table 20. For all but one characteristic the breadboard module did not produce inspection data with the same repeatability as that obtained by conventional means. The repeatability, however, was well within the acceptable tolerance levels. The one characteristic measurement performed on the breadboard gage which compares favorably with the conventional measurement is the two point out-of-roundness. The repeatability of this measurement is better than that produced by the conventional gage and, therefore, is also within acceptable limits when compared to the precision of the roller tolerance requirement for which the measurement is made.

The deviation shown by the end parallel data (4.8×10^{-6}), somewhat larger than that exhibited by the conventional gage (0.9×10^{-6}), is still small enough to assure accurate measurement of that characteristic.

The standard deviation of the crown concentricity measurement produced by the breadboard gage cannot be compared to that resulting from measurements taken by conventional means since no usable conventional data are available. The conventional data were listed as being less than a specific number rather than as a quantitative value.

The remaining data item shown on Table 20 is end runout. For this roller characteristic, the standard deviation of the breadboard gage (12×10^{-6}) is almost 2-1/2 times that of the conventional gage data (5.3×10^{-6}), resulting in a somewhat poorer showing for the repeatability of the breadboard gage when measuring this characteristic. The data for this characteristic measurement, as per the roller length, were taken from strip chart recordings. This recording was made with little or no pen damping and provided data which required interpretation by the person reducing the data leading to possible errors in establishing the dimension of the charted curve envelope.

The errors associated with manual data determination will be eliminated by the electronic data logging and computer function to be used in the automated gage, thereby producing more repeatable measurements.

TABLE 20

TABULATED RESULTS

AXIAL/RADIAL BREADBOARD GAGE

REPEATABILITY EVALUATION

"Dynamic" Measurements

Number of Samples: 100

Mean Value: Within 0.45σ of True Mean with
a Probability of 95%

Characteristic	Standard Deviation	
	Breadboard	Conventional
2 Point O/R	2.4×10^{-6}	3.0×10^{-6}
Crown Concen.	14×10^{-6}	Not Available
End Parallel	4.8×10^{-6}	0.9×10^{-6}
End Runout	12×10^{-6}	5.3×10^{-6}

Measurement Evaluation

At the conclusion of the repeatability test, several rollers in each of the two sizes, (16 mm and 7 mm), were measured in the breadboard module. These data can be compared to similar data taken by conventional gaging techniques. The results of both conventional and breadboard gaging are shown in Table 21.

The method of obtaining the breadboard evaluation data followed the procedure for obtaining the repeatability data and shows acceptable agreement with conventionally obtained data.

An identification problem developed at the start of the measurement evaluation, and as a result, less than 25 rollers in each size were measured. The identification of many rollers was established by attaching a self-sticking numbered label to individually wrapped rollers. During the course of handling the rollers, several labels became detached from their respective packets causing a total loss of roller identity.

The most critical parameter to be established in the direct measurement of rollers is the calibration of the sensors used. In the case of the radial/axial module, the probes used were calibrated in place by inserting gaging blocks of known thickness under each radial probe and between the two axial probes. This calibration technique, although entirely satisfactory for the axial probes, can introduce measurement errors for the radial probes because the capacitance formed by the probe sensing tip and the target is no longer obtained from two parallel surfaces but from one flat surface and a cylindrical surface. (See Appendix C.) Cylindrical plug gages were not obtainable with sufficient accuracy to be used as calibration gages; therefore some differences between conventional and breadboard measurements should be expected from this cause. Given sufficient incentive, the desired plug gages could be obtained from a bearing manufacturer's own shop thereby eliminating any calibration doubt.

The measurements obtained from the breadboard show sufficient accuracy and agreement to justify proceeding to the prototype gage design.

TABLE 21

RADIAL/AXIAL ROLLER DIMENSIONS

(All dimensions in 10^{-6} inch except diameter, length which are in inches)

Roller S/N	7mm Diameter x 7mm Long Rollers									
	Crown				Diameter		Length		Crown Drop	
	End Parallel Bread- Board	Conven- tional	Concen- tricity	Bread- Board	Conven- tional	Bread- Board	Conven- tional	Bread- Board	Conven- tional	Bread- Board
3	26	20	40	0.27551	0.27600	0.27558	0.27555	120	120	14
4	20	16	30	0.27559	0.27599	0.27556	0.27557	86	90	12
5	10	20	25	0.27559	0.27600	0.27558	0.27556	48	80	14
6	6	26	40	0.27543	0.27600	0.27558	0.27556	126	140	14
7	8	20	30	0.27543	0.27600	0.27557	0.27559	119	90	11
9	32	32	30	0.27546	0.27599	0.27557	0.27555	142	60	10
10	18	6	70	0.27557	0.27599	0.27553	0.27555	76	120	14
11	16	10	40	0.27562	0.27599	0.27561	0.27600	74	50	10
12	22	16	30	0.27557	0.27600	0.27567	0.27559	51	110	10
13	32	6	30	0.27558	0.27598	0.27560	0.27556	72	80	12
14	16	8	10	0.27557	0.27600	0.27556	0.27557	84	210	10
15	22	30	30	0.27555	0.27600	0.27562	0.27558	93	80	10
16	16	20	20	0.27553	0.27600	0.27564	0.27557	111	100	10
17	24	16	30	0.27548	0.27599	0.27556	0.27557	144	150	10
18	20	20	30	0.27559	0.27600	0.27562	0.27557	83	200	10
19	24	20	20	0.27549	0.27599	0.27564	0.27557	129	250	12
20	20	20	30	0.27566	0.27601	0.27567	0.27555	119	100	10
21	20	20	40	0.27530	0.27600	0.27566	0.27559	131	20	12
22	10	10	30	0.27559	0.27599	0.27562	0.27547	85	20	10
23	20	8	30	0.27548	0.27599	0.27547	0.27556	63	40	12
25	16	10	10	0.27551	0.27600	0.27570	0.27559	47	160	12
27	24	36	20	0.27554	0.27600	0.27562	0.27553	20	140	14

TABLE 21 (cont'd)

16mm Diameter x 16mm Long Rollers														
Roller S/N	End Parallel		Crown Concentricity		Diameter		Length		Crown Drop		OD Taper		2 Pt Out-of-Round	
	Bread- Board	Conven- tional	Bread- Board	Conven- tional	Bread- Board	Conven- tional	Bread- Board	Conven- tional	Bread- Board	Conven- tional	Bread- Board	Conven- tional	Bread- Board	Conven- tional
97	30	< 20	70	40	0.62973	0.62980	0.62944	0.62950	3400	3400	148	<10	17	60
98	40		20	30	0.62980	0.62981	0.62951	0.62952	3388	3500	37		12	19
99	70		30	40	0.62980	0.62981	0.62955	0.62960	3446	3450	40		8	37
100	40		30	20	0.62975	0.62982	0.62945	0.62950	3412	3520	108		8	28
101	30		70	20	0.62981	0.62979	0.62955	0.62961	3390	3500	16		16	19
104	30		40	30	0.62981	0.62980	0.62942	0.62952	3566	3550	111		8	37
105	20		20	40	0.62976	0.62981	0.62955	0.62951	3270	3450	36		12	47
106	20		20	30	0.62976	0.62981	0.62954	0.62958	3345	3520	48		16	37
107	20		20	30	0.62979	0.62979	0.62942	0.62957	3403	3600	72		8	28
108	30		20	40	0.62979	0.62980	0.62946	0.62959	3397	3680	70		8	37
109	42		24	20	0.62780	0.62980	0.62991	0.62959	3344	3550	35		8	19
110	30		22	35	0.62978	0.62979	0.62955	0.62952	3360	3640	31		16	26
111	42		24	40	0.62978	0.62980	0.62945	0.62953	3417	3620	5		8	28
112	40		52	20	0.62982	0.62980	0.62939	0.62952	3353	3600	19		8	26
113	40		36	60	0.62982	0.62979	0.62960	0.62959	3308	3480	42		8	57
114	20		42	20	0.62982	0.62980	0.62954	0.62956	3419	3600	50		12	37
115	34		25	25	0.62982	0.62979	0.62939	0.62961	3436	3550	26		8	37
116	30		22	30	0.62981	0.62980	0.62951	0.62956	3410	3500	16		8	37
117	20		40	40	0.62981	0.62981	0.62955	0.62956	3406	3500	8		8	28
118	20		6	20	0.62980	0.62979	0.62960	0.62956	3328	3500	2		8	37
119	40		38	25	0.62980	0.62979	0.62952	0.62955	3523	3580	24		8	37
120	40		20	40	0.62979	0.62980	0.62955	0.62955	3385	3550	4		8	37
121	40		20	20	0.62979	0.62980	0.62940	0.62954	3453	3550	7		8	37

3. Contour Gage Module Evaluation

The evaluation of the contour gage module pictured in Figure 30 followed the radial/axial evaluation and was conducted in a similar manner. Three separate tests were performed on this module according to the test plan. These tests are described in the following report sections.

Functional Check

The functional check of the contour gage module was performed in the same manner as the check performed on the radial/axial module. A roller was placed in the gaging position and all the operations necessary to perform the contour inspection were performed. As expected, the same malfunctions which turned up on the radial/axial module appeared on the contour gage module. These malfunctions included:

- Debris from the rubber-covered wheel caused erratic roller movement
- Tungsten carbide plasma spray surface on the "V" block damaged the roller's outer diameter
- Hand-wheel rotation of the roller was erratic

The same corrective procedures were applied to the contour gage module as were successfully used on the radial/axial gage module. These procedures were:

- The rubber covered wheel, used to rotate the roller undergoing inspection, was replaced by a wheel employing a silicon rubber O-ring.
- The tungsten carbide plasma sprayed wear surfaces on the 90° "V" gaging block were replaced with sintered tungsten carbide blocks. These blocks were then ground and lapped flat to an 8 μ rms finish.
- A clock motor was added to the roller rotating mechanism.

A photograph of the modified contour gage module is shown as Figure 34. Identified in the photograph is the new silicone rubber O-ring roller

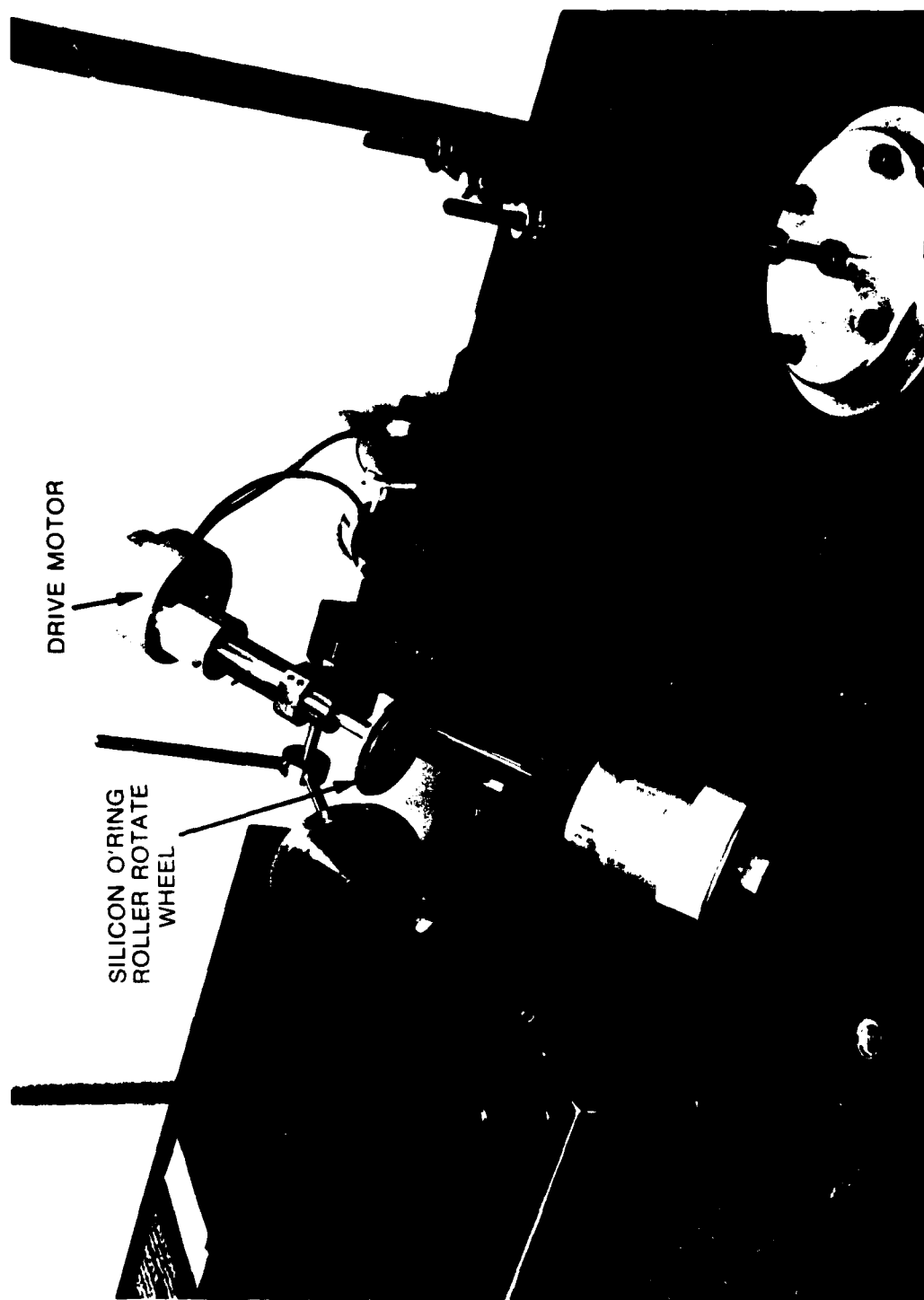


Fig. 34 Modified Contour Gage Module

rotation wheel, and the rotator motor. The tungsten carbide blocks, although installed are not visible under the micrometer shaft.

The successful completion of the functional check modifications permitted continuation of the test plan with the initiation of the repeatability evaluation of the contour gage module.

Repeatability Evaluation

The repeatability evaluation of the contour module was performed by successfully scanning the test roller over a significant portion of the diode array. The scanning process produced a diode count for every horizontal position of the roller within the diode field of view. A 13-step scan, taken at a horizontal translation increment of 0.25 mm, was used and repeated 25 times. The resulting data were statistically analyzed to provide the mean and standard deviation of the diode count data at each incremental position.

At the conclusion of the scanning evaluation, a roller was positioned in the line scan camera's field of view so that diode array looked at the high point of the roller's corner. The roller rotate wheel was then lowered into position and the roller rotated to evaluate the line scan camera's ability to measure corner runout.

The results of both the scan and runout evaluations are shown on Table 22. The standard deviation for the measurement of contour shows a sigma of 1.0 or less which means that the contour data's standard deviation is one diode count or less. This corresponds to a dimensional σ of 43×10^{-6} inch which should be entirely adequate for contour tolerance measurements. A similar result was obtained for the corner runout measurement where the σ was 33×10^{-6} or 0.77 of a diode count.

Conventional measurement techniques showed a $\sigma = 4.9 \times 10^{-6}$ in. for corner runout and a $\sigma = 5.48 \times 10^{-3}$ in. for the flat centrally. Corner breakout dimensions obtained by conventional inspection techniques were shown as having no deviation.

TABLE 22
REPEATABILITY EVALUATION DATA
CONTOUR GAGE MODULE

Curve Plotting

<u>Horizontal Translation*</u> <u>Axial Position Fixed</u>	<u>Mean Diode Count</u>	<u>σ^{**}(Diode Count)</u>
1	1109	.78
2	1307	.91
3	1480	.70
4	1600	1.0
5	1652	.28
6	1664	.27
7	1652	.37
8	1584	1.0
9	1388	.65
10	1172	.49
11	952	.44
12	734	.65
13	515	.93

Corner Runout

<u>Standard Deviation</u>	
<u>Line Scan Camera</u>	<u>Conventional</u>
33×10^{-6} in.	4.9×10^{-6} in.

N = 100, Mean will be 0.45σ of True Mean
with 95 Percent Probability

*Each horizontal translation increment 0.25 mm.

**Each diode count equivalent to 43×10^{-6} inch.

The procedure described on the previous page produced data directly related to the repeatability of the contour gages scanning process. This procedure was selected as an alternate to the complete repetitive measurement of a roller contour since the long and elaborate data collection and reduction effort required by manual data acquisition methods would not provide data any more effective than those described.

Measurement Evaluation

Each of the two roller lots previously measured for radial and axial dimensions were measured for contour in this phase of the contour gage module evaluation. The extreme amount of time required to manually collect and interpret the contour data was instrumental in arriving at the decision to measure only one rather than both ends of all rollers. This decision led to problems in data comparison because rollers measured by conventional means at a bearing manufacture's inspection facility, although identified by serial number, were not identified as to end location (which corner data related to which roller end). As a result, the measurement data cannot be directly related to a roller end; the data however should agree as to magnitude when related to one of the two end choices.

The procedure used in establishing the contour dimensions was identical to that described in section IV-4. The use of this procedure permitted the collection of data outlining a roller end, its corner and crown and a portion of its central straight cylindrical section. Figures 35 and 36 show the typical roller contour results obtained on the contour gage module.

The method used to determine roller contour characteristic dimensions was as follows:

- A line was drawn through the roller end data points establishing the roller end contour.
- A second line, perpendicular to the first line, was drawn through the data points defining the roller's straight cylindrical section.

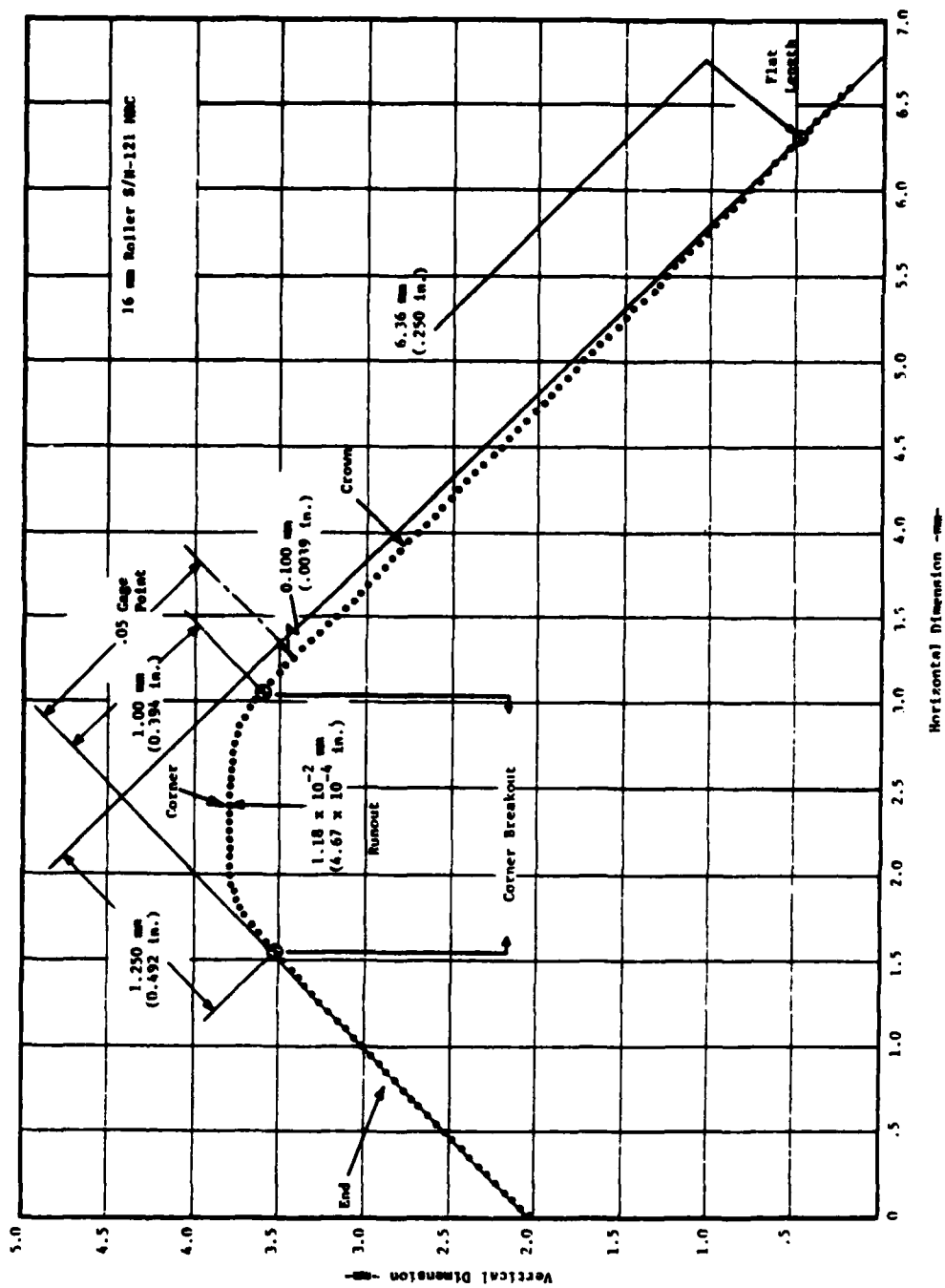


Fig. 35 Contour Scan - 16mm Dia Roller

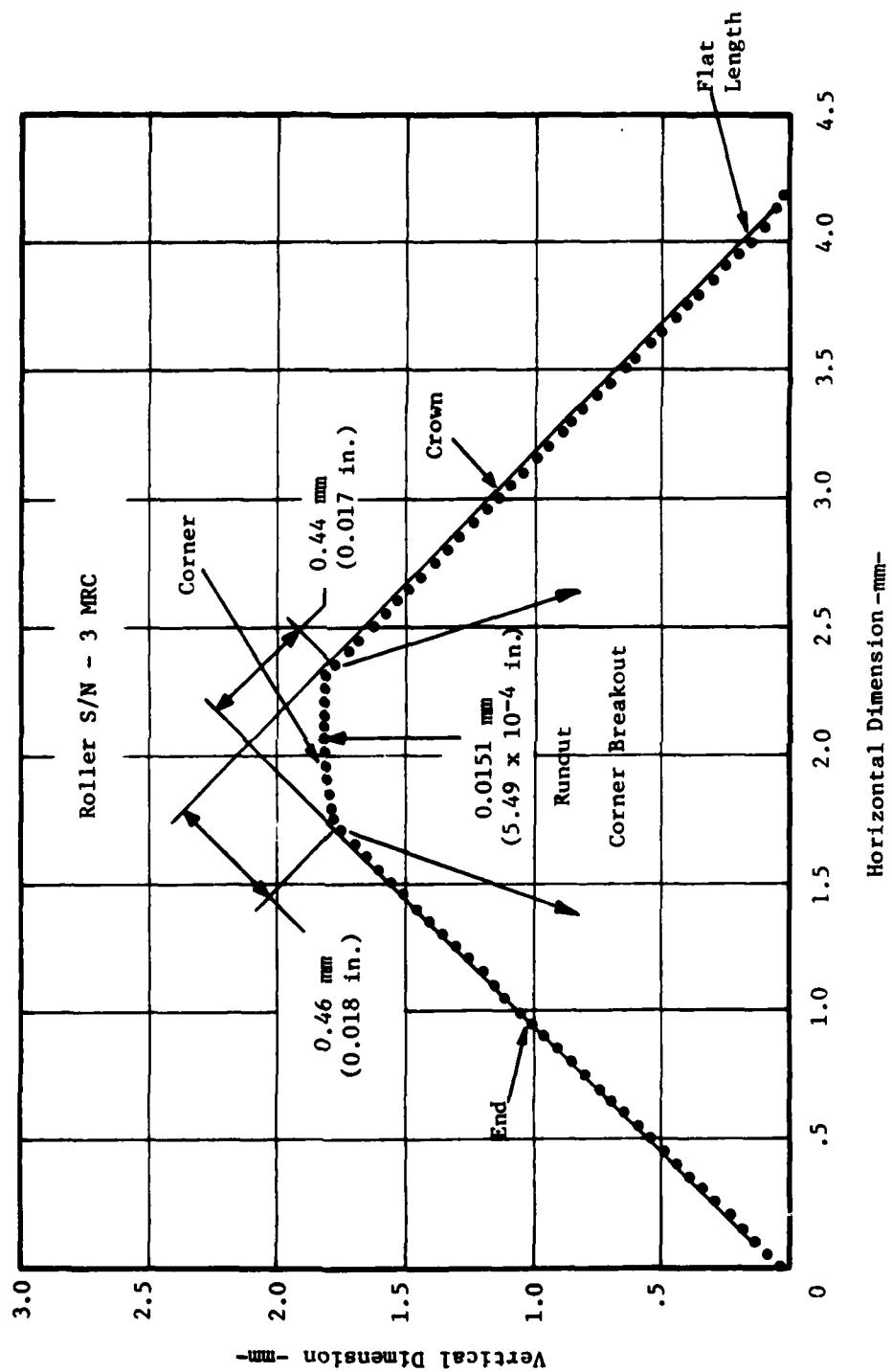


Fig. 36 Contour Scan 7mm Roller

- From the data points defining the roller corner, the location of where a curved line fitting these data and the lines through the end and crown data is estimated.
- In addition where a curved line representing the crown data intersects the straight cylindrical section is also estimated.

Actual roller characteristic dimensions such as corner breakout and the location of the straight cylindrical portion are obtained from the estimated location of the various roller curves relative to the two orthogonal lines originally drawn. In the case of the length and centrality of the central straight portion of the roller, the dimension actually measured is from the roller end to the cylindrical section. The centrality would be determined from the differences of dimension when measured from both roller ends. The length of the cylindrical section would be arrived at by subtracting the sum of the two measurements from the known roller length.

The above procedure was followed for each roller with the results listed on Table 23. For comparison, the contour data established by conventional inspection methods are also listed.

The corner runout of each roller was also measured by the method established in the Contour Measurement Gage Description portion of section IV. The results of these measurements is shown on Table 24.

Each of the readings listed for the contour gage evaluation requires visual interpretation of plotted data to establish the necessary roller dimensions. The probability of obtaining this interpretation manually with a high degree of accuracy is not high. The reasonably close agreement between the breadboard and conventional data is in part a direct function of the care used in the manual data reduction. A significant cause for the differences between breadboard and conventional contour data is discussed herein.

A reason for contour data differences between conventional and breadboard inspection methods is related to the actual profile of the roller's corner radius. In both the 16 mm and the 7 mm roller the corner is not a true radius but rather a nearly straight chamfer blended by small radii into the

TABLE 2.3
ROLLER CONTOUR MEASUREMENTS
(all dimensions in inches)

Roller	7mm Diameter x 7mm Long Rollers										16mm Diameter x 16mm Long Rollers									
	Corner Breakout					Flat Centrality					Corner Breakout					Flat Centrality				
	Outer Diameter		Roller End			Breadboard		Roller End			Outer Diameter		Roller End			Breadboard		Roller End		
	S/N	Breadboard	Conventional	Breadboard	Conventional	S/N	Breadboard	Conventional	Breadboard	Conventional	S/N	Breadboard	Conventional	Breadboard	Conventional	S/N	Breadboard	Conventional	Breadboard	Conventional
3	0.017	0.016	0.018	0.017	0.053	97	0.038	0.035	0.033	0.031	97	0.038	0.035	0.033	0.031	0.201	0.207	0.212	0.201	0.217
4	0.019	0.017	0.021	0.017	0.052	98	0.042	0.036	0.033	0.033	98	0.042	0.036	0.033	0.033	0.207	0.212	0.212	0.207	0.212
5	0.020	0.018	0.022	0.018	0.060	99	0.046	0.038	0.033	0.032	99	0.046	0.038	0.033	0.032	0.210	0.210	0.210	0.210	0.210
6	0.021	0.019	0.024	0.021	0.068	100	0.044	0.038	0.034	0.036	100	0.044	0.038	0.034	0.036	0.214	0.214	0.214	0.214	0.214
7	0.018	0.019	0.022	0.017	0.063	101	0.042	0.038	0.031	0.035	101	0.042	0.038	0.031	0.035	0.212	0.212	0.212	0.212	0.212
9	0.020	0.017	0.023	0.018	0.070	102	0.043	0.039	0.039	0.035	102	0.043	0.039	0.039	0.035	0.218	0.218	0.218	0.218	0.218
10	0.021	0.018	0.020	0.018	0.059	103	0.044	0.039	0.044	0.036	103	0.044	0.039	0.044	0.036	0.214	0.214	0.214	0.214	0.214
11	0.018	0.018	0.021	0.021	0.062	104	0.039	0.032	0.048	0.031	104	0.039	0.032	0.048	0.031	0.204	0.204	0.204	0.204	0.204
12	0.017	0.019	0.022	0.016	0.064	105	0.039	0.036	0.047	0.035	105	0.039	0.036	0.047	0.035	0.210	0.210	0.210	0.210	0.210
13	0.019	0.018	0.023	0.018	0.059	106	0.040	0.039	0.046	0.034	106	0.040	0.039	0.046	0.034	0.224	0.224	0.224	0.224	0.224
14	0.021	0.018	0.025	0.019	0.055	107	0.040	0.040	0.050	0.035	107	0.040	0.040	0.050	0.035	0.201	0.201	0.201	0.201	0.201
16	0.019	0.018	0.020	0.020	0.060	108	0.041	0.038	0.044	0.035	108	0.041	0.038	0.044	0.035	0.215	0.215	0.215	0.215	0.215
17	0.017	0.017	0.020	0.017	0.061	109	0.039	0.038	0.045	0.031	109	0.039	0.038	0.045	0.031	0.206	0.206	0.206	0.206	0.206
18	0.016	0.017	0.015	0.013	0.062	110	0.037	0.037	0.046	0.036	110	0.037	0.037	0.046	0.036	0.219	0.219	0.219	0.219	0.219
19	0.018	0.018	0.020	0.018	0.060	111	0.036	0.036	0.043	0.034	111	0.036	0.036	0.043	0.034	0.220	0.220	0.220	0.220	0.220
20	0.018	0.017	0.017	0.017	0.054	112	0.034	0.034	0.047	0.035	112	0.034	0.034	0.047	0.035	0.195	0.195	0.195	0.195	0.195
21	0.019	0.018	0.020	0.015	0.052	113	0.035	0.035	0.044	0.032	113	0.035	0.035	0.044	0.032	0.209	0.209	0.209	0.209	0.209
22	0.015	0.017	0.016	0.017	0.048	114	0.033	0.033	0.032	0.034	114	0.033	0.033	0.032	0.034	0.216	0.216	0.216	0.216	0.216
23	0.019	0.017	0.019	0.014	0.058	115	0.047	0.047	0.041	0.031	115	0.047	0.047	0.041	0.031	0.203	0.203	0.203	0.203	0.203
25	0.019	0.019	0.020	0.020	0.051	116	0.038	0.038	0.051	0.035	116	0.038	0.038	0.051	0.035	0.196	0.196	0.196	0.196	0.196
27	0.015	0.016	0.018	0.016	0.050	117	0.038	0.038	0.051	0.035	117	0.038	0.038	0.051	0.035	0.200	0.200	0.200	0.200	0.200
						118	0.049	0.049	0.039	0.031	118	0.049	0.049	0.039	0.031	0.216	0.216	0.216	0.216	0.216
						119					119									
						120					120									
						121					121									

TABLE 24

ROLLER CORNER RUNOUT MEASUREMENTS

- All Dimensions in 10^{-4} Inch -

7 mm Dia			16 mm Dia		
S/N	Breadboard	Conventional	S/N	Breadboard	Conventional
3	5.9	6.0	97	3.8	1.5
4	4.2	4.0	98	6.7	3.0
5	7.6	6.0	99	3.8	2.5
6	4.2	4.0	100	2.1	3.0
7	4.7	9.0	101	4.6	4.0
9	5.1	4.5	102	5.5	4.0
10	4.2	4.0	103	1.7	2.0
11	5.1	6.0	104	5.0	4.0
12	6.8	6.0	105	2.1	3.0
13	3.8	3.0	106	3.8	3.5
14	7.2	7.0	107	2.5	4.0
16	8.4	6.0	108	4.2	4.0
17	5.5	4.5	109	2.1	2.0
18	5.9	3.5	110	3.4	4.0
19	6.7	5.0	111	5.5	5.0
20	4.7	5.0	112	25.0	30.0
21	3.0	5.0	113	6.7	6.0
23	4.2	5.5	114	4.2	4.0
25	5.1	5.0	115	6.3	5.0
27	5.5	5.0	116	6.3	4.0
			117	2.5	5.5
			118	3.8	4.0
			119	3.4	4.0
			120	4.6	5.0
			121	5.5	4.0

roller's end and crown. There is no reason to believe that the intersection of the radii with both the roller end and crown will track as a true circle when looking at the roller end or will lie in a plane perpendicular to the rollers longitudinal axis in the case of the crown intersection. The actual corner breakout locations will, therefore, depend on the circumferential location on which they are measured.

The corner runout measurement would also suffer from this problem, since the exact location of where the runout is taken will affect the runout data. Since there is no practical method of establishing the exact circumferential location for taking both the conventional and breadboard data, differences in data should be expected.

The contour data arrived at by use of the breadboard gage is accurate enough to conclude that development of a prototype gage using the breadboard gage inspection principles should proceed. The use of analytically computed intersection data obtained from least square fit calculated contour curves should significantly improve the data accuracy.

SECTION VI

PROTOTYPE AUTOMATIC GAGE DESIGN

The successful conclusion of the breadboard gage evaluation confirmed the adequacy of the basic design philosophy. From that point the design of automated gages proceeded. As a minimum, it was determined that each of the automatic gage modules would include computer controlled gaging functions and data analysis for all functions manually performed on the breadboard gages. It was also established that the axial and radial gages would be combined into a single gage to minimize their operating complexity, and that no transfer or sorting functions would be designed.

The decision not to provide for transfer between modules or for sorting of fully inspected rollers was based on the cost effectiveness study. This study indicated that the added expense for those functions would inhibit roller manufacturers and users from procuring the gage and not substantially improve its usability. In the following subsection, the cost effectiveness study is discussed. The final prototype automatic gages are discussed in subsequent sections.

1. Cost Effectiveness Study

The need of a manufacturer or user of quality machine parts, such as bearing rollers, to obtain some level of economic justification before acquiring new and expensive inspection equipment requires that studies be performed by the equipment supplier. These studies must prove that the new machine will provide an improvement in either quality, cost or both before the final equipment configuration is established.

In order to establish the need for automated gages, several facts must be ascertained. One is the production rate of rollers for which 100 percent inspection is required. The remaining required information includes the production rate of rollers for which sampling inspection techniques are now employed, the present cost of inspection on a per unit basis, and the desire or ability of manufacturers or users to make the capital investment necessary to acquire automated inspection equipment.

In an attempt to develop the cost and production factors necessary to establish the automation level which is economically justifiable, contact was made with both suppliers and users of military aircraft roller bearings. No production or usage rates or costs were made available by anyone with the exception of the Air Force ALC's. In the case of roller bearing suppliers, proprietary reasons were given for not divulging cost figures; bearing users such as engine manufacturers, cited Air Force restrictions as the reason for not providing such data.

Additionally, in many inspection facilities, costs attributed to a specific inspection operation are not maintained since the overall cost for maintaining and operating such a facility is already part of a factory's overhead account. This means that along with a company's natural reluctance to divulge production or cost data, the actual cost of a specific inspection process, which is part of a much broader inspection operation, may not even exist.

To circumvent the restricted availability of roller inspection cost and production data quotations obtained from bearing manufacturers to inspect specific rollers were used to establish unit inspection costs.

Inspection Costs

Although inspection costs billed to a customer can be established, it is practically impossible to estimate capital investment costs. Each bearing manufacturer or user tends to develop nonstandard gage fixtures which are employed on many roller sizes. Prorating these costs is possible, but the basic dollar value of the investment is both unknown and unobtainable.

The only benchmarks for inspection cost which were billable to a customer were two inspection procurements by MTI and one inspection estimate which was not purchased. Table 25 indicates the level of cost actually experienced. From the data included in this table, it is estimated that the expense of inspecting rollers was somewhere near \$100 per roller. The lowest cost paid was felt to be under bid and was not weighed as high as the other two figures.

TABLE 25

Roller Inspection Costs

<u>Roller Size</u>	<u>No. of Rollers Inspected</u>	<u>Type of Inspection</u>	<u>Total Cost</u>	<u>Cost/Roller</u>
16mm	1	100 consecutive measurements on one roller each of 12 characteristics	\$4400 ^(a)	\$ 44.00
16 mm	25 each size	12 characteristics on 25 rollers in- cludes cost of 25	\$1120 ^(b)	\$ 22.40
7 mm*		7 mm rollers	\$3540 ^(c)	\$142.00

* 7 mm rollers were not required to be suitable for bearing installation,
only the inspection data was required

a Vendor #1 - 100 consecutive measurement on each of 12 characteristics.
Only one side of roller was measured.

b Vendor #2 - All characteristics on 25 rollers of two sizes.

c Vendor #1 - All characteristics on 25 16 mm rollers.

Production Rates

A typical military aircraft turbine engine bearing production lot will most likely consist of 100 to 200 bearings with each containing 25 to 35 rollers. Assuming that the attrition rate for roller inspection is 50 percent, a production lot of 10,000-14,000 rollers will be inspected. It is very likely that the automated gage throughput will be 2 min/roller; at this rate, the entire bearing lot of rollers would be inspected in 2.9 weeks. If additional lots of the same roller size or other roller sizes could be 100 percent inspected effectively, the long idle time, which would make investment in an expensive automatic gage difficult to justify could be overcome. Even accepting the fact that estimates are off by 100 percent still leaves the automatic gage for a considerable period of time to inspect more than one roller size.

When considering the tooling changes and recalibrations which would result from roller size changes, it appears prudent to minimize the final gage cost as much as practical. In relation to investment cost, bearing manufacturers were asked what cost limit should be set on the automatic gages to make procurement attractive. Unfortunately, no answer was forthcoming. The conclusion as to ultimate cost, therefore, is based on work completed under Air Force Contract 33615-72-C-1226 which produced an automated radial play gage for miniature ball bearings. The production cost that turned out to be unacceptable was \$50,000 to \$70,000 per unit.

In summary, the present cost of inspecting military aircraft turbine engine bearing rollers is sufficiently high to warrant improving the inspection process. The present roller production requirements, however, along with what has appeared in the past to be a reluctance of manufacturers to heavily invest in new inspection equipment, precludes the construction of the ultimate all inclusive automated roller gage.

From a cost effective standpoint, therefore, the semi-automated gage is considered the most appropriate design. In this design, rollers are manually loaded into a gaging module at which time the complete gaging cycle is performed automatically. These modules will be designed in a configuration which will

permit the easy addition of automatic transfer and sorting functions should industry acceptance and revised production rates indicate the need for less operator intervention in the gaging process.

2. Radial/Axial Gage Module Prototype

Drawing 633E001, listed as Figure 37, and the parts list PL633E001, presented in Appendix D, comprise the final prototype design for the axial/radial module of the automatic roller inspection system. A description of how the design was arrived at and how the gage functions is presented in this section. By definition the function of the prototype design for this module is to automatically place a roller in the gaging position, provide all the measurement manipulations and then to remove the roller from the gaging position. The design goals established for the module were:

- Minimum number of changeover parts and adjustments for roller size change
- Ease and reliability of operator loading
- Accessibility of automation mechanisms for adjustment
- Reduction of precision motions in handling the roller so that the mechanism does not require fine tuning
- Use of standard commercial components whenever possible
- Minimal use of precision fabricated components

The basic module design is described as follows:

- Operating Cycle

The roller to be measured is placed in bearing holder (22) by an operator. The operator then presses a cycle start button which causes the following automatic events. The traction wheel (58) is lifted, the end loading shaft (63) is retracted, and the roller is transported into the "V" block. The end shaft (63) is then loaded against the bearing, and the traction wheel is energized. The roller then is revolved for a predetermined initial time. Measurement of the roller bearing then takes place and data are logged into the computer. When the measurement cycle is complete

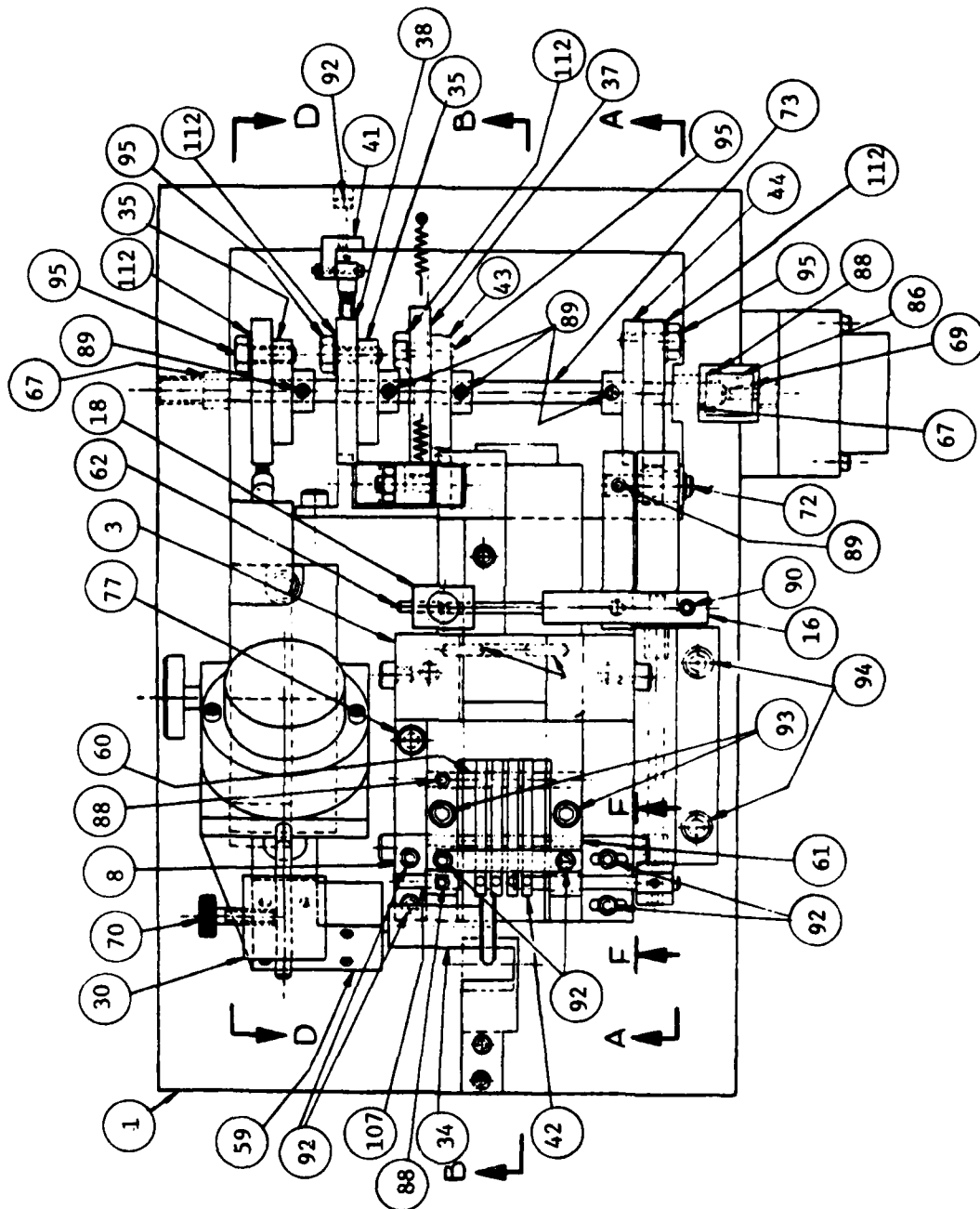


Fig. 37 Axial/Radial Module of the Automatic Roller Inspection System

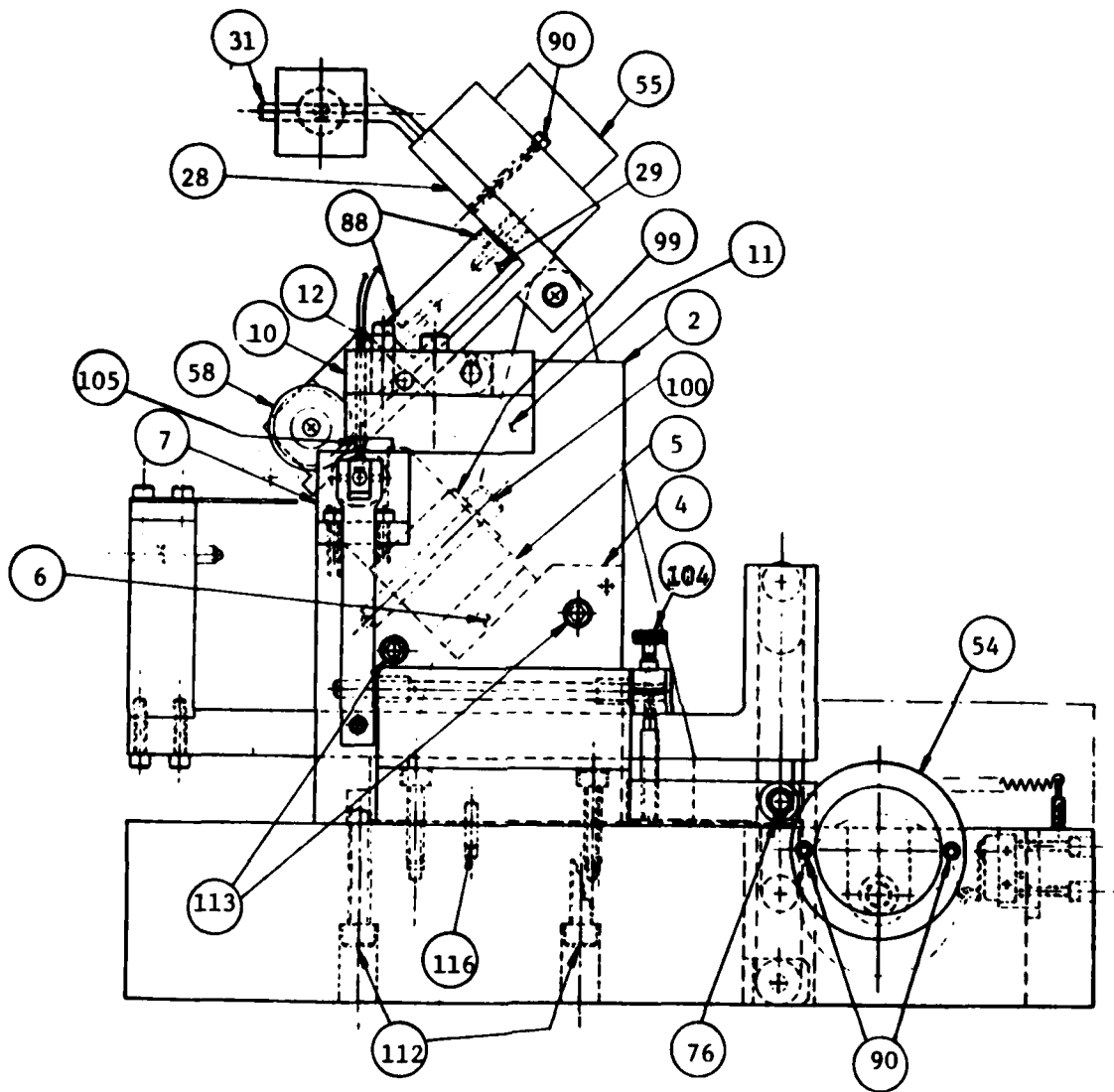


Fig. 37 Cont'd

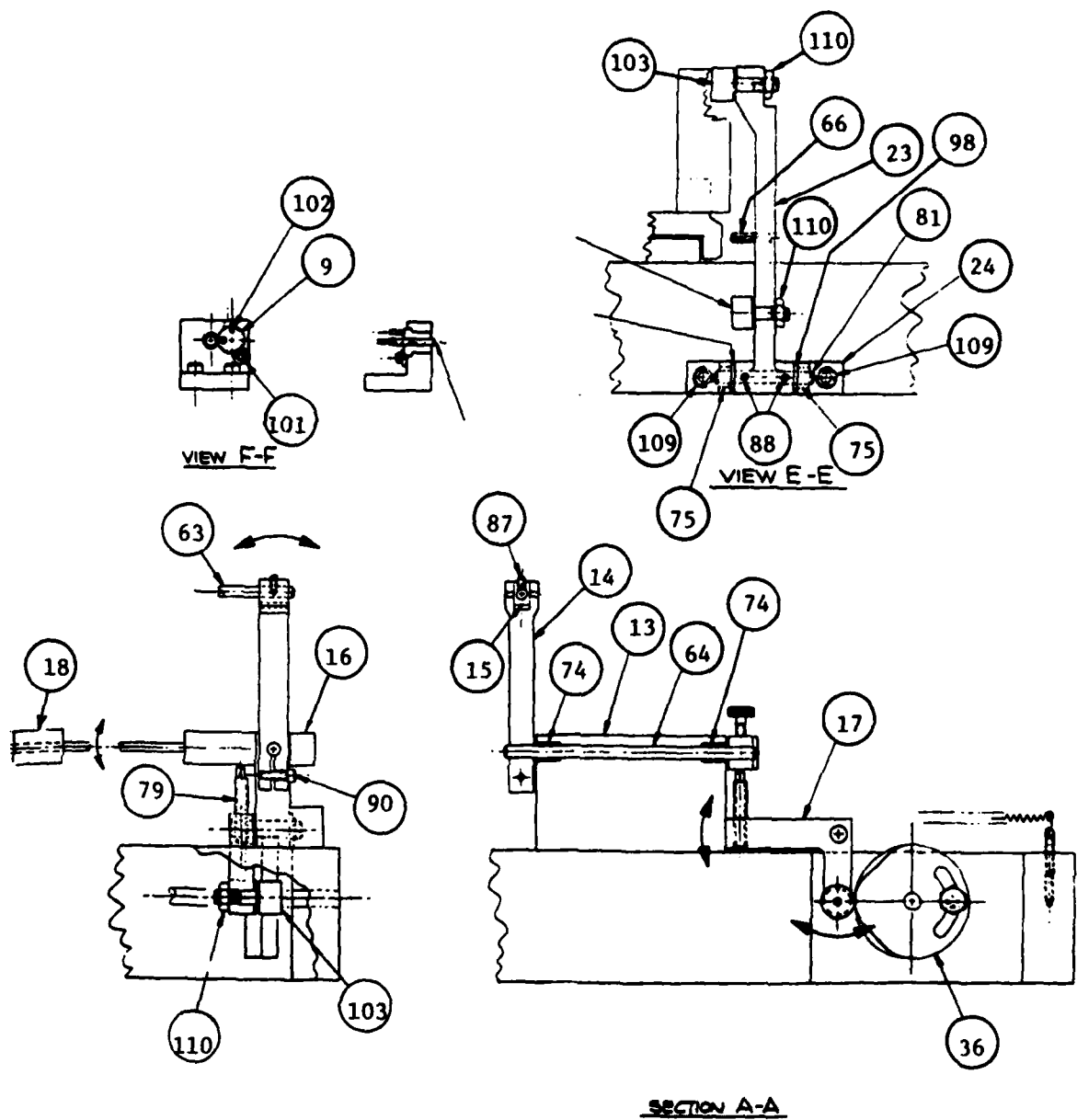


Fig. 37 Cont'd

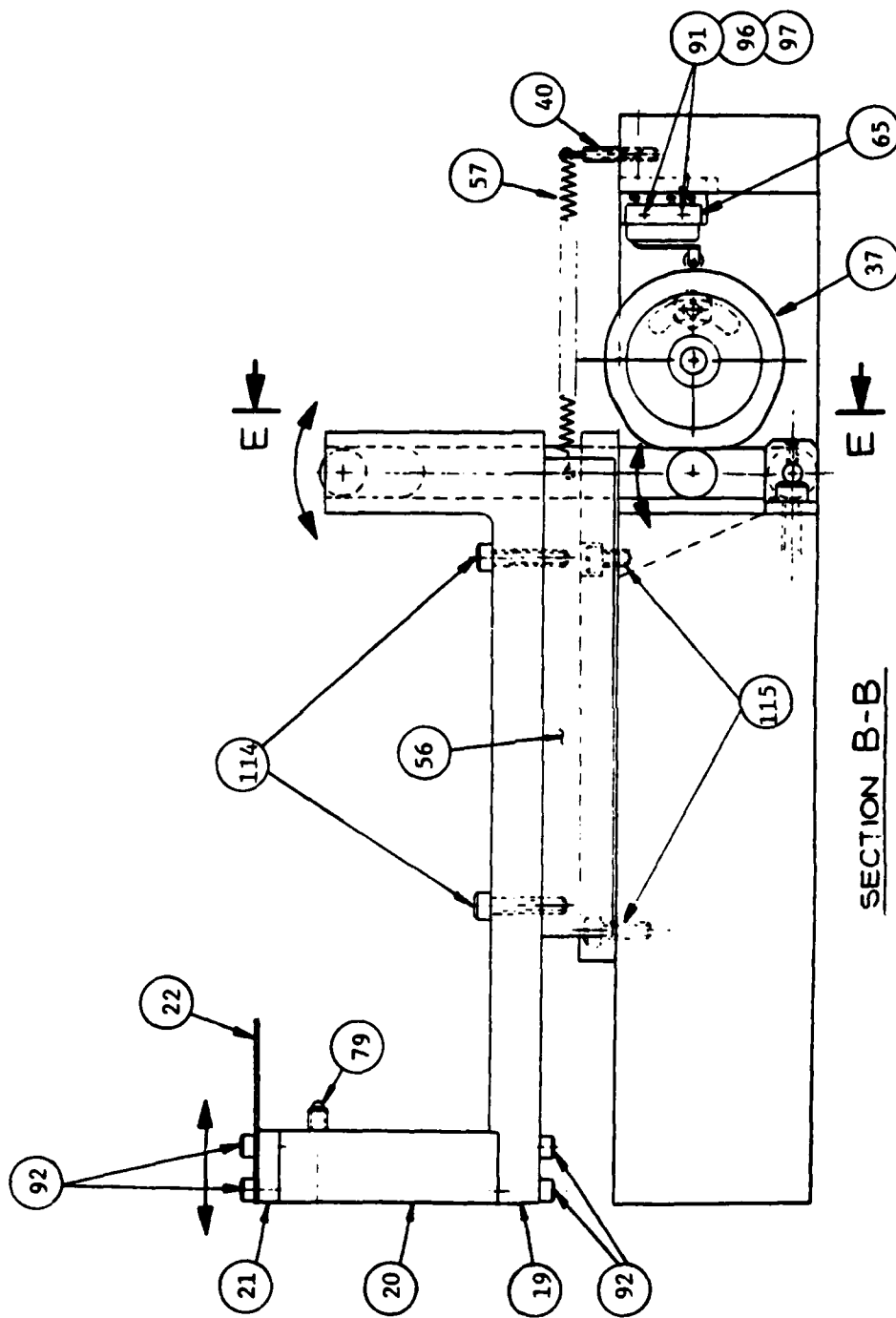
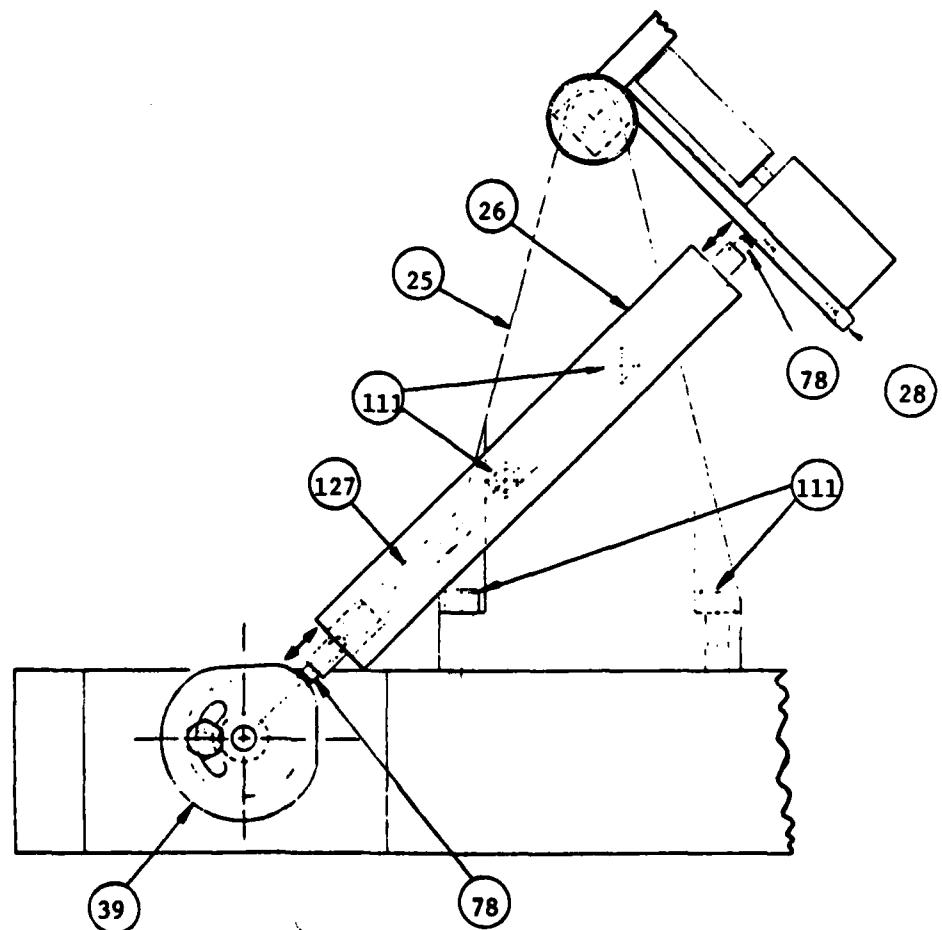
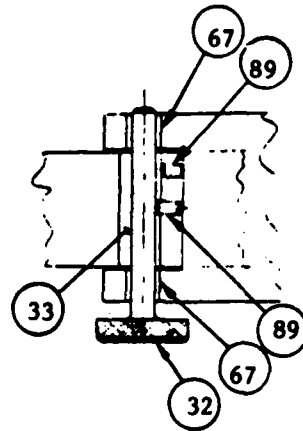


Fig. 37 Cont'd

30361



SECTION D-D

Fig. 37 Cont'd

the traction wheel is automatically lifted, the roller end positioning shaft (61) is retracted and the roller is transferred to the operator load position. This concludes the machine cycle and it is now ready for the next roller loading by the operator.

• Description of Machine Elements

- Vertical Probe Holders - A vertical probe bracket (10) is held in place by two socket head screws (93). This bracket holds a maximum of four capacitance probes which are an integral part of the vertical probe holders (42). The probe holders are maintained in position by means of a vertical probe spacer (12) which is a change part special for each roller length. The vertical probe holders (42) are spaced by sliding them on the probe holder shaft (60), and then are locked in place with the probe spacer (12) as described previously. The vertical probe holder is repositioned vertically for different roller diameters by changing the vertical probe spacer (11).
- Axial Probe Holders - The right-hand angle block (7) is adjustable and is held in position by clamping screws (92). This block and block (8), the left-hand angle block, contain the axial probe holders (9) which can be revolved to position the axial probe circumferentially with reference to the roller bearing diameter. This repositioning is accomplished by loosening the motor mount cleat (101) and moving the probe holder which is expedited by pushing against roll pin (102). Scribe lines on probe holder item (9) are used for initial probe alignment.
- End Shaft Loading Mechanism - The end shaft (63) is loaded against the bearing end by motion of the end pin lever (14). This lever supports the end pin holder (15) and shaft (63). During the loading cycle, cam (36) pushes the end pin actuator arm (17) which results in a vertical motion of the Vlier plunger (79). This vertical motion raises the end pin actuator arm (16), resulting in retraction of the end pin

lever (14). End pin weight (18) is adjustable on shaft (62) for bearing end loading.

- Traction Motor Lift Mechanism - While a roller is being loaded, cam (39) activates push rod (27) which pushes the pivoted motor bracket (28) and lifts traction drive out of the way. An eccentric traction drive pivot rod (32) and eccentric bushing (33) are provided for changing the traction wheel point of contact on the roller. The traction wheel is driven by a timing motor (55) which transmits power through a right-angle drive (59). Centering of the traction wheel against the roller in the length-wise direction is accomplished by repositioning the traction wheel.
- Roller Bearing Loading and Unloading Transport Mechanism - The bearing is loaded into the roller holder item (22) which then transports the roller into position on the "V" block. The roller holder is moved by a loader cam (37) which activates loader lever (23) that in turn imparts motion to the ball slide (56). The loader lever (23) is spring loaded by (57) to hold it against the cam. The final position of the loading device is precisely held by an adjustable stop screw (79). Upon entering the "V" block, the roller is lifted out of the roller holder (22) by a very small amount to prevent any contact between the bearing and the bearing holder during gaging. This permits the loader to remain in position in the "V" block during the gaging cycle. After the forward loading cycle is complete, limit switch (65) is actuated to stop the cam drive timing motor (54).
- Drive Shaft - All of the automatic motions are generated by cams securely mounted on a cam shaft (73). The shaft is located at the rear of the machine which permits easy access for adjustment.

Provision is made for cam timing adjustments by use of slotted cam bodies which are rotated on hubs and then locked in position.

The mounting of the cam shaft in the rear of the machine permits an unencumbered loading area for easy operator accessibility.

● Tooling Change Requirements

The guiding philosophy used in designing this module was to minimize the tooling changes required when the module is changed over to different diameter rollers. This is accomplished by moving the gaging "V" block on a 45° incline in the module. The employment of this principle, requires only five fixture changes for roller diameter changeover.

These changes are:

- Movement of the "V" block (5) by insertion of an appropriate spacer (6) behind the "V" block.
- Raising the capacitance probes in a vertical direction by introducing the appropriate spacer (11) under the probe vertical bracket (10).
- Adjustment of roller holder (22) by changing to appropriate bearing holder spacer (21).
- Repositioning of axial probe holders (9).
- Adjustment of the right-hand angle block (7).

3. Contour Gage Module

The contour gage module design is shown on Drawing 640E001 which is listed as Figure 38. The parts list for this module, identified as PL633E001 is presented in Appendix E. Figure 38 illustrates the final configuration of the contour gage portion of the automatic roller inspection system. Following is a description of the reasoning behind the particular design selected and how this roller inspection module functions.

The significant design requirements, such as ease and reliability of operator loading and minimizing the number and complexity of changeover parts, along with the other items listed for the radial/axial gage module, were also applied to the contour module.

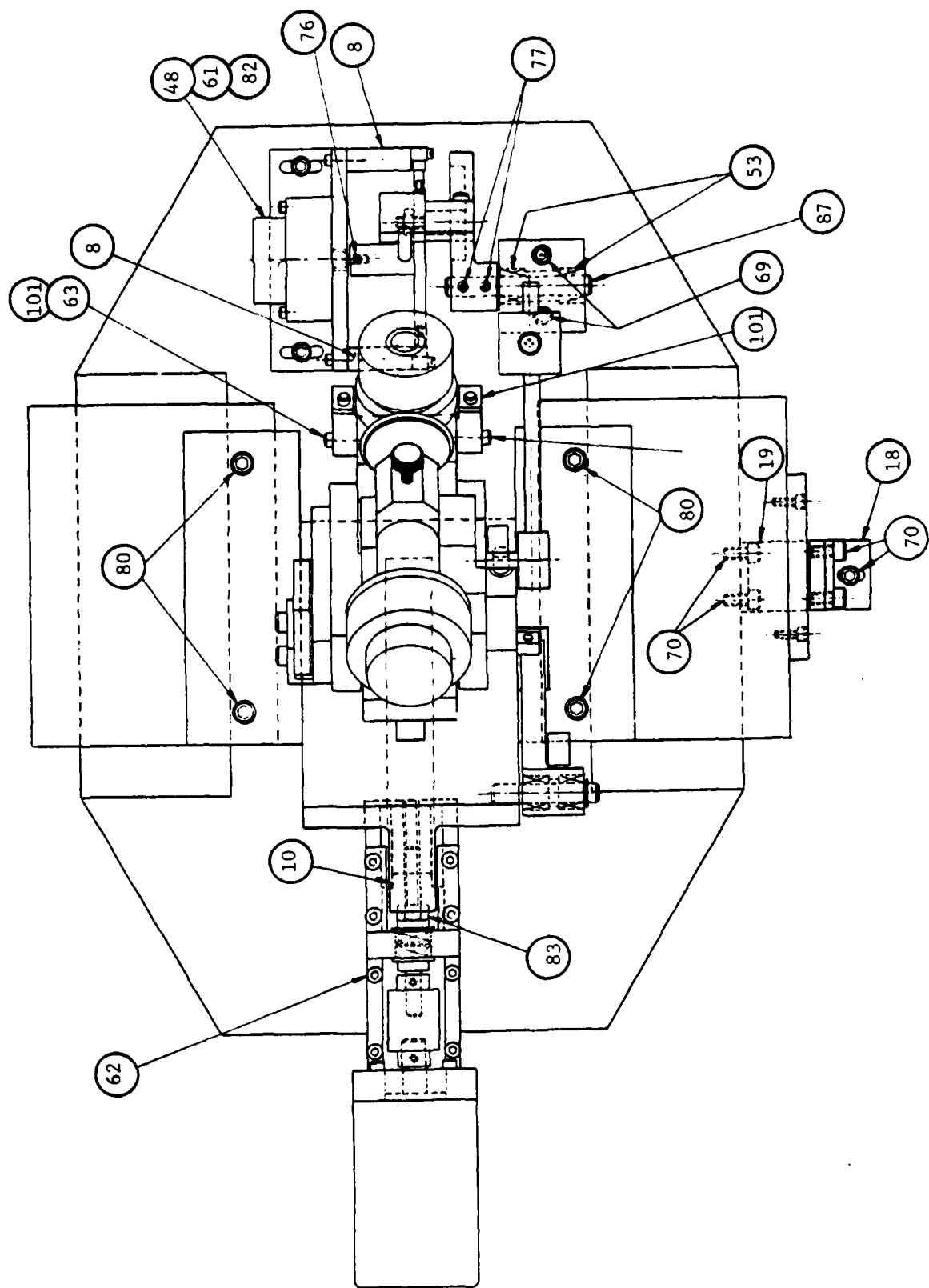


Fig. 38 Contour Gage Module Design

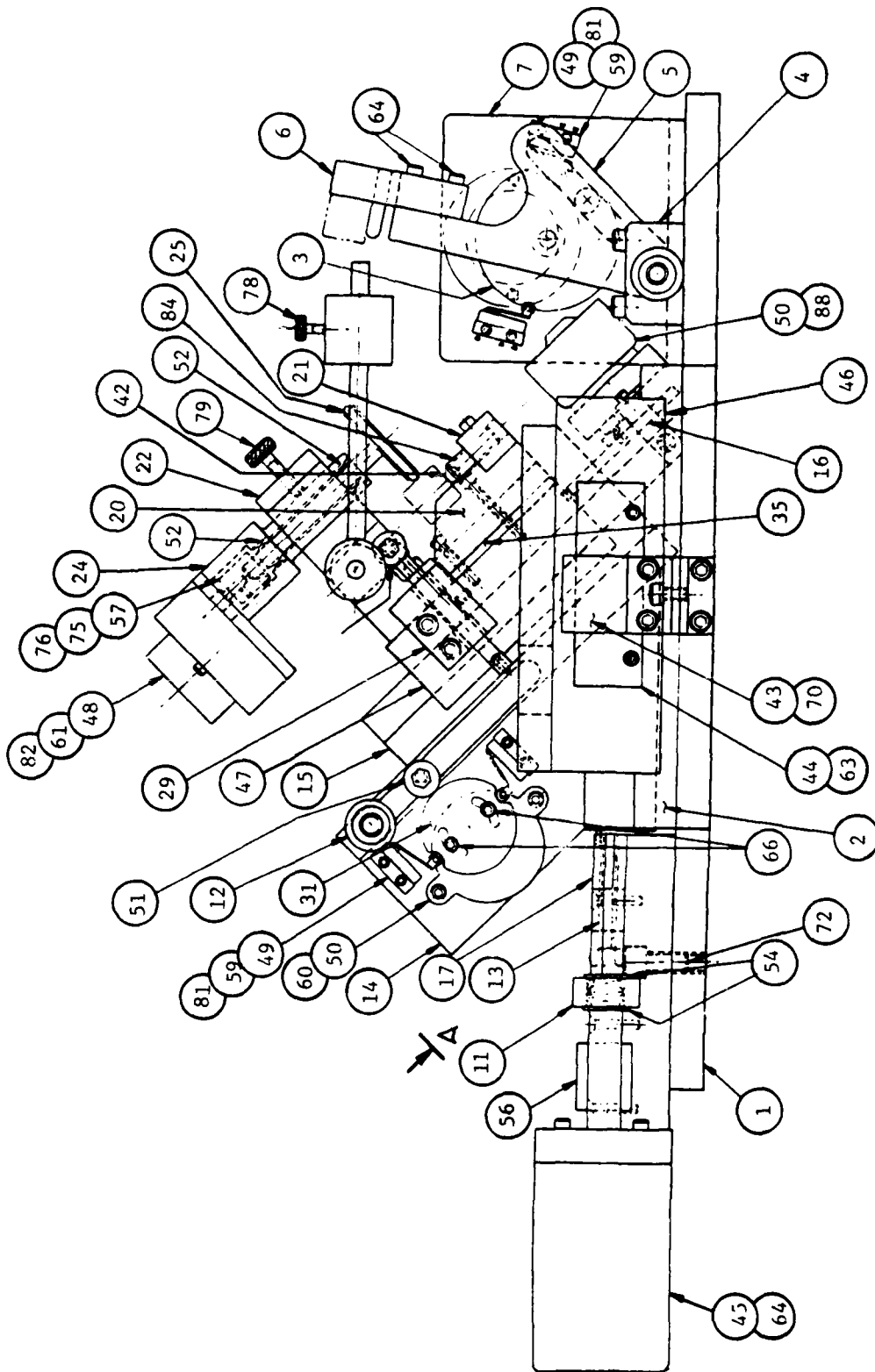


Fig. 38 Cont'd

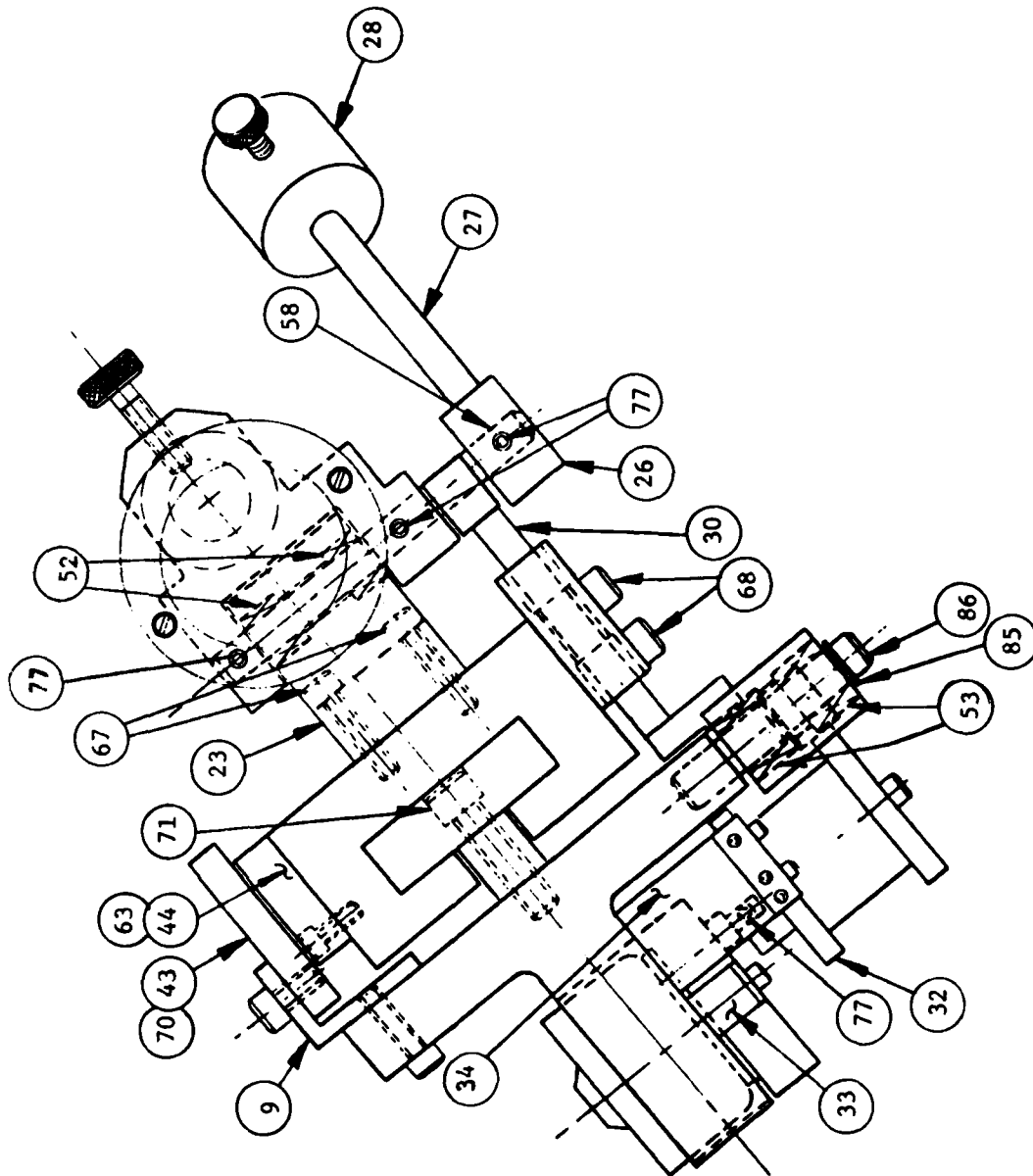


Fig. 38 Cont'd

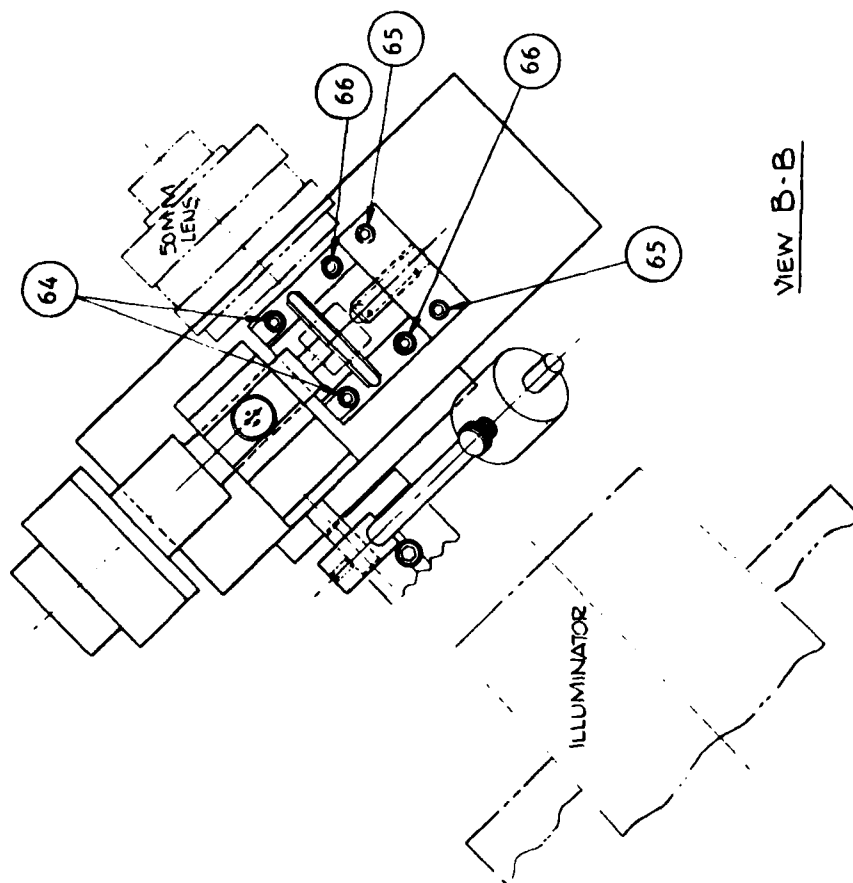
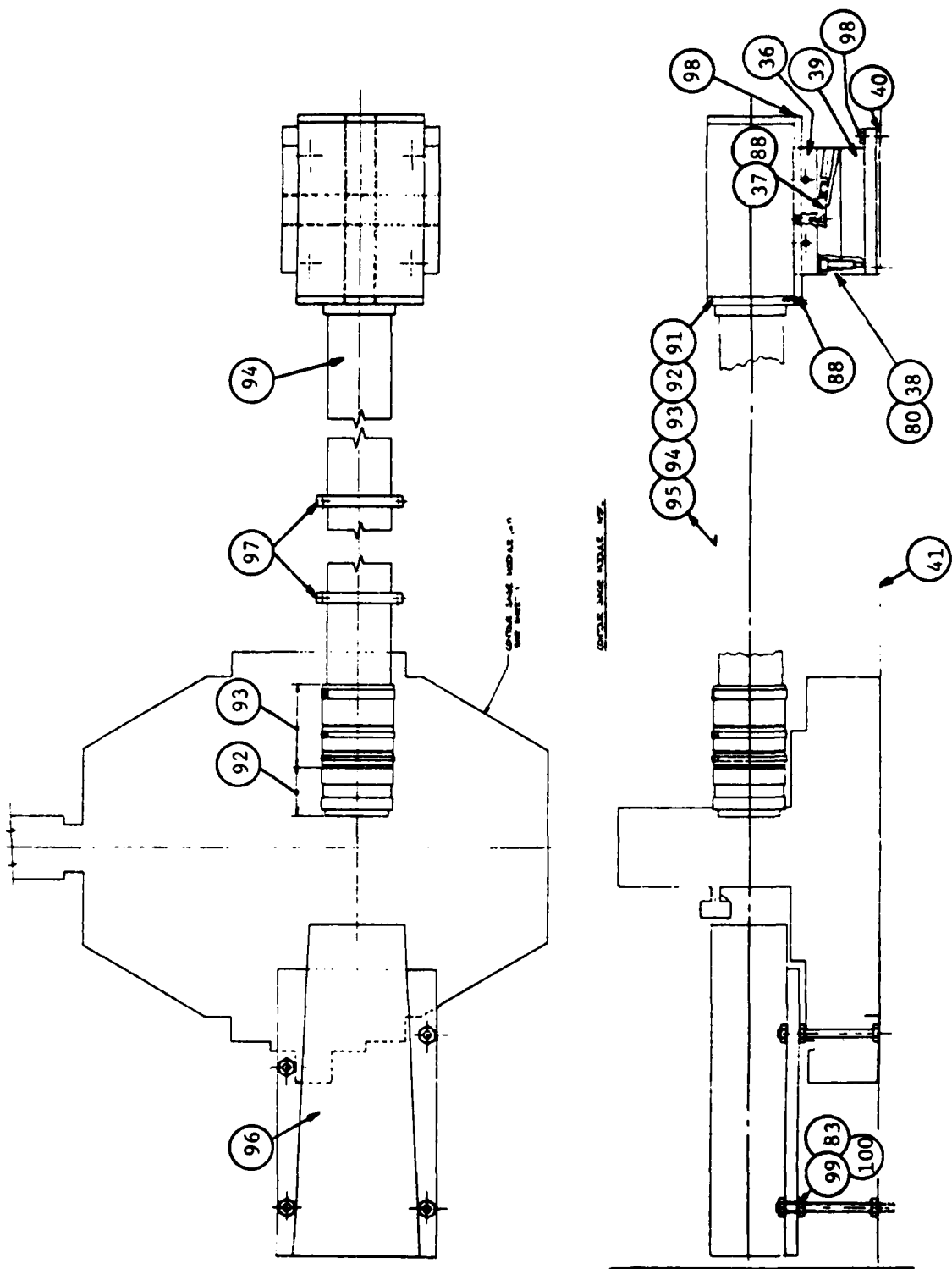


Fig. 38 Cont'd



The contour gage module uses the same measurement techniques shown to be successful in the breadboard evaluation. These techniques include:

- Back lighting the roller with a collimated light source to provide a sharp shadow image of the roller.
- Orienting the line scan camera's diode array vertically to permit a simple scanning track.
- Orientating the roller to be inspected at an inclination of 45 degrees to the axis of the diode array to eliminate the poor resolution which occurs when the roller shadow crosses the diode at a small angle from the vertical.

Two features added to the automatic gage module, other than the actual automation mechanisms, which were not included in the breadboard gage are:

- A gas bearing slide on the 45 degree axis to eliminate any roller sliding during the inclined axis translation.
- Two position encoders, one on the horizontal axis and one on the 45 degree axis, to replace the micrometers so that slide position data could be directly read into the system's computer.

Motions along both axes of the gage module are now supported on gas bearing slides and the micrometers have been replaced by motors and encoders.

The design of the contour module is described as follows:

- Operating Cycle

The operator places the roller to be inspected in the roller holder (6) and initiates the measurement cycle start by pushing a start button. Vacuum is then applied to the roller holder (6) and the loader arm (5) is pivoted to load the roller into the "V" block (20). The loader arm is driven by motor (48), and cam (3).

At the completion of the loaders downward stroke, the limit switch (49) is actuated and appropriate mechanisms shut off the vacuum and retract the loading arm. At this time the roller is positioned in the "V" block against the end stop mounting block (21) and end stop (84).

The traction wheel (25) which is in the retracted position during loading is lowered temporarily to rotate the roller slightly for proper seating in the "V" block.

The computer controlled gage then performs all the gaging functions necessary to gage the roller according to a pre-selected schedule according to roller size.

After initial roller seating, the gaging sequence described in report section IV-4 is automatically performed after which the loading sequence is activated in reverse to remove the roller from the gage.

● Description of Machine Elements

The entire gage module is mounted on two externally pressurized gas bearing slides (46) which establishes a stiff frictionless foundation for the gage. The movable portion of the slides provides the axis of motion to provide the horizontal scan capability.

- Horizontal Scan Mechanisms - Motion for the horizontal scan is provided by a torque motor (45) which is energized after roller loading is complete. The motor turns the scan positioning screw (13) which drives the scanning slide (46) via the scan positioning nut (10).

Note: the positioning nut is not attached to the moving part of the slide but only pushes against it. Attaching the nut to the slide would induce moments on the air bearing slide and interfere with the bearing's effectiveness.

The slide follows the nut on a return cycle because of a very slight inclined mounting.

A Farrand Inductosyn position transducer consisting of scale (44) and sensor (43) is mounted on the slide to provide position readout. The scale (44) is mounted on the moving part of the slide and the sensor (43) is fixed to the stationary member of the slide.

- Inclined Axis Motion - At the magnification established by the lens (92) and lens extension tubes (93) and (94) the total diode array of the line scan camera (91) will have only an approximate 0.070 in. field of view.

Since this field of view is not large enough to capture the entire roller, it is necessary to index the roller in steps and scan between each step. A second frictionless gas bearing called the index slide (47) is provided for this purpose.

After completion of the initial scan, the roller and the "V" block are indexed upward at a 45° angle. By rotating the cam motor (50) which drives the index positioning cam (16) the index slide is moved. Its position is obtained with a second Farrand Inductosyn position transducer. The transducer scale (44) is mounted to the movable member of the index slide, and the sensor (43) is mounted to the fixed slide member. Gravity retains the index slide against the index cam.

- Traction Wheel Mechanism - While a roller is being loaded into the gaging position the traction wheel mechanism is lifted out of the way. This is accomplished automatically by having the lift motor (50) and attached push rod cam (31) activate the push rod (30) which in turn pivots the traction motor holder (22) via cam follower (51). At the end of the lift, limit switch (49) is activated, which stops the motor. Upon loading

a new roller, the motor is reversed and the traction wheel is lowered to contact the roller.

Energizing the traction wheel motor (48) drives the traction wheel which revolves the roller.

Traction wheel pressure is adjustable with moveable weight (28).

● Tooling Change Requirements

Simplicity of changeover requirements has guided the design of the contour gage module. This simplicity is accomplished by providing a small number of changeover requirements when a different size roller is inspected.

The new changes required are:

- A new roller holder (6) for each diameter change
- A new "V" block spacer (35) for each diameter change
- Repositioning of the end stop (84) for each length change
- A repositioning of the traction wheel (25) in its holder with clamp screw (79) for each length change.

4. Data Acquisition and Machine Control

Each gaging station contains some combination of position sensing instrumentation that includes either capacitance probes or light sensing diodes and position encoders. From these instruments the information necessary to evaluate all the required roller characteristics will be obtained, but not in a manner easily recognized by an operator. In order to convert all the sensor readings into meaningful data, to provide control over the measuring sequences, to initiate and conclude a measurement process and to provide data relative to the measured roller characteristics, a computer controlled data acquisition and control system will be provided.

The data acquisition system will determine and identify all the required roller characteristics and provide:

- A calculation capability to convert the sensor signals to roller dimensions.
- A classification capability to compare the calculated roller characteristics to the required values, to retain the ordered sequence of the rollers as they pass through the automatic gage and to print out the results for a permanent inspection record.
- A classification control capability to activate the appropriate accept-reject or classification alarms.
- A measurement control circuit which will act upon cycle-start signals from the mechanical gage to initiate a measurement sequence, which will initiate a cycle-end for the mechanical gage when the measurement cycle is complete and will coordinate the measurement process for all gage modules.

Radial and axial roller dimension will be taken while the roller being inspected is revolved in the gaging module. Data from the two probes measuring the central land position will be analyzed for the least square fit to a polynomial. From this computation, the diameter and the location of the roller center will be obtained for each end of the central land. Data from the two probes measuring the crown drop will be analyzed in the same manner and will result in the determination of the crown diameter and centroid location.

A comparison of inspection data to fitted curves and the comparison of various centroid locations will establish all the desired diametral roller characteristics including: runouts (differences in fitted data to straight lines), crown drops (differences in fitted curve mean values), concentricities (differences in mean values at two locations), and taper (differences in mean values of fitted curves for central cylindrical portion).

In a similar manner the axially-oriented probes would provide all the axial inspection data. Roller length would be established by relating mean probe readings from each roller end to a reading established from a known calibrated length. Runout at each roller end would be determined from the variation in individual probe readings, while end parallelism would be calculated from the maximum and minimum differences in the opposed probe readings.

An additional computer function will be the calculation of roller contour characteristics; the calculation method follows. The contour measurements, as established by the position encoders on the gage slides and the light emitting diodes in the line scan camera of the contour gage module, will be analyzed by the computer to produce the roller's contour characteristics. The procedure used for the analysis has been previously described in report section III-3 and Figure 15. An additional calculation will provide the least square fit to the central straight cylindrical roller contour data. The equation for this contour is given by $y = -\frac{1}{m}x + b_6$, which is a straight line orthogonal to the roller end contour $y = mx + b_1$, and will permit calculations for the radial corner breakout and the location of the central land.

To summarize, the computer will be programmed to calculate roller contour by establishing mathematical curves which are least square fit to the contour data. From these curves the contour characteristics will be calculated. Figure 39 schematically demonstrates the mathematical curves to be generated and how these curves establish contour characteristics. On Figure 39, the roller end contour segment is specified as $y = mx + b_1$, the roller corner contour segment as $(x+b_2)^2 = (y+b_3)^2 = R_2^2$, the crown contour segment as $(x+b_4)^2 + (y+b_5)^2 = R_1^2$, and the straight cylinder contour segment as $y = -\frac{1}{m}x + b_6$. At each contour segment, intersection at the "x" and "y" coordinates of the segments will be identical and their slopes (d_y/d_x) will be equal. At these boundary conditions, the individual contour segment equations will be solved to determine the intersection coordinates; these coordinates will in turn be used to calculate the contour characteristics.

Control of the automated roller inspection station, and analysis of each roller is accomplished using a microprocessor based system. With the use of an Intel Corporation 8080A based microprocessor system, all required control functions, all data storage, and all mathematical functions and requirements are met. Figure 40 is a block diagram of the automated roller inspection station.

The microprocessor is an 8 bit processor with a 1.9 microsecond instruction time, six general registers, 16 bit addressing (65 KB), and over 100 unique

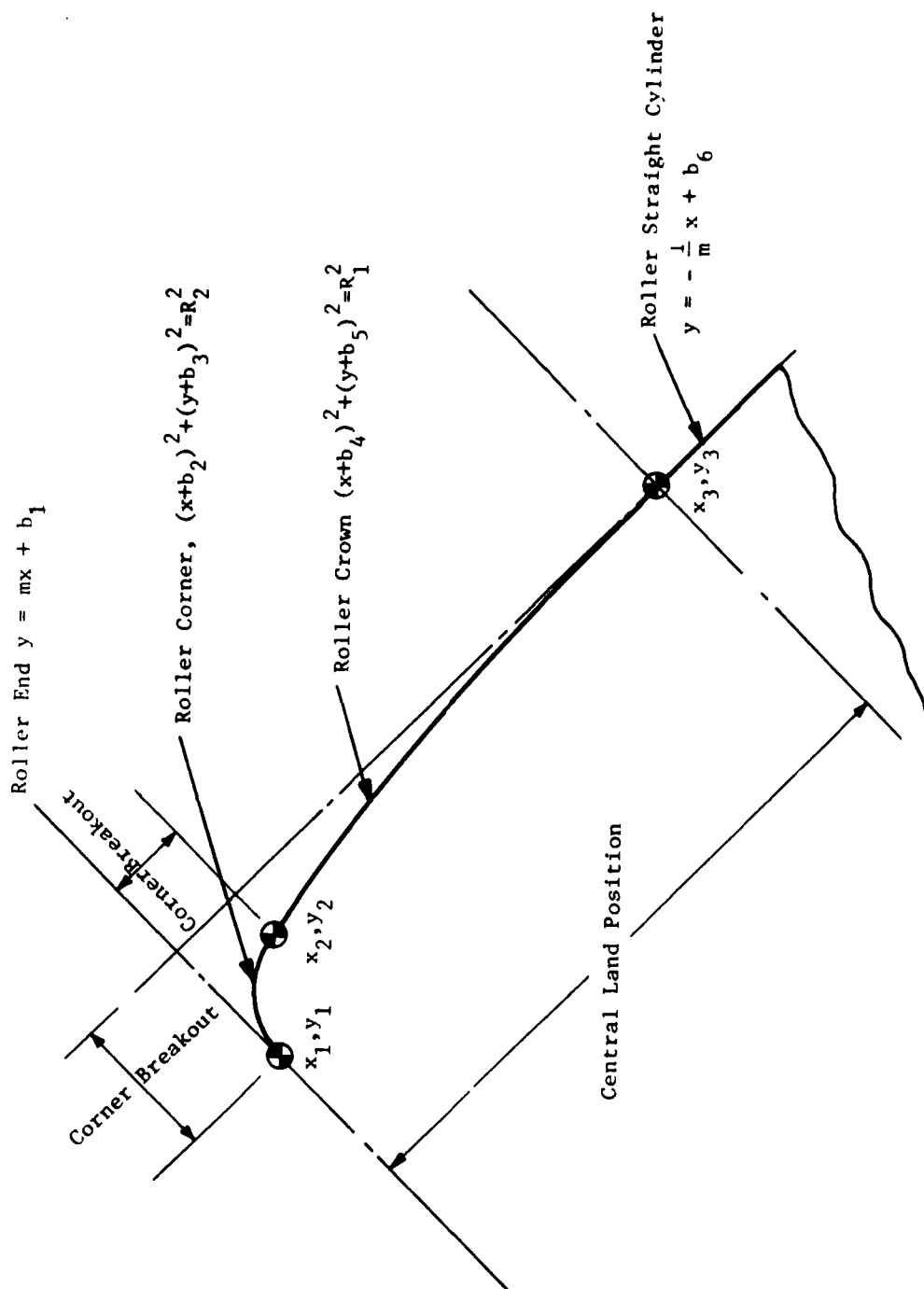
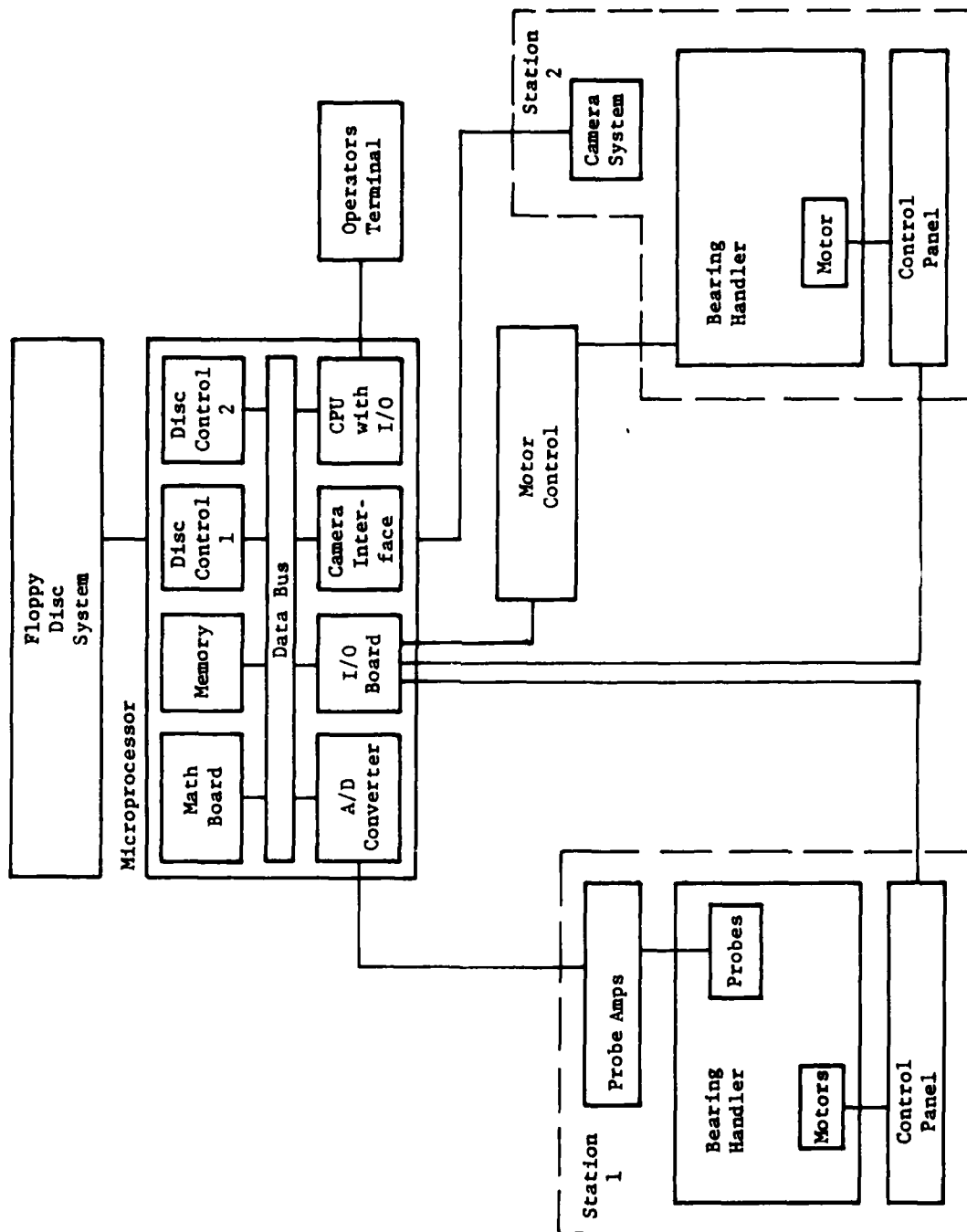


Fig. 39 Mathematical Curves for Roller Contour Calculations

793497



793496

Fig. 40 Automated Roller Inspection System
Block Diagram

instructions. It is part of the total system which includes a dual-drive dual density floppy disc system, 65,000 bytes of MOS memory, 120 input and output bits for control, a camera image processor, an analog to digital converter, and a hardware math processor. An operator's terminal is also provided for system control and hard copy of inspection results.

Processor

The processor used in the system is the Intel 80/20 single board computer. The heart of this processor is the Intel 8080A single chip microprocessor. It is a complete central processing unit which supports vectored interrupts, serial I/O Port, decimal, binary, or double precision arithmetic and over 65K bytes of memory. It has six general purpose registers and operates at better than 2 micro seconds per instruction cycle. In addition to the 8080A processor, the 80/20 board also includes a programmable baud rate RS 232 compatible I/O port, two programmable 16 bit binary timers, 48 programmable I/O lines, and an eight level interrupt control system.

Floppy Disc System

A dual transport, dual density floppy disc system is included for program and data storage. Each floppy disc has a half mega-byte storage capacity. Two circuit cards are used for control of the disc transports. Up to 500,000 bits/second can be transferred on or off the IBM-compatible soft sectored discs.

Memory

A single circuit card contains all 65K bytes of memory for the system. The memory is constructed using MOS devices, and on-board refresh capability is provided. Typical access time for the memory is 450 nano-seconds.

Math Processor

A high-speed hardware-based math processor is included in the system to provide a parallel processing capability during involved calculations. The Intel 310 Processor is contained on a single circuit card. This processor supports 16- and 32-bit formats in fixed point operation and 32-bit formats in floating point mode. Standard mathematic operations are supported as well

as floating point square and square roots, compare-and-test functions, and fixed point to floating, and floating point to fixed conversions.

A/D Converter

A high-speed analog to digital (A/D) converter is provided to interface with the capacitance probes of Station One. The converter samples the outputs of the probe amplifiers and generates a double precision digital word for the processor's use. It is a 12-bit converter with 16 multiplexed input channels, jumper selectable input ranges, programmable gain, 100 meg-ohm input impedance, and is contained on a single circuit card compatible with the Intel Data Bus.

I/O Board

Discrete control lines for system functions are provided via an I/O Interface Board. Seventy-two control lines are provided on a dedicated board, and an additional 48 are provided on the CPU board for a system total of 120 control lines. These lines are program controlled to input or output function, and may also be jumpered on-board to function as interrupts. The bits are electrically constrained to 4-bit slices and software grouped into 8-bit bytes of input or output functions.

Camera Interface

An interface for the roller imaging camera is also used to process the camera data. This interface, which is a Reticon 6020, accepts video data from the camera, and digitizes the data without the need for CPU control. Two 512 byte RAM memories are used for data storage. This memory is then considered as part of system memory by the CPU for processing.

Operator's Terminal

The operator's terminal is a 30 character per second Dec Writer. Manufactured by Digital Equipment Co., this terminal operates at 300 baud over an RS232 serial link. Initial system start-up and final roller analysis are done through this terminal.

System Chassis

All the computer hardware, i.e., CPU, Memory, A/D Converter, etc., is placed in an Intel system chassis. This chassis has an eight slot card rack, power

supply and power control. Fans are also included to provide forced air cooling. Figure 41 shows the proposed card slot allocations for the system.

System Packaging

The complete roller inspection station electronics system will be mounted in a 60-inch cabinet. All subassemblies are standard 19-inch rack mountable units that will go into the cabinet. The cabinet will include a rear door, a power distribution system and an air circulation system. All cables will exit the cabinet from the lower rear area of the cabinet.

System Operation - Station 1

Station 1 of the automated roller inspection station is used to check the following roller characteristics:

- diameter
- length
- crown drop
- crown runout
- end parallel
- end runout
- O. D. taper
- two-point out-of-round

After the computer system has been initialized at the system console, the operator may place the roller to be tested into the loading position for Station 1. A "Begin-Test" button is pushed which commences automatic operation. A light will be illuminated to signify the station is in operation. During the course of operation the roller being tested will be automatically moved into position, static measurements will be made, followed by dynamic measurements where the roller is rotated while data are gathered. Once completed, the roller is automatically returned to the loading position, the "In-Operation" light is extinguished and the "load/un-load" light will be illuminated. A new roller may now be tested simply by reloading and then pressing the "Begin-Test" button.

System Operation - Station 2

Station 2 of the automatic roller inspection station is used to check the following roller characteristics:

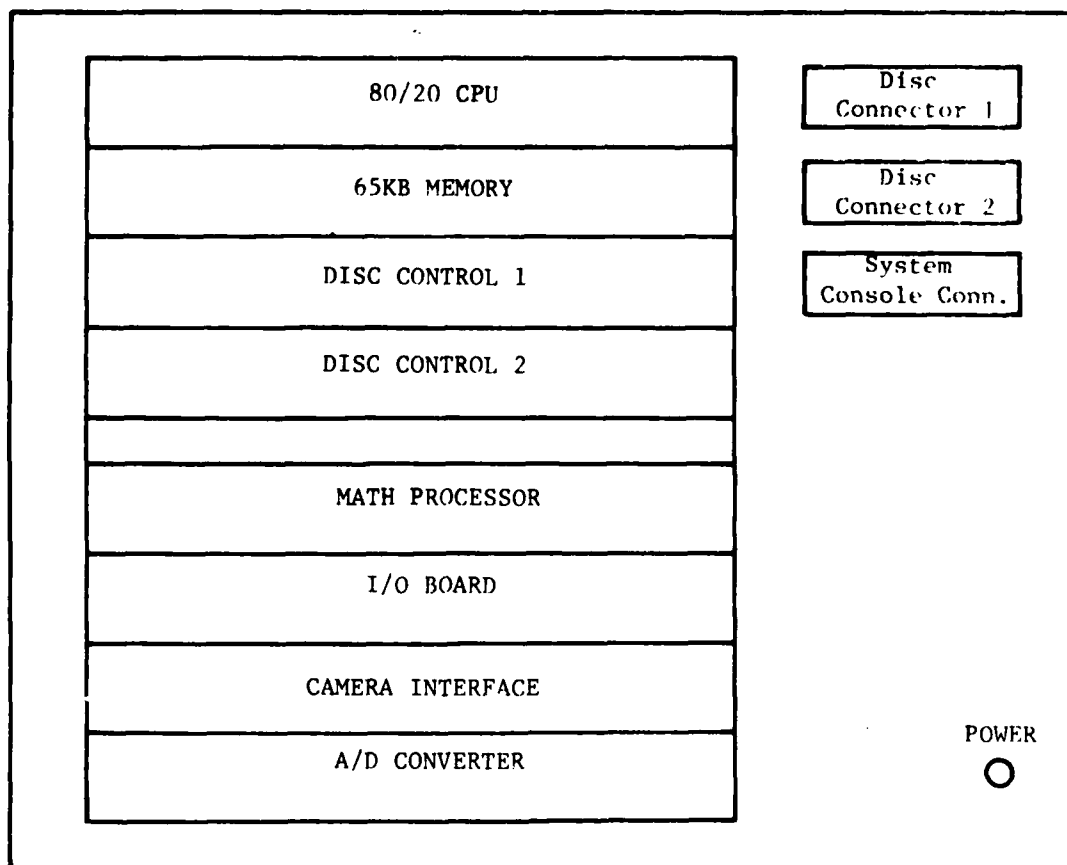


Fig. 41 System Chassis Configuration

- corner breakout
- corner runout
- flat length
- flat centrality

After the roller under test has been removed from Station 1, it may be inserted into the loading position of Station 2. Again the Station 2 "Begin-Test" button is depressed to begin the testing. A light is also provided on Station 2 to indicate "In-Operation" status.

Once testing has been completed, the "In-Operation" lamp will be extinguished, and the "Load/Un-load" light will be lit.

Following the end of testing a summary of the various roller characteristics will be printed at the system console.

5. Environmental Considerations

Present methods of roller inspection permit the periodic cleaning of individual rollers, particularly before making an inspection measurement. For this reason, the cleanliness of the inspection room, although significantly better than the normal shop area, need not be a clean area as defined by AMS standards.

Hand cleaning of the rollers prior to their insertion into the gaging modules will still be required. The development of an automatic cleaning and recoiling system was felt to be impractical.

Vibration isolation of the complete automatic gage assembly including both the radial/axial module and the contour module will be accomplished by providing air bag isolation mounts for the automatic gage mounting block and stand. A large seismic mass consisting of a 1500 lb granite surface plate will be used to mount the gage hardware. The installation should make the gage insensitive to all normal shop floor vibrations.

SECTION VII
DISCUSSIONS AND RECOMMENDATIONS

The inspection data produced by the breadboard versions of the automated roller inspection system generally indicated an acceptable level of accuracy and repeatability when compared to similar data generated by conventional methods. By far the most difficult dimensions to measure and the area where more differences between the breadboard and conventional inspection results occurred fell within the high precision requirements of the radial and axial dimensions. In all measurement categories, particularly for the absolute dimensions of length and diameter, differences to a greater or lesser degree exist throughout the data. Since the repeatability of the breadboard gage was shown to be adequate, then differences from other sources must be examined. While variations in conventional inspection data cannot be assessed, differences in the data which may originate in the breadboard gage can be and are discussed as follows.

One important consideration in reviewing the radial/axial module data is capacitance probe calibration. It was previously mentioned that when a flat plate capacitor (such as a sensing probe) senses a curved surface, the capacitor or probe integrates the separation (gap) length over the active probe area to establish the gap dimension. The parameter used as an indication of the level of curvature effect is the ratio of the sensor sensing tip diameter to the diameter of the target. For the 7mm diameter roller used in this program, the miniature probe to target diameter ratio is 0.112; a large enough ratio to raise questions relative to the accuracy of flat gage block calibrations.

The error in calibration is compounded for the probes positioned to measure crown drop. These probes view a compound curve since they actually look at a surface which curves in two directions.

The use of calibration cylinders would eliminate any significant calibration accuracy questions. Several attempts to procure cylindrical gaging standards were made during the evaluation of the radial/axial module. The cylindrical rolls eventually examined contained more variability than the tolerance levels they were intended for and were discarded. It is felt that proper

standard rollers could be selected from bearing rollers in actual production which could then be certified as to dimension by the U.S. Bureau of Standards.

The fact that capacitance probes integrate over both the target area and probe to target gap seriously affects the positioning of the probe relative to a rapid change in roller contour such as a corner. To eliminate the errors in measurement caused by rapid gap changes within the probes target area, the probe must be positioned sufficiently away from such contour discontinuities. In many instances therefore, positioning of the probes will not be in accordance with present gaging specifications. The difference of the probe positioning in the breadboard gage, coupled with the difficulty in establishing accurate calibrations, would explain some of the differences noted in the data.

Additional variability between the roller inspections, performed by the breadboard and conventional gage, could be attributed to operational characteristics of the breadboard gage. These characteristics may have resulted from:

- work performed on the module during the functional checks,
- possible operator error in not permitting sufficient time for the roller to become seated in the gage or,
- lack of cleanliness.

An additional factor affecting the radial/axial gage is that the diameter of the sensors limits the number of probes which can be axially displaced along a roller, while still permitting placement at satisfactory gaging locations. The capacitance probes developed for this program are the smallest practical size which can be used in automatic roller gaging; they will not be suitable for gaging rollers less than 7mm in diameter without gaging each roller twice, once at each end.

In summary, the radial/axial gage module, while demonstrating good repeatability, did not demonstrate the expected high level of agreement with conventional gaging techniques. It is felt that these disagreements can be attributed primarily to the following causes:

- Calibration with parallel gaging surfaces which tended to produce lower than actual readings on curved surfaces.
- Differences in gage point locations due to probe positioning requirements.
- Slightly higher variability in the breadboard gage, particularly with respect to axial measurements.

None of the difficulties discussed above should deter the construction of the automated version of the gage.

The two steps that must be taken if the automated gage is to become accepted are:

- Calibration cylinders with known and acceptable levels of accuracy in each roller size must be used for all the dimensions to be measured on the gage. In essence, master rollers for gage calibration will be required.
- An acceptance modification of the "gage point" location and/or definition must be agreed on by both the supplier and user of the rollers to be automatically inspected.

In addition to the questions raised by the use of the miniature capacitance probes, the repeatability of the breadboard gage, although basically as good as conventional gaging did not always produce the same results. It is felt that improved computer based data acquisition and calculation techniques will reduce the differences discussed.

The evaluation of the contour gage module showed that it produced data with less variability than the radial/axial gage module. Not only was the repeatability of the gage excellent, as evidenced by the standard deviation of less than + or - one diode count, but the individual roller inspections were also well within acceptable levels of agreement with conventional inspection methods.

Some variation in both the contour and corner runout data can be attributed to the manual interpretation of gage data, both for the conventional as well as the breadboard gage rather than by variability of the gaging process.

Some variability, however, must also be expected due to the impossibility of taking a contour reading at exactly the same circumferential location on the roller for both gaging processes. The only significant measurement difference to surface was for the corner breakout measurements taken from the roller end location; the contour change where the corner radius intersects the crown. The manual interpretation of the line scan camera data for this measurement has a high judgment factor which can lead to the differences shown.

The introduction of a mini-computer controlled data acquisition and interpretation system to the gage module will eliminate manual data reduction errors and improve the accuracy of the contour characteristic measurements.

The contour gage, like the radial/axial gage, requires some modification to quality assurance specifications due to the manner in which the data must be collected. As a result of the scanning process described in this report, the location of the roller's central cylindrical section is measured from the roller end. This is the data listed for the flat centrality measurement. The actual length of the central flat would be obtained by performing the end measurement from both roller ends and then subtracting the sum of these measurements from the known roller length. The conventional flat centrality listed in the test data was obtained by subtracting the central flat length and one-half the flat centrality from the length of the roller. Although the dimensions resulting from the contour module measurements provide the same information as the conventional gage measurements, they are not obtained in the same manner and therefore, must be subject to both supplier and user approval.

Each of the measurement systems designed and studied as breadboard versions of an automatic gaging system produced measurements more or less with the accuracy requirements of high DN bearing roller tolerances. Both the radial/axial gaging module and the contour gage module, however, presented some areas of disagreement with conventional gaging techniques which cannot be answered by this program, (particularly those areas concerned with gaging location specifications).

An additional aspect of the automatic inspection system design is the question of industry acceptance. It is quite feasible to construct an automatic roller inspection system which is entirely free of operator interaction. The problem in building such a system is that it may not be entirely practical. The introduction of new techniques to an established industry must not only demonstrate improved performance, but must also be cost effective. A cost effectiveness study was undertaken as part of this program as a method of establishing the level of automation to be built into the system.

The decision regarding the complexity of the final automated gage, however, must rely more on estimates of use, of investment cost to the user, and limited inspection cost data rather than on actual production rates and firm costs since no production data, inspection costs nor user's procurement levels were made available.

In conclusion, the present cost of inspecting military aircraft turbine engine bearing rollers is sufficiently high to warrant improving the inspection process. Current roller production requirements, however, along with what has appeared in the past to be a reluctance of manufacturers to heavily invest in new inspection equipment, precludes the construction of the ultimate all inclusive automated roller gage at this time.

From a cost effective standpoint, therefore, the semi-automated gage presented in this report is considered the most appropriate design. In this design, rollers are manually loaded into a gaging module at which time the complete gaging cycle is performed automatically. These modules are designed in a configuration which will permit the easy addition of automatic transfer and sorting functions should industry acceptance and revised production rates indicate the need for less operator intervention in the gaging process.

The results of this program have so far demonstrated both the usability of the gaging techniques discussed and the cost effectiveness of the gage designs, thus fully justifying the continuation of this program with the construction of the computer controlled automatic gaging system presented.

REFERENCES

1. Modular Automatic Radial Play Gage for Miniature Bearings: AFML-TR-73-64, April 1973.
2. AFAPL TR77-32, Advanced High Speed Roller Bearing Inspection Techniques, TRW Report 5515.3.77-36, April 1977.

APPENDIX A

STATISTICAL EVALUATION OF COMPARABLE INSPECTION DATA

(Ref: Hays, W.L., Statistics, Holt, Rinehart and Winston, 1963)

In order to evaluate the degree of improvement, if any obtained by one support method over another, it will be required to test statistical hypothesis about differences in means of the data. Basically, if we denote mean measurements as M_1 and M_2 for two different support methods, respectively, we are interested in the hypothesis that the two means are equal. Let us call this the null hypothesis and also state the alternate hypothesis as the two means not being equal. Symbolically, we have

$$\text{Null Hypothesis } H_0 : M_1 - M_2 = 0$$

$$\text{Alternate Hypothesis } H_1 : M_1 - M_2 \neq 0$$

If we could conclude that the two means are indeed different at a given "significance level" then the question of how much difference may be answered by computing the "strength of association". We have introduced two statistical terms here. Another term which is important is "power of the test" by which the appropriate decision about H_0 may be reached, given a true alternate hypothesis. $H_1: M_1 - M_2 = c$. Before we can define all these three terms, it will be necessary to briefly talk about the sampling distribution of means and differences in means.

A. Sampling Distributions of Means

If a normally distributed population has a mean M and standard deviation σ , then the sampling distribution of means obtained by samples of size N , follows a t-distribution whose variance is $\frac{\sigma^2}{N}$. Thus, if we have two populations, M_1 , σ_1 and M_2 , σ_2 and we select samples of sizes N_1 and N_2 , then variance of the difference in means is easily determined and the t-distribution for difference in means is completely defined.

$$\sigma_{\text{diff.}}^2 = \sigma^2 \left(\frac{1}{N_1} + \frac{1}{N_2} \right)$$

where

$$\sigma^2 = \frac{\sigma_1^2 + \sigma_2^2 N_2}{N_1 + N_2 - 2}$$

The degrees of freedom for the t-distribution for the difference are given by

$$v = N_1 + N_2 - 2$$

The so called t-ratio for the difference is given by

$$T = \frac{(M_1 - M_2) - E(M_1 - M_2)}{\sigma_{diff.}} = \frac{M_1 - M_2}{\sigma_{diff.}}$$

Where M represents the observed sample mean and the second equality holds when the null hypothesis is true. It should be noted that the variance of the sampling distribution depends on the sample size and thus by having large samples, this could be substantially reduced. We shall get into a slight detail about this relationship later.

B. Significance Level for a Hypothesis

Once the sampling distribution of any statistic is defined the possibilities that the statistic lies in a certain interval may be easily computed. Let us represent the distribution of differences in means by the solid curve in Figure (A1). This also represents the null hypothesis H_0 . The probability that the observed absolute difference in means M_1 and M_2 is greater than $k \sigma_{diff.}$ is given by the shaded area α . The basis for either accepting or rejecting H_0 , is set by assigning the probability α . Thus, if the observed $(M_1 - M_2)$ is greater than $k \sigma_{diff.}$, then we reject H_0 at "significance level" of α . This is also equivalent to saying the null hypothesis is rejected with a significance level α , when the observed statistic lies outside the confidence band associated with the probability $(1-\alpha)$.

C. Power of the Test

The power of the test is defined by the probability of correctly rejecting H_0 in favor of a given true alternative H_1 . Let H_1 be represented by a dashed line in Figure (42) and H_0 is rejected when the observed difference in means is greater than $k \sigma_{diff.}$, then the probability β of error in decision given the true H_1 is given by the shaded area under the dashed curve. Now the probability $(1-\beta)$ represents the probability of being right in rejecting H_0 given that H_1 is true. This probability $(1-\beta)$ is called the "power" of the

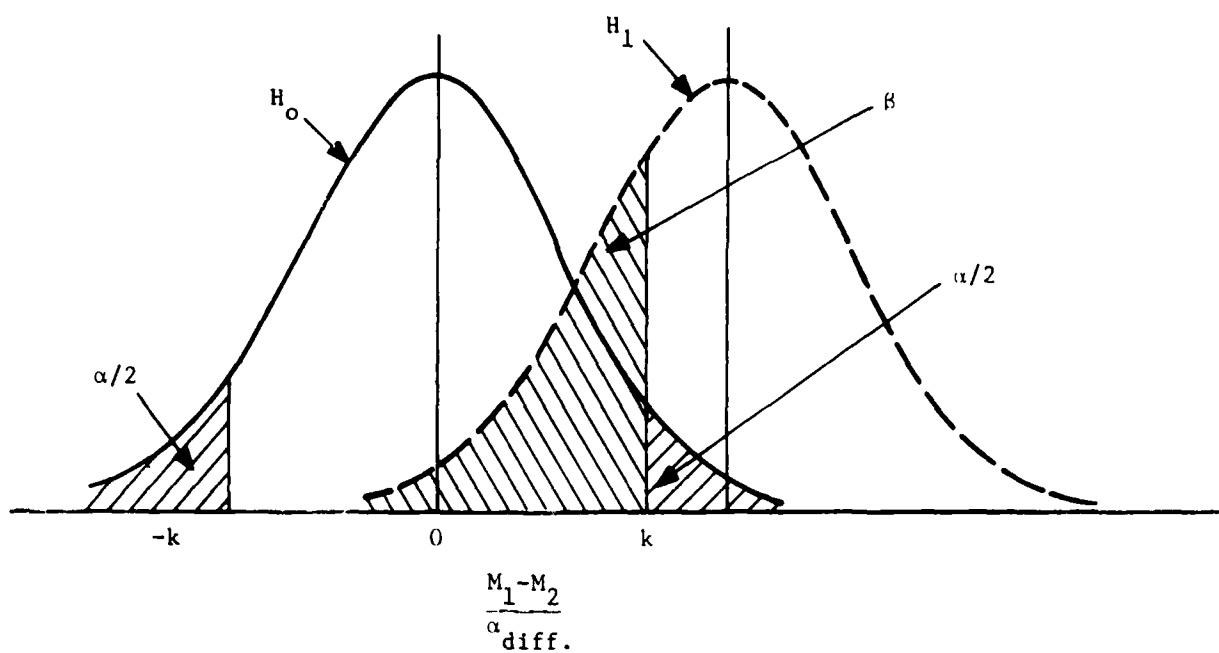


Fig. 42 Definition of Power of a Statistic Test Given a True Alternate Hypothesis H_1

792366

statistical test. It is clear that as the difference between H_1 and H_0 increases the power approaches unity. It is easily shown that

$$T_{\beta} = T_{\alpha/2} - \frac{c}{\sigma_{\text{diff}}} \quad (\Lambda-1)$$

where c is the difference between means given by the two hypotheses.

D. Strength of Association

If we have a large population of specimens, we sample a group of size N , subject each group to different experimental conditions given by an independent variable X and experimentally measure a dependent variable Y , the distribution of Y over all possible values of X is called the marginal distribution of Y . With a specified X , we have the conditional distribution of Y . The strength of statistical association is essentially the relative reduction in variance of Y obtained by specifying X . Or, symbolically

$$\omega^2 = \frac{\sigma_Y^2 - \sigma_{Y/X}^2}{\sigma_Y^2}$$

It is clear that if X defines Y , exactly (i.e., $\sigma_{Y/X}^2 = 0$) then ω^2 is unity. On the other hand, when X has no control over Y (i.e., $\sigma_{Y/X}^2 = \sigma_Y^2$) ω^2 is zero. So the value of ω^2 defines the strength of the association between X and Y .

It is quite interesting to note the significance of ω^2 in cases where we test for differences in means of two population. In terms of the mounting block experiments, if we argue that the strength of the relationship between the block configuration and the measurement capability is zero, then the observed test data will be the same by using any mounting method. Thus, the null hypothesis H_0 is equivalent to the hypothesis $\omega^2 = 0$.

A rough estimate of ω^2 is obtained by the expression

$$\text{est. } \omega^2 = \frac{T^2 - 1}{T^2 + N_1 + N_2 - 1} \quad (\Lambda-2)$$

E. Sample Size in Statistical Test

The sample size N required to estimate the means of population within $k\sigma$ with a probability of at least ρ may be estimated directly from Tchebycheff's inequality.

$$\text{prob } (|M - M_0| \leq k\sigma) \geq 1 - \frac{\sigma_M^2}{(k\sigma)^2},$$

where M_0 is the true mean.

For sample of size N , the variance of sampling distribution of means σ_M^2 is σ^2/N . Thus

$$\text{prob } (|M - M_0| \leq k\sigma) \geq 1 - \frac{\sigma^2}{N(k\sigma)^2}$$

If we desire that $\text{prob } (|M - M_0| \leq k\sigma) = \rho$, then

$$1 - \frac{\sigma^2}{N(k\sigma)^2} = \rho$$

or

$$N = \frac{1}{(1-\rho) k^2} \quad (\text{A-3})$$

As an example, let us consider that $\rho = 95$ percent then

$$N = \frac{20}{k^2}$$

Thus, if we require that the estimate of the mean be within 1σ with at least 95 percent probability, then $N = 20$, whereas if the estimate is required to be within 0.1σ with the similar confidence, then $N = 2000$. This simple way to estimate the sample size is useful in cases when we want a precise estimate of the mean.

In hypothesis testing, however, the sample size should be related to the strength of association ω^2 , the significance level for rejecting the

hypothesis α , and the power of the test $1-\beta$. It can be shown that given these three parameters, the sample size N is given by

$$\sqrt{\frac{N}{2}} = \frac{[z_{(1-\alpha/2)} - z_{\beta}]}{\Delta} \quad (\Lambda-4)$$

where

$$\Delta = 2 \sqrt{\frac{\omega^2}{1-\omega^2}}$$

and z is the standardized normally distributed variable. As an example, let us say α is 0.10 and we want the power to be 50 percent, which means that there is 50 percent chance of correctly rejecting H_0 in favor of a true H_1 , then $z_{\beta} = 0$, and $z_{(1-\alpha/2)} = 1.65$, hence

$$N = \frac{(1.65)^2 (1-\omega^2)}{\omega^2}$$

Thus, if we would like to detect a statistical association of say 0.05 then $N = 85.2$, that means we should have a sample of at least 86 elements before we can even have a 50 percent chance of detecting any small difference in means of the two groups.

If $N = 22$, then for $\alpha = .10$ and $\beta = .10$ we have

$$\Delta = \frac{1.65 + 1.28}{\sqrt{11}} = 0.883$$

which gives $\omega^2 = 0.163$.

This means that if we are looking for a strength of statistical association of 0.163, then a sample of 22 specimens is enough to correctly detect the difference in means of the two groups with a 90 percent confidence when the null hypothesis is rejected at $\alpha = .10$ in a two tailed t-test.

All of the above analysis is based on the assumption that the populations are normally distributed and when testing hypothesis about differences in means, the variance of the two populations are equal. It may be shown that relatively

large deviations from normality contribute very little errors. The assumption of homogeneity of variance is more important. In fact, when the variances are quite unequal, the use of different sample sizes can have serious effects on the conclusions. So it will always be safe to select samples of equal sizes from each population. In the case of support method evaluation the variances are not largely different, so the conclusions may not be in a substantial error. To be more exact, it will be required to perform a test for homogeneity of variance before performing a t-test.

In the relation between sample size and statistical association, a normal distribution is used instead of the t-distribution. This is done to avoid mathematical complications and to "guess" a smallest possible sample size required. In practice the sample must be somewhat larger than the size determined.

APPENDIX B

AUTOMATED ROLLER INSPECTION DEMONSTRATION TEST PLAN

AUTOMATED ROLLER INSPECTION DEMONSTRATION TEST PLAN

CONTRACT F33615-77-C-3142

MTI PROJECT 48806

1.0 PURPOSE

The purpose of the test plan is to provide a logical sequence of action items necessary to demonstrate the ability of the breadboard roller inspection modules to adequately inspect aircraft turbine engine quality bearing rollers.

2.0 INTRODUCTION

The test plan is divided into two sub tasks, one sub task will be a functional evaluation of the breadboard gage modules in which the performance of each module will be evaluated with respect to roller handling and manipulation. All the necessary sensors will be activated during this task and data will be recorded, however, an evaluation of accuracy will be made only to the extent that proper roller manipulation within each gage module can be determined.

The second sub task within the test program will be the evaluation of each breadboard gage module's accuracy and repeatability. In this sub task an individual roller will be inspected for all characteristics listed in Table 1 at least 100 times. From these data the repeatability of the gage will be evaluated by statistically comparing the results with similar data taken by presently used roller manufacturers' gaging methods. A second evaluation test within this subtask will consist of measuring a population of 25 identified rollers and comparing these measurements with the same measurements taken on the same rollers but with the use of present inspection equipment. It is understood that one roller design to be inspected will be the 16 x 16 mm roller used in the #4 bearing position of the F-100 engine. A second smaller roller of a size mutually agreed to by MTI and the Air Force will also be inspected.

3.0 FUNCTIONAL TESTS

The function test sequence will be performed to ascertain the following:

1. Ability of radial gage to determine
 - a. Diameter
 - b. Runout (cylindrical)
 - c. Crown Drop
 - d. Runout (crowd)
 - e. Flat Length Taper
2. Ability of Axial Gage to Determine
 - a. Length
 - b. End Parallel
 - c. End Squareness
3. Ability of Contour Gage to Determine
 - a. Corner Breakout
 - b. Corner Runout
 - c. Flat Length
 - d. Flat Centrality

An individual roller will be inserted into each gage module and a normal gaging cycle initiated. The roller will be dithered in the gaging fixture to assure proper seating after which a complete gaging sequence will be performed. Measurement accuracy will not be attempted at this time but the breadboard model's ability to properly handle the rollers and the techniques of measurement data reduction will be examined.

The following gage functions will be evaluated during the functional tests.

- Axial clamping requirements of roller in fixture
- Ability to rotate a roller in fixture
- Slide and roller indexing
- Prism alignment
- Line scan camera alignment and focus

Correction of any deficiencies discovered during the functional test sequence will be implemented prior to initiation of the accuracy and repeatability test sequence.

4.0 ACCURACY AND REPEATABILITY TEST

- 4.1 Repeatability test will be performed by obtaining 100 readings for each roller characteristic listed in Table 1. The tests will be conducted using a 16 mm roller and will be performed on both the current industry employed instruments and on the breadboard gage modules. A statistical analysis will be performed on the resulting data to determine whether a significant difference exists between the means of the two sets of data.

- 4.2 Accuracy tests will be conducted on two roller populations consisting of 25 15 mm x 16 mm rollers and 25 additional rollers of a size mutually agreeable to by MTI and the Air Force PCO. The two roller populations will be inspected by conventional means and by using breadboard gage modules. A statistical analysis will be performed on the test results to determine whether the breadboard gage modules duplicate the results of the conventional gaging techniques.

TABLE 1

ROLLER CHARACTERISTICS TO BE MEASURED

Diameter
Length
Crown Drop
Crown Runout
End Parallel
End Runout
Corner Breakout
Corner Runout
Flat Length
Flat Centrality
O. D. Taper

APPENDIX C

CALCULATION OF ERROR FOR STANDARD CIRCULAR
PROBE USED WITH A CYLINDRICAL SURFACE

Assume that a flat probe of effective radius r is facing a cylindrical surface of radius R as illustrated in fig. 43. An end view of the inner electrode of the probe is shown in fig. 43 (a) and a plan view showing the gap between the probe electrode and the cylindrical surface is given in fig.43 (b).

Assuming that the electric field in the gap between the probe electrode and the curved surface is uniform and parallel, the capacity due to the elemental strip, shaded in fig.43(a), is given by:

$$dC = \frac{m l dx}{y} \dots\dots\dots (1)$$

Where $m =$ a constant
 $l dx =$ area of the strip.
 $y =$ distance from strip to curved surface (a function of x)

Changing the variable from x to θ gives:

$$\begin{aligned} l &= 2 r \cos \theta) \\ x &= r \sin \theta) \dots\dots\dots (2) \\ dx &= r \cos \theta d\theta) \end{aligned}$$

$$\text{Thus } dC = \frac{m 2r^2 \cos^2 \theta d\theta}{y} \dots\dots\dots (3)$$

Integrating equation (3) between the limits $\theta = 0$ and $\theta = \pi/2$ will give half the total capacitance between the probe and the curved surface, i. e. the capacitance C is given by:

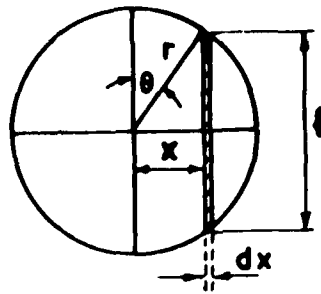
$$\begin{aligned} C &= 2 \int_0^{\pi/2} \frac{m 2r^2 \cos^2 \theta d\theta}{y} \\ &= 4mr^2 \int_0^{\pi/2} \frac{\cos^2 \theta d\theta}{y} \dots\dots\dots (4) \end{aligned}$$

When the radius R tends to infinity, i. e. when the surface to be measured becomes parallel to the probe surface, y is a constant equal to the fixed distance a . The capacitance C_0 between the probe and the surface under these conditions is given by:

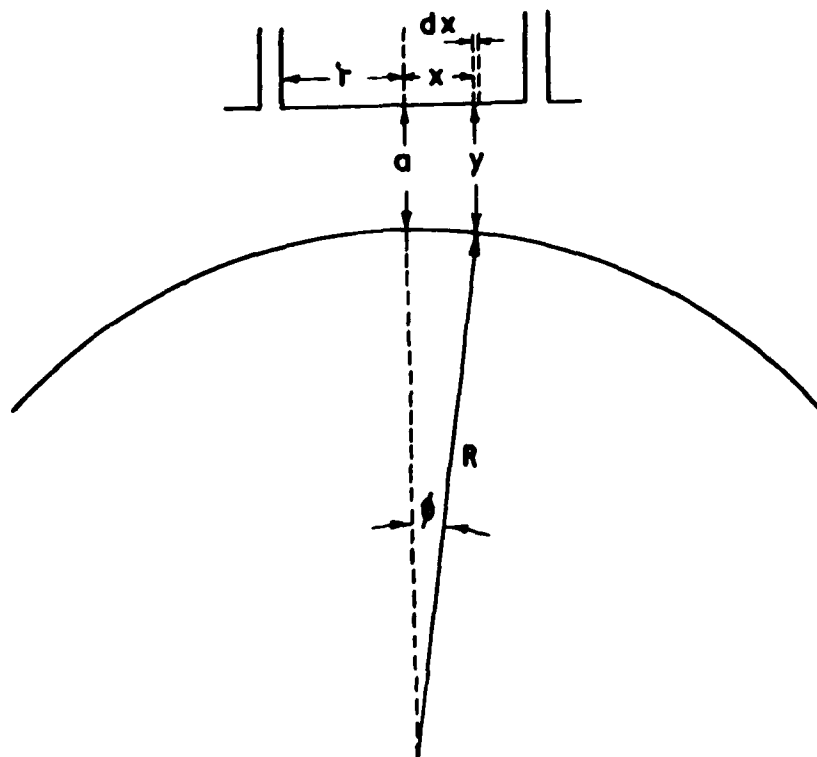
$$C_0 = \frac{4 \pi r^2}{a} \int_0^{\pi/2} \cos^2 \theta d\theta$$

i. e. $C_0 = \frac{\pi r^2}{a} \dots\dots\dots (5)$

In this case the calibrations are correct.



(a)



(b)

Fig. 43 Probe to Target Geometry

APPENDIX D

RADIAL/AXIAL MODULE AUTOMATED ROLLER INSPECTION PROTOTYPE



MECHANICAL TECHNOLOGY INCORPORATED
Latham, New York

PL 633E001

TITLE

SHEET 1 OF 6

RADIAL/AXIAL MODULE
AUTOMATED ROLLER INSPECTION PROTOTYPE

QTY./GROUP				ITEM NO.	AUTOMATED ROLLER INSPECTION PROTOTYPE	
4	3	2	G1		PART NO.	DESCRIPTION
				—	G33E001-G1	AXIAL RADIAL MODULE - AUTOMATED ROLLER INSPECTION PROTOTYPE
			1	1		BASE
			1	2		FIXTURE END PLATE R.H.
			1	3		FIXTURE END PLATE L.H.
			1	4		FIXTURE SPACER
			1	5		VEE BLOCK
			1	6		VEE BLOCK SPACER
			1	7		ANGLE BLOCK - R.H.
			1	8		ANGLE BLOCK - L.H.
			1	9		END PROBE HOLDER
			1	10		VERTICAL PROBE BRACKET
			1	11		VERTICAL PROBE BRACKET SPACER
			1	12		VERTICAL PROBE SPACER
			1	13		PIVOT BLOCK
			1	14		END PIN LEVER
			1	15		END PIN HOLDER
			1	16		END PIN ACTUATOR ARM
			1	17		END PIN ACTUATOR ARM
			1	18		END PIN WEIGHT
			1	19		LOADER YOKE
			1	20		LOADER POST
			1	21		ROLLER HOLDER SPACER
			1	22		ROLLER HOLDER
			1	23		LOADER LEVER
			1	24		LOADER LEVER CLEVIS
			1	25		TRACTION DRIVE SUPPORT
			1	26		PUSH-ROD GUIDE
			1	27		PUSH-ROD
			1	28		TRACTION DRIVE BRACKET
			1	29		TRACTION DRIVE COUPLING

DRAWN	J. Romano 8-8-79	SYN	REVISIONS	DATE	CODE IDENT. NO.	26741
ISSUED		A	ISSUED	9-21-79	PL 633E001	A
DESIGNED	W.W. Sures 9/21/79					
	H. JONES 9/21/79					
			170			
					SHEET 1 OF 6	REV

MECHANICAL TECHNOLOGY INCORPORATED
Latham, New York

PL 633E001

SHURET 2 of 6

TITLE

RADIAL/AXIAL MODULE
AUTOMATED ROLLER INSPECTION PROTOTYPE

[illegible]

MECHANICAL TECHNOLOGY INCORPORATED
Latham, New York

PL 653E001

SHEET 3 of 5

TITLE

RADIAL/AXIAL MODULE
AUTOMATED ROLLER INSPECTION PROTOTYPE

QTY./GROUP				ITEM NO.	AUTOMATED ROLLER INSPECTION PROTOTYPE	
4	3	2	G1	PART NO.	DESCRIPTION	
			1	57	E0240-022-2000	SPRING-ASSOCIATED SPRING BR-FOL. CONN. (.65 #/IN SPRING RATE)
			1	58	GZ10-1340606	FRICTION DRIVE WHEEL-STOCK DRIVE PRODUCT NEW HYDE PARK N.Y. (B & J FACE)
			1	59	2Z27MC1010	RIGHT ANGLE DRIVE-STOCK DRIVE PRODUCT NEW HYDE PARK N.Y.
			1	60	A3-20	SHAFT - 1/4" DIA x 2" LG - PIC DESIGN, CONN.
			1	61	A2-20	SHAFT - 3/16" DIA x 2" LG - PIC DESIGN, CONN.
			1	62	A1-22	SHAFT - 1/8" DIA x 2 1/4" LG - PIC DESIGN, CONN.
			1	63	A2-25	SHAFT - 3/16" DIA x 2 1/2" LG - PIC DESIGN, CONN.
			1	64	A2-40	SHAFT - 3/16" DIA x 4" LG - PIC DESIGN, CONN.
			1	65	111SM2-T	TYPE 5M SUBMINIATURE SWITCH-STYLE 16 MICRO SWITCH - FREEZE-T
			1	66	C3-B	ROLL PIN - 3" DIA x 3/8" LG - PIC DESIGN CONN OR EQUIV
		4	67	B10-10	BEARING-OIL IMPREGNATED BRONZE 1/4" I.D. x 3/8" LG - PIC DESIGN, CONN.	
			68			
			1	69	D1-10	PRECISION SLEEVE COUPLING PIC DESIGN, CONN.
			1	70	# 4041	KNURLED TUMB SCREW - # 0-32 x 3/4" LG PIC DESIGN, CONN. OR EQUIV.
			71			
			1	72	A3-11	SHAFT - 1/4" DIA x 1 1/8" LG - PIC DESIGN, CONN.
			1	73	A3-70	SHAFT - 1/4" DIA x 7" LG - PIC DESIGN, CONN.
		2	74	B10-6	BEARING-OIL IMPREGNATED BRONZE 3/16" I.D. x 3/8" LG. - PIC DESIGN, CONN	
DRAWN		S. Romano 8-8-79		SYN		REVISIONS
CHECKED						DATE
APPROVED		J. M. [unclear] 8-11-79				CODE IDENT. NO. 26741
		ridgines 9/21/79				PLG33E001 A
						SHEET 3 OF 6 REV



MECHANICAL TECHNOLOGY INCORPORATED
Latham, New York

PL633E001

TITLE

SHEET 4 OF 6

RADIAL/AXIAL MODULE
AUTOMATED ROLLER INSPECTION PROTOTYPE

QTY./GROUP				ITEM NO.	PART NO.	DESCRIPTION
4	3	2	G1			
			2	75	B10-5	BEARING-OIL IMPREGNATED BRONZE 3/16" I.D. x 1/4" LG (MODIFY TO 3/16" LENGTH) PIC DESIGN, CONN.
			1	76	Z2-3	RETAINING RING - FOR 1/4 DIA SHAFT PIC DESIGN, CONN.
			1	77	Z0D25	PRECISION JIG BUTTON - 3/8 HD DIA. x 1/4" LG - ALLIED DEVICES, BALDWIN NY, ORER
			2	78	SSB-52	BALL PLUNGER - (10-32 THDS) (STN STL) VLIER, BURBANK, CA.
			2	79	SSS-52	STN STL PLUNGER - (10-32 THDS) VLIER, BURBANK, CA.
			1	81	A2-15	SHAFT - 3/16" DIA x 1 1/2" LG - PIC DESIGN, CONN.
			1	86	CS-8	SET SCREW - "NO-MAR" #2-56 THD x 5/32 LG PIC DESIGN, CONN.
			1	87	CS-9	SET SCREW - "NO-MAR" #4-40 THD x 5/32 LG PIC DESIGN, CONN.
			7	88	CS-10	SET SCREW - "NO-MAR" #6-32 THD x 5/32 LG PIC DESIGN, CONN.
			7	89	CS-11	SET SCREW - "NO-MAR" #8-32 THD x 15/64 LG
			6	90		SOC HD CAP SCREW #4-40 x 1/2" LG STN STL
			2	91	Y5-2-W-N	SOC HD CAP SCREW SELF LCK. #3-56 x 1/2 LG STN STL - PIC DESIGN, CONN.
			10	92	Y5-4-W-N	SOC HD CAP SCREW SELF LCK #4-40 x 1/2 LG STN STL - PIC DESIGN, CONN.
DRAWN				REVISED		DATE
J. Romano 8-8-79				SYN		CODE IDENT. NO. 26741
CHECKED						PL633E001 A
APPROVED						SHEET 4 OF 6
H. Jones 9/14/79						REV



MECHANICAL TECHNOLOGY INCORPORATED
Latham, New York

PL633E001

TITLE

SHEET 5 OF 6

RADIAL/AXIAL MODULE
AUTOMATED ROLLER INSPECTION PROTOTYPE

QTY./GROUP					ITEM NO.	AUTOMATED ROLLER INSPECTION PROTOTYPE	
4	3	2	G1	PART NO.		DESCRIPTION	
			2	93		SOC. HD. CAP SCREW #10-30 x 1 1/2 LG STN STL	
			2	94		SOC. HD. CAP SCREW #10-32 x 3/4 LG STN STL	
			4	95		HEX BOLT #10-32 x 1/2 LG STN STL	
			2	96		# 2 FLAT WASHER STN STL	
			2	97		# 2-56 HEX NUT STN STL	
			2	98	YW-7	NYLON WASHER #10 - PIC DESIGN CONN.	
			1	99		WASHER , FLAT - 5/16" (.34 I.D. x .75 O.D. x .062 THK) STN STL	
			1	100		SOC. HD. CAP SCREW 1/4-20 x 1 3/4 LG STN STL	
			1	101	L3-20	MOTOR MOUNT CLEAT (SEE # 2-56 SC2) PIC DESIGN , CONN.	
			1	102	C3-2	ROLL PIN - 1/16" DIA x 1/2 LG PIC DESIGN , CONN	
			2	103	CF-1/2-SB	CAM FOLLOWER , MCGILL CORP. (SEE TEK BRG CAT.)	
			1	104	4019	KNURLED THUMB SCREW - #6-32 x 1/2 LG PIC DESIGN , CONN.	
				105		PROBE	
				106		PROBE	
			1	107	D9-875	DOWEL PIN - 3/16" DIA x 7/8 LG PIC DESIGN , CONN.	
			1	108	CF-1/2-NSB	CAM FOLLOWER , MCGILL CORP. (SEE TEK BRG CAT.)	
DRAWN		J. Romano 8-8-79		SYN	REVISIONS		
CHECKED							
DESIGNED		H. Jones 9/21/79					
		H. JONES 9/21/79					

APPENDIX E

CONTOUR GAGE MODULE

MECHANICAL TECHNOLOGY INCORPORATED
Latham, New York

PL 640E00

SECRET 1 OF 5

TITLE

CONTOUR GAGE MODULE

QTY./GROUP				ITEM NO.	PART NO.	DESCRIPTION
4	3	2	G1			
			X	X	640E001G1	
			1	1		BASE
			1	2		SCAN SLIDE SPACER
			1	3		LOADER ARM CAM
			1	4		LOADER ARM PIVOT BRACKET
			1	5		LOADER ARM
			1	6		ROLLER HOLDER
			1	7		LOADER ARM DRIVE BRACKET
			2	8		LIMIT SWITCH SPACER
			1	9		SCANNER MOUNTING BRACKET
			1	10		SCAN POSITIONING NUT
			1	11		SCAN POSITIONING NUT ASSY BRACKET
			1	12		PUSH ROD CAM FOLLOWER
			1	13		SCAN POSITIONING SCREW
			1	14		INDEX SLIDE MOUNT. BRACKET
			1	15		INDEX SLIDE SPACER
			1	16		INDEX SLIDE CAM
			1	17		COVER PLATE
			1	18		SCANNER MOUNTING BRACKET
			1	19		SCANNER MOUNTING BRACKET
			1	20		VEE BLOCK
			1	21		END STOP MOUNTING BLOCK
			1	22		TRACTION MOTOR HOLDER
			1	23		TRACTION MOTOR PIVOT BLOCK
			1	24		TRACTION MOTOR BRACKET
			1	25		TRACTION WHEEL
			1	26		COLLAR
			1	27		COUNTER-WEIGHT SHAFT

DRAWN *J. Remond* OCT 26/75

CHECKED *H. Jones* 10/30/75

APPROVED *W. S. Jones* 10/29/75

REVISIONS:

ISSUED

DATE: 10/26/75

CODE IDENT. NO. 26741

PL 640E001 A

177



MECHANICAL TECHNOLOGY INCORPORATED
Latham, New York

PL 340E00

SHEET 2 OF 5

TITLE

CONTOUR GAGE MODULE

QTY./GROUP				ITEM NO.	PART NO.	DESCRIPTION
4	3	2	G1			
			1	28		TRACTION WHEEL COUNTER-WEIGHT
			1	29		PUSH-ROD BEARING BLOCK
			1	30		PUSH-ROD
			1	31		PUSH-ROD CAM
			1	32		LIMIT SWITCH CAM
			2	33		TRACTION WHEEL LIFT MOTOR SPACER
			2	34		LIMIT SWITCH SPACER
			1	35		VEE BLOCK SHIM
			1	36	383C47 PI	SLIDE BASE
			1	37	383B46 PI	SLIDE
			1	38	383C45 PI	SLIDE BASE
			1	39	383C44 GI	CAMERA MOUNT ASSY
			1	40		CAMERA MOUNT SHIM
			1	41		GRANITE SURFACE PLATE-30x43x0.7-K
			1	42		TUNGSTEN CARBIDE STEEL BALL 1.32 DIA
			2	43	# 216324	SLIDER-FARRAND CONTROLS, VALHALLA, NY
			2	44	# 216343	SCALE-FARRAND CONTROLS, VALHALLA, NY
			1	45	MH 2005-001-	"C-LINE" DC SERVO MOTOR
						TORQUE SYSTEMS INC, WALTHAM, MASS
			2	46	LABS-20	AIR BEARING SLIDE, PNEUMO PRECISION, INC., KEENE, N.H.
			1	47	LABS-10	AIR BEARING SLIDE, PNEUMO PRECISION, INC., KEENE, N.H.
			2	48	# 530-27D	TIMING MOTOR -THE BRISTOL SAYBROOK CO., CONN.
			4	49	1115M2-T	TYPE SM SUBMINIATURE SWITCH -
						STYLE 16 - MICRO SWITCH, FREEPORT, ILL.
			2	50	3Z15M00300D	DC GEAR MOTOR
						STOCK DRIVE PRODUCTS NEW HYDE PARK, N.Y.
DRAWN				J. Romano Oct 26, 1979		REVISIONS
CHECKED				H. Jones 10/30/79		
APPROVED				Oct 20, 1979		
						DATE
						CODE IDENT. NO.
						26741
						PL340E001
						A
						SHEET 2 OF 5
						1979



MECHANICAL TECHNOLOGY INCORPORATED
Latham, New York

PL640E001

SHEET 3 OF 5

TITLE

CONTOUR GAGE MODULE

QTY./GROUP				ITEM NO.	PART NO.	DESCRIPTION
4	3	2	G1			
			1	51	CF-1/2-NSB	CAM FOLLOWER, MCGILL CORP. (SEE TEK BRG. CAT.)
			4	52	GB-45	NEEDLE BRG. TORRINGTON CORP. (SEE TEK BRG. CAT.)
			4	53	GB-55	NEEDLE BRG. TORRINGTON CORP. (SEE TEK BRG. CAT.)
			2	54	F-3	FLANGED ROLLER BRG. BARDEN CORP. DANBURY CONN. (SEE TEK BRG. CAT.)
				55		
			1	56	TI-3	COUPLING, BELLOWS-1/4" I.D. x 1/4" I.D. PIC DESIGN, CONN.
			1	57	DI-10	PRECISION SLEEVE COUPLING 1/8" I.D. x 1/4" I.D. PIC DESIGN, CONN.
			1	58	A3-30	SHAFT - 1/4" DIA x 3" LG STN STL PIC DESIGN, CONN.
			8	59		#2-56 x 1/2" LG SOC HD CAP SCREW STN STL
			2	60		#4-40 x 3/4" LG SOC HD CAP SCREW STN STL
			4	61		#4-40 x 1" LG FILLISTER HEAD MACHINE SCREW STN STL
			8	62		#6-32 x 3/4" LG FLAT HEAD CAP SCREW STN STL
			6	63		#6-32 x 1/2" LG SOC HD CAP SCREW STN STL
			8	64		#6-32 x 3/4" LG SOC HD CAP SCREW STN STL
			2	65		#6-32 x 7/8" LG SOC HD CAP SCREW STN STL
DRAWN				REVISED		DATE
F. Romano Oct 26/1979				SYN		CODE IDENT. NO. 26741
H. Jones 1/9/30/79						PL640E001 A
M. S. Jones Oct 21/79						SHEET 3 OF 5



MECHANICAL TECHNOLOGY INCORPORATED
Latham, New York

PL640E001

TITLE

SHEET 4 of 5

CONTOUR GAGE MODULE

QTY./GROUP				ITEM NO.	PART NO.	DESCRIPTION
4	3	2	G1			
			4	66		#6-32 x 1 1/8 LG SOC HD CAP SCREW
						STN STL
			2	67		#8-32 x 3/4 LG SOC HD CAP SCREW
						STN STL
			2	68		#10-32 x 3/4 LG SOC HD CAP SCREW
						STN STL
			2	69		#10-32 x 1 1/4 LG SOC HD CAP SCREW
						STN STL
			9	70		#10-32 x 3/8 LG SOC HD CAP SCREW
						STN STL
			2	71		M6 x 25 MM LG SOC HD CAP SCREW
						STN STL - METRIC - MULTISTANDARD COMP. INC.
			2	72		M8 x 16 MM LG SOC HD CAP SCREW
						STN STL - METRIC - MULTISTANDARD COMP. INC.
			1	73		#6-32 x 3 3/4 LG DOG POINT
						SETSCREW - STN STL
				74		
			1	75	CS-8	SETSCREW - NO-MAR" #6-56 THD x 5/32 LG
						STN STL - PIC DESIGN, CONN.
			2	76	CS-10	SETSCREW - NO-MAR" #6-32 THD x
						5/32 LG STN STL - PIC DESIGN, CONN.
			6	77	CS-15	SETSCREW - NO-MAR" #6-32 THD x
						9/32 LG STN STL - PIC DESIGN, CONN.
			1	78	4016	#6-32 x 3/4 LG KNURLED THUMB
						SCREW - STN STL - PIC DESIGN, CONN.
			1	79	4038	#10-32 x 3/4 LG KNURLED THUMB
						SCREW - STN STL - PIC DESIGN, CONN.
			8	80		1/4-20 UNC x 3/4 LG SOC HD CAP SCREW
						STN STL
DRAWN	J. Romano OCT 26, 1979				SYN	REVISIONS
CHECKED	H. JONES 10/31/79					DATE
APPROVED	W. S. Jones OCT 29, 1979					CODE IDENT. NO.
						26741
						PL640E001 A
						SHEET 4 OF 5

MECHANICAL TECHNOLOGY INCORPORATED
Latham, New York

PL 640 E.C.

PAGE 5 OF 5

TITLE

CONTOUR GAGE MODULE

[illegible]